

Utah State University

DigitalCommons@USU

---

All Graduate Theses and Dissertations

Graduate Studies

---

5-2011

## Water and Energy Balance of a Riparian and Agricultural Ecosystem along the Lower Colorado River

Saleh Taghvaeian  
*Utah State University*

Follow this and additional works at: <https://digitalcommons.usu.edu/etd>



Part of the [Civil and Environmental Engineering Commons](#)

---

### Recommended Citation

Taghvaeian, Saleh, "Water and Energy Balance of a Riparian and Agricultural Ecosystem along the Lower Colorado River" (2011). *All Graduate Theses and Dissertations*. 949.

<https://digitalcommons.usu.edu/etd/949>

This Dissertation is brought to you for free and open access by the Graduate Studies at DigitalCommons@USU. It has been accepted for inclusion in All Graduate Theses and Dissertations by an authorized administrator of DigitalCommons@USU. For more information, please contact [digitalcommons@usu.edu](mailto:digitalcommons@usu.edu).



WATER AND ENERGY BALANCE OF A RIPARIAN AND AGRICULTURAL  
ECOSYSTEM ALONG THE LOWER COLORADO RIVER

by

Saleh Taghvaeian

A dissertation submitted in partial fulfillment  
of the requirements for the degree

of

DOCTOR OF PHILOSOPHY

in

Irrigation Engineering

Approved:

---

Christopher M.U. Neale  
Major Professor

---

Gary P. Merkle  
Committee Member

---

David G. Tarboton  
Committee Member

---

Esmail Malek  
Committee Member

---

Lawrence E. Hips  
Committee Member

---

Byron R. Burnham  
Dean of Graduate Studies

UTAH STATE UNIVERSITY  
Logan, Utah

2011

Copyright © Saleh Taghvaeian 2011

All Rights Reserved

## ABSTRACT

Water and Energy Balance of a Riparian and Agricultural  
Ecosystem along the Lower Colorado River

by

Saleh Taghvaeian, Doctor of Philosophy

Utah State University, 2011

Major Professor: Dr. Christopher M. U. Neale  
Department: Civil and Environmental Engineering

Spatially-distributed water consumption was modeled over a segment of the Lower Colorado River, which contains irrigated agricultural and Tamarisk-dominated riparian ecosystems. For the irrigation scheme, distributed evapotranspiration data were analyzed in conjunction with point measurements of precipitation and surface flow in order to close daily and annual water balance. The annual closure error was less than 1% of the total water diversion to the area. In addition, it was found that the soil water storage component of the water balance cannot be neglected if the analysis is performed over time frames shorter than annual (e.g. growing season).

Water consumption was highly uniform within agricultural fields, and all the full-cover fields were transpiring close to their potential rates. Mapping several new and existing drainage performance indicators showed that neither soil salinization nor water-logging would be of concern in this irrigation scheme. However, the quality of high-volume return flow must be studied, especially since the degraded water quality of the

western US rivers is believed to act in favor of the invasive riparian species in outcompeting native species.

Over the Tamarisk forest, the remotely-sensed evapotranspiration estimates were higher than the results of an independent groundwater-based method during spring and winter months. This was chiefly due to the fixed satellite overpass time, which happened at low sun elevation angles in spring and winter and resulted in a significant presence of shadows in the satellite scene and consequently a lower surface temperature estimate, which resulted in a higher evapotranspiration estimate using the SEBAL model. A modification based on the same satellite imagery was proposed and found to be successful in correcting for this error. Both water use and crop coefficients of Tamarisk estimated by the two independent methods implemented in this study were significantly lower than the current approximations that are used by the US Bureau of Reclamation in managing the Lower Colorado River.

Studying the poorly understood stream-aquifer-phreatophyte relationship revealed that diurnal and seasonal groundwater fluctuations were strongly coupled with the changes in river stage at close distances to the river and with the Tamarisk water extraction at further distances from the river. The direction of the groundwater flow was always from the river toward the riparian forest. Thus the improved Tamarisk ET estimates along with a better understanding of the coupling between the river and the riparian aquifer will allow the Bureau of Reclamation to re-asses their reservoir release methodology and improve efficiency and water savings.

## ACKNOWLEDGMENTS

I deeply appreciate my family members for their never-ending love and encouragement that have motivated me to overcome all the difficulties in my path. I am specifically grateful to my parents, who raised me and taught me to always be eager to learn. I would not be able to reach this point without the love and support of my wife, Khatoon, who has been beside me in every step during my PhD program. I am also grateful to my brothers, Saber and Sadegh, for their friendship and for fulfilling the responsibilities that I could not accomplish due to my educational constraints. Especial thanks to my uncle and aunt, Mahmood and Sandy Akhavan. With them, I never felt I was away from my parents.

My deepest gratitude to the committee members, Drs. Hipps, Malek, Merkley, and Tarboton, for their teaching and guidance. I am especially grateful to my major advisor, Dr. Neale, for being a wonderful mentor not only with my research, but also in other aspects of my life. His advice has always been enlightening during the past several years while I have had the pleasure of being his student.

I am thankful to Mr. Roger Henning (PVID chief engineer), Mr. Michael Mullion (Red River Farms, PVID), Mr. John Weiss (hydrologic technician, Blythe Hydrographic Office, River Operations Group, USBR), and Dr. Marvin Jensen for kindly sharing their extensive knowledge and experience with me and for providing me with detailed information required to carry out the present study. My sincere appreciation to all other individuals who have graciously helped me in every single step of my life and education, including my good friends Kevin Kerr and Mark Hargreaves, and the hardworking staff

of the BE and CEE departments: Ms. Ann Martin, Ms. Rebeca Olsen, Ms. Carolyn Benson, Ms. Marlo Bailey, and Mr. Jed Moss.

This research was funded in part by the US Bureau of Reclamation under a contract with the Alliance of Universities with a sub-contract to Utah State University. Additional funding was provided by the Utah Agricultural Experiment Station and the Remote Sensing Services Laboratory, Department of Civil and Environmental Engineering, Utah State University.

Saleh Taghvaeian

## CONTENTS

	Page
ABSTRACT.....	iii
ACKNOWLEDGMENTS .....	v
LIST OF TABLES.....	ix
LIST OF FIGURES .....	x
CHAPTER	
1. GENERAL INTRODUCTION.....	1
Problem statement.....	6
Research significance.....	10
Objectives .....	12
References.....	14
2. REMOTE SENSING AND GIS TECHNIQUES FOR MANAGING IRRIGATION SCHEMES: A CASE STUDY IN SOUTHERN CALIFORNIA .....	19
Abstract .....	19
Introduction.....	20
Methods and materials .....	22
Study area.....	22
Water balance components .....	23
Irrigation and drainage performance.....	27
Results and discussion .....	33
Groundwater fluctuations.....	33
Water balance components .....	34
Irrigation and drainage performance.....	41
Summary and conclusions .....	49
References.....	52
3. REMOTE SENSING OF CROP COEFFICIENTS AND WATER REQUIREMENTS OF IRRIGATED COTTON.....	56



	viii
Abstract .....	56
Introduction.....	57
Methods and materials .....	60
Study area.....	60
Cotton agricultural practices in PVID.....	61
Energy balance model.....	62
Field selection .....	62
Comparing crop coefficients.....	64
Results and discussion .....	65
Remotely-sensed crop coefficients .....	65
Water consumption .....	68
SAVI- $K_{cb}$ relationship.....	71
Summary and conclusions .....	72
References.....	73
4. WATER CONSUMPTION AND STREAM-AQUIFER- PHREATOPHYTE INTERACTION ALONG A TAMARISK- DOMINATED SEGMENT OF THE LOWER COLORADO RIVER.....	75
Abstract.....	75
Introduction.....	76
Methods and materials .....	82
Study area.....	82
Groundwater characteristics.....	85
Tamarisk evapotranspiration.....	87
Closing water balance .....	91
Results and discussion .....	92
Groundwater characteristics.....	92
Tamarisk evapotranspiration.....	98
Closing water balance on the river.....	112
Summary and conclusions .....	114
References.....	116
5. GENERAL SUMMARY AND CONCLUSIONS.....	121
APPENDIX.....	125
CURRICULUM VITAE.....	128

## LIST OF TABLES

Table	.Page
2.1 Total annual amounts of water balance components and associated percentages.....	40
4.1 Characteristics of measuring stations.....	84
4.2 Annual and seasonal water consumption in mm over Slitherin and Diablo. Values in parentheses are the percentage of the corresponding (annual or seasonal) grass-based reference ET .....	109
4.3 Total annual amounts of water balance components. Depth values are estimated by dividing the volume of water consumption by the total studied area (73,862 ha).....	113
A.1 Reported coefficients of variation (among and within field, $CV_s$ and $CV_w$ respectively) of actual ET estimated over sites with diverse agro-climatological conditions .....	126
A.2 Previously developed $K_c$ -VI relationships for cotton in the literature.....	127

LIST OF FIGURES

Figure	Page
2.1 Palo Verde Irrigation District (PVID) in southern California, within the Colorado River basin .....	23
2.2 (a) Monthly average of all piezometer readings and (b) Cumulative frequency distribution of depth to groundwater for three months: February, June, and September 2008 .....	33
2.3 SEBAL-derived spatially distributed daily ET on July 29th, 2008 (DOY: 211).....	36
2.4 (a) Frequency distribution of $K_c$ on a pixel-by-pixel basis for two dates in 2008: April 8th (DOY: 99) and July 13th (DOY: 195) and (b) the cumulative frequency of $K_c$ for the same dates .....	38
2.5 Stacked bars of daily depths of a water inputs; and, b outputs .....	39
2.6 Adjusted values of daily PT parameter ( $\alpha$ ). Dashed and solid gray lines represent 1.26 and 1.4, respectively .....	42
2.7 Average RET over all and full-cover fields of PVID, under hypothetical non-advective and actual advective conditions.....	43
2.8 Average $DF_g$ and $DF_n$ for each month in 2008 .....	46
2.9 Frequency distribution of RGD of all PVID fields for February and September .....	47
2.10 Field-specific DDU (left) and RGD(right) of larger PVID fields for September 2008 .....	48
3.1 Palo Verde Irrigation District (PVID) in southern California .....	60
3.2 2008 crop classification layer of PVID fields (left) and ground-truthed fields (right) .....	63
3.3 Average cotton crop coefficient during the 2008, estimated by (a) the SEBAL model and (b) the SAVI method. Vertical dashed lines represent the range of values for all 22 studied fields .....	66

3.4	Piece-wise crop coefficients from: SEBAL- $K_c$ (solid black line), SAVI- $K_{cb}$ (dashed black line), FAO-56- $K_c$ (solid gray line), and LCRAS- $K_c$ (dashed gray line).....	67
3.5	(a) Daily and (b) seasonal cotton water use: SEBAL- $K_c$ (solid black line), SAVI- $K_{cb}$ (dashed black line), FAO-56- $K_c$ (solid gray line), and LCRAS- $K_c$ (dashed gray line) .....	69
3.6	SEBAL- $K_c$ versus SAVI. Each point represents one Landsat TM5 overpass and one field. A total of 21 satellite scenes were used to study 22 cotton fields. The solid black line represents the lower envelope to the estimated $K_c$ -SAVI pairs .....	71
4.1	The stretch of the Lower Colorado River between Palo Verde diversion dam and USBR gaging station at Cibola .....	83
4.2	The lower Cibola National Wildlife Refuge (CNWR) and the location of study sites. Left: False-color multispectral airborne image and Right: LiDAR-derived canopy height, both at 1 m resolution.....	85
4.3	Average groundwater EC during 2008 at Diablo (light gray), Swamp (dark gray), and Slitherin (black).....	93
4.4	Average daily depths to groundwater during 2008 at Diablo (light gray), Swamp (dark gray), and Slitherin (black).....	94
4.5	Daily average (a) depths to groundwater and (b) groundwater elevation, at five observation wells of the Diablo station. ....	96
4.6	Daily average groundwater elevation (m) at Diablo (light gray), Swamp (dark gray), and Slitherin (black), along with the river stage (double blue line). All elevation data are based on the same datum.....	96
4.7	Daily average inter-station hydraulic gradient expressed in percentage (a) before and (b) after correcting for the effect of southward flow .....	98
4.8	2008 daily groundwater consumption estimated by White method (black), overlaid by the measured depth to groundwater (gray), average for all the five observation wells at (a) Slitherin and (b) Diablo.....	99
4.9	Daily ET rates over Slitherin station, estimated by SEBAL model and two different extrapolation techniques: EToF (black) and EF (gray).....	101
4.10	Spatially-distributed ET rates modeled by the SEBAL-EF methods over CNWR.....	103

4.11	A comparison of daily ET rates estimated by SEBAL-EF method (black) with the White method (gray) over (a) Slitherin and (b) Diablo .....	104
4.12	A comparison of daily ET rates estimated by SAVI-adjusted SEBAL-EF method (black), the White method (light gray), and measured by the Bowen-Ratio tower (dark gray) over (a) Slitherin and (b) Diablo.....	107
4.13	Piece-wise Kc curves over, a Slitherin; and, b Diablo, using the following methods: adjusted SEBAL-EF (solid black), White (solid gray), LCRAS (dashed black), and LCRAS modified by Westenburg et al. (2006) (dashed gray).....	108

## CHAPTER 1

### GENERAL INTRODUCTION

Historically, the western US has been known for its arid climate, low precipitation, and long droughts, which have made water management a very complex issue in this part of the world. Increasingly scarce water resources of the western US need to be allocated in such a way that not only supply increasing human and agricultural demands, but also protect ecosystems and critical habitat for flora and fauna. In addition, new scientific evidence of future climate change has concerned both policy makers and the public. For Western water supplies possible consequences of global warming include, but are not limited to: more mountains precipitation in the form of rainfall and less snow, earlier spring run-off, change in timing of vegetation growth stages, and higher evapotranspiration rates. Water governance in such an environment is not possible without having a thorough knowledge of where the water is most needed and where it can be saved.

The fate of water after diversion from surface resources and/or extraction from aquifers can be categorized into consumptive and non-consumptive uses (Perry 2007). The consumed fraction of water essentially consists of evaporative losses in forms of evaporation from land and water surfaces and transpiration by vegetation, which are usually treated as the combined process of evapotranspiration (ET). Other consumptive uses of water such as human uses or the water that is incorporated in plant tissues are significantly smaller compared to the ET from vegetative surfaces, especially in arid/semi-arid regions. For example, irrigation withdrawals to meet crop ET demand

have been the largest use of fresh water in the United States since 1950, accounting for about 65% of the total water withdrawals. Not surprisingly, the majority of withdrawals (86%) and irrigated area (75%) were in the seventeen contiguous western states (Hutson et al. 2004). The irrigation sector has also been occasionally accused of wasting huge amounts of water and several researchers have concluded that by increasing irrigation efficiency in arid/semi-arid areas, water can be saved and assigned to other purposes. Therefore, it is crucial to study the amount of water that needs to be diverted for irrigation and how it is partitioned into different consumptive and non-consumptive uses in order to identify any water saving potential.

Traditionally, evapotranspiration and consequently irrigation efficiencies have been addressed based on point measurements. A major caveat of this approach is that the results represent only the local conditions of the usually small footprint of measuring instruments. Considering that the hydro-climatological conditions are highly variable, the results of traditional methods are less useful as the size of study area increases from field to scheme and basin. Recent advances in earth observing systems have made remote sensing techniques an efficient tool that can be used either independently or in conjunction with point measurements to assist decision makers with managing water resources.

Remotely-sensed data can be useful at different levels of water consumption studies, from very basic levels of determining land surface type to the more complicated modeling of the spatially-distributed evapotranspiration. One example of using satellite imagery at a basic level is the Lower Colorado River Accounting System (LCRAS), which has been developed by the US Bureau of Reclamation (USBR) to estimate the

water demand of agricultural crops and riparian species along the Lower Colorado River. In LCRAS, the Lower Colorado River Basin is classified into different land cover groups using five satellite images per year. For every land cover group, a tabularized single crop coefficient ( $K_c$ ), estimated based on previous point measurements, is multiplied by the reference evapotranspiration in order to approximate the actual water use of that specific group (Jensen 2003). The total volume of water consumption by each group is then estimated by multiplying the actual ET and the total area associated with each land cover. Integrating all these volumes over appropriate time scale determines the amount of water that needs to be released at each diversion point.

Although this method has been applied for many years, it is subject to many different sources of errors, such as the error in classifying land cover type, the error introduced by assuming that all the fields under the same crop are planted and harvested at the same time, the uncertainty due to applying oversimplified  $K_c$  values, and the uncertainty due to ignoring variability within fields. Stehman and Milliken (2007) showed that in 2002, LCRAS classification error alone ranged from about 7% for alfalfa to about 67% for small vegetables. Fortunately, the errors for different crops were partially offsetting in under- or overestimating total volume of water demand, and therefore resulted in a small overall error.

A higher level of incorporating air- or space-borne imagery is in spatial extrapolation of ET estimates. An example of this approach that has been extensively implemented over agricultural areas is developing a relationship between crop coefficients ( $K_c$ ) and vegetation indices (VI's), obtained from remotely-sensed surface reflectance in different wavebands. Reflectance-based crop coefficients have been



developed for many agricultural crops such as: potato (Jayanthi et al. 2007), sugar beet and green bean (Koksal 2008), soybean, sorghum, and alfalfa (Singh and Irmak 2008), cotton (Shuhua et al. 2003; Hunsaker et al. 2005a), corn (Bausch and Neale 1987; Neale et al. 1989; Bausch 1993, 1995; Singh and Irmak 2008), and wheat (Choudhury et al. 1994; Ray and Dadhwal 2001; Duchemin et al. 2006; Hunsaker et al. 2005b, 2007). This approach is similar to LCRAS in which that classification of agricultural crops is required in order to assign the appropriate VI- $K_c$  relationship to each type of crop. However, the advantage of this method is in the use of remotely-sensed VIs, which provides information on the actual growth condition of crops, rather than assuming a similar condition over all fields under the same crop. The effects of other agricultural and water management practices and within field variations are also reflected in this method.

Compared to land surface classification and ET extrapolation, an even higher level of using remotely-sensed data is the modeling of surface energy balance components. Although energy balance models have existed since the early 1970's (Brown and Rosenberg 1973; Stone and Horton 1974), recent improvements in estimating sensible heat flux (Norman et al. 1995; Bastiaanssen et al. 1998a) have significantly enhanced their accuracy. One of the best performing energy balance models in irrigated areas is "Surface Energy Balance Algorithm for Land (SEBAL)" (Bastiaanssen et al. 1998a). Being applied in more than thirty countries, SEBAL estimates of ET have been validated against ground measurements and showed that this model has the ability to accurately model ET (Bastiaanssen et al. 1998b; Ramos et al. 2009) at field and catchment scales (Bastiaanssen et al. 2005). In this model, net radiation ( $R_n$ ) is calculated through estimating all components of incoming and outgoing

radiation. Once net radiation is determined, soil heat flux ( $G$ ) is modeled as a fraction of  $R_n$ . The ratio of  $G$  over  $R_n$  is a function of surface vegetative fraction, which is estimated using Normalized Difference vegetation Index (NDVI).

SEBAL utilizes an innovative approach in modeling sensible heat flux ( $H$ ). This approach is based on the assumption that over a wet surface, the transfer of water between land and atmosphere is solely controlled by atmospheric demand. In other words, since there is no shortage of water, most of the available energy is used for evapotranspiration; therefore, the temperature gradient over the wet surface, and, consequently, sensible heat flux, would be negligible. In contrast, since there is little or no water to evaporate over a very dry surface, the vertical vapor pressure gradient and latent heat flux would approach zero. Spatially anchoring these two extreme limits makes it possible to interpolate  $H$  over all other surfaces in between, using the surface temperature estimated from the thermal infrared band (Bastiaanssen et al. 1998a). After  $R_n$ ,  $H$ , and  $G$  are identified, latent heat flux ( $LE$ ) can be calculated as the residual of energy balance equation, assuming that the energy used in photosynthesis and the canopy storage of energy are both insignificant.

Space- or airborne imagery – as input data to models such as SEBAL – is only a snapshot of latent heat flux at a specific time during the day. As a result, remote sensing techniques offer only an instantaneous estimate of ET that needs to be scaled up to longer periods (hourly, daily, and seasonal) for most practical purposes (e.g. water balance analysis). In the earlier versions of SEBAL, and some other energy balance models, instantaneous ET is extrapolated to daily values using Evaporative Fraction (EF or  $\Lambda$ ). This concept is based on the assumption that the ratio of instantaneous ET to

instantaneous available energy ( $R_n - G$ ) is constant during the day (Brutsaert and Sugita 1992; Crago 2000), especially under cloud-free conditions (Zhang and Lemeur 1995). Once this ratio is determined, daily ET could be calculated by multiplying EF ratio and the daily value of available energy. Although the EF technique has provided reliable results in many studies (Gowda et al. 2008), its accuracy decreases in arid regions, where afternoon advection is common. To overcome this problem, Trezza (2002) suggested a new concept (ETrF method), which modifies EF ratio by replacing available energy with estimated alfalfa-base reference evapotranspiration ( $ET_r$ ). Since measured daily  $ET_r$  contains some information about the energy imported from dry neighboring areas, up-scaled daily ET estimates would be significantly improved (Romero 2004; Allen et al. 2007 a, 2007b). Alternatively, grass-based reference ET ( $ET_o$ ) could also be used in extrapolating instantaneous ET values (EToF method). Colaizzi et al. (2006) compared estimates of five different up-scaling techniques with measurements of precision weighing lysimeters at Bushland, Texas, where strong advection of heat usually occurs. For cropped surfaces, the EToF method performed better than ETrF and EF methods. Chavez et al. (2008) also indicated that for irrigated agricultural crops under advective condition, the performance of EToF is better than ETrF and EF mechanisms.

### **Problem statement**

As the demand for water increases in the western US, the need to better estimate the evaporative losses from irrigated agriculture becomes significantly more important. However, accurately identifying evapotranspiration alone would not answer all of the questions and concerns about agricultural uses of water. As summarized by Jensen

(2007) there are many misunderstandings about the agro-hydrological water cycle that have led to false conclusions. The most important misunderstanding is that by improving irrigation efficiency, water can be saved and assigned to other purposes. However, the possibility of any water saving can be evaluated only if in addition to ET, other water balance components are also quantified. Spatially-distributed ET has been estimated over many irrigation schemes, but a thorough water balance closure to identify the fate of water after irrigation is lacking in the literature. This is mainly due to the mismatch between hydrological and irrigation scheme boundaries, as well as the difficulties in obtaining information on other water balance components.

Irrigation managers are also interested in evaluating the performance of different components of irrigation and drainage systems. Remotely-sensed energy and water balance components can be used in addressing irrigation performance at a wide variety of spatial and temporal scales. Spatially-distributed performance indicators (PIs) provide water managers with a powerful tool that can be used for locating poor-performing fields and for investigating the factors responsible for that, rather than going through the time and expense-extensive point evaluation of every single field. Although remote sensing techniques have been occasionally applied in performance evaluation studies, there is still a gap between research projects and practical application of these techniques in irrigation management (Ambast et al. 2002). Bastiaanssen and Bos (1999) stated that more demonstration projects and case studies should be carried out to bridge this gap and to show the potential of remote sensing to water managers. In addition, combining water balance analysis and remotely-sensed performance evaluation can standardize the

definition and interpretation of the existing PIs, which is very important in developing benchmarks and in comparing performance of different irrigation schemes.

Addressing the performance of drainage systems has an equal, if not greater, importance compared to the irrigation performance, since the sustainability of irrigation schemes is strongly affected by the functioning of agricultural drains and their effectiveness in removing extra water and salts from the crop root zone. Soil salinization and water-logging has been responsible for the failure of several ancient agriculture-based civilizations in the world, and unless drainage systems are evaluated appropriately, even the new and modern irrigation projects are in danger of a similar system failure. However, spatially-distributed drainage performance and its linkage to irrigation performance have not been investigated before. Bos (1997) defined a few drainage PI's to be studied along with irrigation PI's, but his ideas have never been developed beyond the theory level.

Besides the evaporative losses from irrigated areas, the amount of water extraction by phreatophytes is also of great concern, especially in arid/semi-arid regions. The issue of riparian water consumption is even more complicated along the western US watercourses, where invasive species such as Tamarisk (*Tamarix* spp.) have replaced with high density native riparian species such as Mesquite (*Prosopis* spp.) and Willows (*Salix* spp.). For decision makers in the semi-arid western US with scarce water resources, it is of crucial importance to accurately estimate Tamarisk evapotranspiration and the amount of water that can be salvaged by its removal.

However, the debate over the actual amount of Tamarisk ET is still unresolved. For example, in estimating riparian water consumption along the Lower Colorado River,

USBR applies a coefficient of 0.86 as the ratio of annual Tamarisk ET to grass reference ET, while Murray et al. (2009) estimated a value of only 0.42 over the same area. Such large differences have resulted in contrasting opinions on the effectiveness of Tamarisk control efforts for water salvage purposes. Fostering an aggressive eradication program, Zavaleta (2000) reported that the negative effects of Tamarisk water consumption on agricultural and municipal water supplies, hydropower generation, and flood control reach an annual value as high as 285 million USD. On the other hand, Vandersande et al. (2001) found that water use of Tamarisk is similar to other native species and Murray et al. (2009) concluded that water salvage from Tamarisk removal in the Lower Colorado River would be negligible.

The existing remote sensing methods for estimating riparian ET are those that have been developed for agricultural crops. However, agricultural crops and phreatophytes are very different in nature. Analyzing spatially-distributed energy and water balance components over these areas requires proper understanding of different processes that are involved. In irrigated agriculture, the water cycle is artificially enhanced by human interference in such a way that crops are provided with sufficient water at the appropriate time and location. On the other hand, riparian vegetation in arid regions relies on groundwater availability. If the groundwater level drops below the effective root depth, evapotranspiration would decrease, regardless of atmospheric demand. In addition, the quality of soil and water may be different for agricultural and riparian ecosystems. In a well-managed irrigation scheme, excessive water is drained and even sometimes water is applied just to wash the salts out of root zone. While in a

riparian area, diurnal and seasonal fluctuations of ground water and continuous extraction by phreatophytes may deposit salts in the top layer of the soil.

Although an accurate estimation of spatially-distributed riparian ET is needed, it does not provide a comprehensive understanding on the mechanisms that control riparian water use; unless it is supported by a detailed investigation of stream-aquifer-phreatophytes interaction (Devitt et al. 1997). Carrying out a comprehensive study to accurately identify the amount of riparian ET and its inter-relationship with respect to groundwater availability and quality, as well as river stage fluctuations would answer the questions of many decision makers in arid/semi-arid parts of the world.

### **Research significance**

In this study, satellite-derived evapotranspiration estimates at high spatial resolution were integrated with point measurements of surface flow at high temporal resolution to study water balance over co-occurring agricultural and riparian ecosystems along a segment of the Lower Colorado River. Integrating the fine spatial and temporal resolutions resulted in a water balance analysis that has rarely been performed at these scales before, especially over mixed ecosystems.

Over the studied irrigation scheme, distributed groundwater dynamics were investigated using more than 260 piezometers. The current literature is lacking such a detailed analysis of groundwater dynamics and the effects of irrigation and drainage on the observed water table fluctuations. The results of this study revealed that the soil water storage component of agricultural water balance can be neglected only if an appropriate time frame is selected based on the local agro-hydrological conditions of the

study area. Specifying the appropriate time frame is particularly important if one of the components (e.g. evapotranspiration) is estimated as the residual of the water balance equation.

In arid/semi-arid regions, it is of crucial importance to accurately evaluate the performance of different components of irrigation schemes in order to identify if water quality and quantity can be preserved. However, current literature focuses primarily on the performance of irrigation conveyance and water application components rather than the performance of drainage system. In addition, most of the reported values on system performance are based on point measurements. In this study, besides a comprehensive evaluation of distributed irrigation uniformity and adequacy, GIS techniques were implemented to estimate drainage efficiency on a pixel-by-pixel basis to locate areas of concern and areas that performance can be improved. One of the studied drainage performance indicators (PIs) has been introduced by Bos (1997), but it has never been applied in a case study before and no actual estimate of this PI is available. In addition, a new drainage PI is introduced and mapped, using the actual groundwater depth measurements. This PI determines if the agricultural fields are uniformly drained or not.

A novel approach for modifying the results of energy balance models to account for the effect of low sun elevation angles at the time of sensor overpass was introduced. Since the proposed modification is based on the same remotely-sensed data used in running energy balance models rather than ground-based data, it is transferable to other riparian ecosystems at different parts of the world (especially those that are poorly gaged). Tamarisk ET was also estimated using another independent method based on high-frequency diurnal groundwater fluctuations measurements. The results of this



method were in agreement with the results of the modified energy balance approach, and both were significantly lower than the Tamarisk water use approximations currently

Another original aspect of this research was in shedding light on the poorly-understood river-aquifer-phreatophytes interaction in the studied Tamarisk-dominated riparian forest. The lack of knowledge about this complex interaction and more specifically about the direction of the groundwater flow between river and aquifer poses operational challenges in the management of over-allocated Colorado River. With knowledge of these interactions, the new estimates of Tamarisk water consumption were projected over the entire Lower Colorado River Basin to provide decision maker with an insight into the consumptive use of water by Tamarisk monocultures.

The findings of this study will significantly assist water managers in allocating limited water resources of the Lower Colorado River Basin in a more efficient way, as well as in performing a more accurate cost-benefit analysis of the expensive riparian eradication activities.

### **Objectives**

The general objective of this study is to apply different satellite-based remote sensing techniques over a composite agricultural and riparian ecosystem in order to study water consumption and use the information for closing the water balance over the entire river reach. In addition, a study of the complex stream-aquifer interaction will be conducted. To accomplish these objectives the following tasks will be conducted:

1. Estimate spatially-distributed ET of agricultural crops, using two different remote-sensing techniques: a surface energy balance model and a reflectance-based crop coefficient method;
2. Conduct a daily water balance analysis and close the water budget over the studied irrigation scheme at different time scales;
3. Study groundwater dynamics over the irrigated area and identify the effect of irrigation and drainage on groundwater seasonal patterns;
4. Map several new and existing performance indicators in order to evaluate the performance of irrigation and drainage systems;
5. Study the water consumption of Tamarisk forests using a remotely-sensed energy balance model and another independent method based on diurnal water table fluctuations;
6. Modify the energy balance model to account for the different bio-physical characteristics of riparian thickets;
7. Investigate the effect of groundwater availability and quality on riparian ET;
8. Identify the stream-aquifer interaction and the direction of groundwater flow; and,
9. Conduct a daily water balance analysis and close the water budget over a stretch of the river that contains both agricultural and riparian ecosystems.

To address the different objectives of this study, three papers were prepared. The first paper presents the results of the SEBAL model applied to the irrigated agricultural area, along with the spatially-distributed irrigation and drainage performance indicators. The results of the water balance study on daily and annual bases will be provided as well. The second paper focuses on cotton, as the second major crop of the studied area. Cotton

growing season is extracted from the remotely-sensed data. Cotton crop coefficients from the energy balance model are compared with the estimates of an existing reflectance-based crop coefficient, as well as with tabulated values suggested in two separate publications. In addition, a new regression model that approximates cotton  $K_c$  from a satellite-based vegetation index is developed. Finally, the third paper deals with water consumption of the studied riparian communities and introduces modifications to the SEBAL model to be able to apply this model over riparian ecosystems. A detailed investigation of stream-aquifer-phreatophyte interaction, including the effect of water availability on Tamarisk ET and the source-sink relationship of riparian aquifer and the Colorado River are also presented in this paper.

### References

- Allen RG, Tasumi M, Morse A, Trezza A, Wright JL, Bastiaanssen W, Kramber W, Lorite-Torres I, Robison CW (2007a) Satellite-based energy balance for Mapping Evapotranspiration with Internalized Calibration (METRIC)-Applications. *Irrig Drain Eng* 133(4):395–406.
- Allen RG, Tasumi M, Trezza R (2007b) Satellite-based energy balance for mapping evapotranspiration with internalized calibration (METRIC)-model. *Irrig Drain Eng* 133(4):380–394.
- Ambast SK, Keshari AK, Gosain AK (2002) Satellite remote sensing to support management of irrigation systems: concepts and approaches. *J Irrig Drain* 51:25–39.
- Bastiaanssen WGM, Bos MG (1999) Irrigation performance indicators based on remotely sensed data: a review of literature. *Irrig Drain Sys* 13:291311.
- Bastiaanssen WGM, Menenti M, Feddes RA, Holtslang AA (1998a) A remote sensing surface energy balance algorithm for land (SEBAL): 1. Formulation. *J Hydrol* 212–213:198–212.

- Bastiaanssen WGM, Pelgrum H, Wang J, Ma Y, Moreno JF, Roerink GJ, van der Wal T (1998b) A remote sensing surface energy balance algorithm for land (SEBAL): 2. Validation. *J Hydrol* 212–213:213–229.
- Bastiaanssen WGM, Noordman EJM, Pelgrum H, Davids G, Thoreson BP, Allen RG (2005) SEBAL model with remotely sensed data to improve water-resources management under actual field conditions. *Irrig Drain Eng* 131(1):85–93.
- Bausch WC (1993) Soil background effects on reflectance-based crop coefficients for corn. *Remote Sens Environ* 46:213–222.
- Bausch WC (1995) Remote sensing of crop coefficients for improving the irrigation scheduling of corn. *Agric Water Manag* 27:55–68.
- Bausch WC, Neale CMU (1987) Crop coefficients derived from reflected canopy radiation: a concept. *Trans ASAE* 30(3):703–709.
- Bausch WC, Neale CMU (1989) Spectral inputs improve corn crop coefficients and irrigation scheduling. *Trans ASAE* 32(6):1901–1908.
- Bos MG (1997) Performance indicators for irrigation and drainage. *Irrig Drain Sys* 11:119–137.
- Brown KW, Rosenberg NJ (1973) A resistance model to predict evapotranspiration and its application to a sugar beet field. *Agron J* 65:341–347.
- Brutsaert W, Sugita M (1992) Application of self-preservation in the diurnal evolution of the surface energy budget to determine daily evaporation. *J Geophys Res* 97:18377–18382.
- Choudhury BJ, Ahmed NU, Idso SB, Reginato RJ, Daughtry CST (1994) Relations between evaporation coefficients and vegetation indices studied by model simulations. *Remote Sens Environ* 50:1–17.
- Chavez JL, Neale CMU, Prueger JH, Kustas WP (2008) Daily evapotranspiration estimates from extrapolating instantaneous airborne remote sensing ET values. *Irrig Sci* 27:67–81.
- Colaizzi PD, Evett SR, Howell TA, Tolk JA (2006) Comparison of five models to scale daily evapotranspiration from one-time-of-day measurements. *Trans ASABE* 49(5):1409–1417.
- Crago RD (2000) Conservation and variability of the evaporative fraction during the daytime. *J Hydrol* 180(1–4):173–194.

- Devitt DA, Sala A, Mace KA, Smith SD (1997) The effect of applied water on the water use of saltcedar in a desert riparian environment. *J Hydrol* 192:233–246.
- Duchemin B, Hadria R, Erraki S, Boulet G, Maisongrande P, Chehbouni A, Escadafal R, Ezzahar J, Hoedjes JCB, Kharrou MH, Khabba S, Mougenot B, Olioso A, Rodriguez JC, Simonneaux V (2006) Monitoring wheat phenology and irrigation in Central Morocco: on the use of relationships between evapotranspiration, crops coefficients, leaf area index and remotely-sensed vegetation indices. *Agric Water Manag* 79:1–27.
- Gowda PH, Chavez JL, Colaizzi PD, Evett SR, Howell TA, Tolk JA (2008) ET mapping for agricultural water management: present status and challenges. *Irrig Sci* 26:223–237.
- Hunsaker DJ, Barnes EM, Clarke TR, Fitzgerald GJ, Pinter Jr. PJ (2005a) Cotton irrigation scheduling using remotely sensed and FAO-56 basal crop coefficients. *Trans ASAE* 48 (4):1395–1407.
- Hunsaker DJ, Pinter Jr. PJ, Kimball BA (2005b) Wheat basal crop coefficients determined by normalized difference vegetation index. *Irrig Sci* 24:1–14.
- Hunsaker DJ, Fitzgerald GJ, French AN, Clarke TR, Ottman MJ, Pinter Jr. PJ (2007) Wheat irrigation management using multispectral crop coefficients: I. Crop evapotranspiration prediction. *Trans ASABE* 50(6):2017–2033.
- Hutson SS, Barber NL, Kenny JF, Linsey KS, Lumia DS, Maupin MA (2004) Estimated use of water in the United States in 2000. U.S. Geological Survey Circular 1268, Reston, VA.
- Jayanthi H, Neale CMU, Wright JL (2007) Development and validation of canopy reflectance-based crop coefficient for potato. *Agric Water Manag* 88:235–246.
- Jensen M (2003) Vegetative and open water coefficients for the lower colorado river accounting system (LCRAS) addendum to the 1998 report. (Available from the Bureau of Reclamation Boulder Canyon Operations Office in Boulder City, Nevada).
- Jensen M (2007) Beyond irrigation efficiency. *Irrig Sci* 25:233–245.
- Koksal ES (2008) Evaluation of spectral vegetation indices as an indicator of crop coefficient and evapotranspiration under full and deficit irrigation conditions. *Intern Remote Sens* 29(23):7029–7043.
- Murray RS, Nagler PL, Morino K, Glenn EP (2009) An empirical algorithm for estimating agricultural and riparian evapotranspiration using MODIS enhanced vegetation index and ground measurements of ET. II. Application to the Lower Colorado River, U.S. *Remote Sens* 1:1125–1138.

- Neale CMU, Bausch WC, Heermann DF (1989) Development of reflectance-based crop coefficients for corn. *Trans ASAE* 32(6): 1891 – 1899.
- Norman JM, Kustas WP, Humes KS (1995) A two-source approach for estimating soil and vegetation energy fluxes from observations of directional radiometric surface temperature. *Agric For Meteorol* 77:263–293.
- Perry C (2007) Efficient irrigation; inefficient communication; flawed recommendations. *Irrig Drain* 56:367–378.
- Ramos JG, Cratchley CR, Kay JA, Casterad MA, Martinez-Cob A, Dominguez R (2009) Evaluation of satellite evapotranspiration estimates using ground-meteorological data available for the Flumen District into the Ebro Valley of N.E. Spain. *Agric Water Manag* 96:638–652.
- Ray SS, Dadhwal VK (2001) Estimation of crop evapotranspiration of irrigation command area using remote sensing and GIS. *Agric Water Manage* 49:239–249.
- Romero MG (2004) Daily Evapotranspiration estimation by means of evaporative fraction and reference evapotranspiration fraction. Dissertation, Utah State University, Logan, UT.
- Shuhua Q, Changyao W, Zheng N, Chunyan Y, (2003) Retrieving the crop coefficient spatial distribution for cotton under different growth status with Landsat ETM+ image. *Geosciences and Remote Sensing Symposium Proceedings, IEEE International* 4:2212–2214.
- Singh R, Irmak A (2008) A modified approach for estimation of crop coefficients using satellite remote sensing data. Presented at the 2008 ASABE Annual International Meeting, Providence, Rhode Island, June 2008. Paper Number: 083542.
- Stehman SV, Milliken JA (2007) Estimating the effect of crop classification error on evapotranspiration derived from remote sensing in the lower Colorado River basin, USA. *Remote Sens Environ* 106:217–227.
- Stone LR, Horton ML (1974) Estimating evapotranspiration using canopy temperatures: field evaluation. *Agron J* 66(3):450–454.
- Trezza R (2002) Evapotranspiration using a satellite-based surface energy balance with standardized ground control. Dissertation, Utah State University, Logan, UT.
- Vandersande MW, Glenn EP, Walworth JL (2001) Tolerance of five riparian plants from the lower Colorado River to salinity drought and inundation. *J Arid Environ* 49:147–159.

Zavaleta E (2000) The economic value of controlling an invasive shrub. *AMBIO* 29(8):462–467.

Zhang L, Lemeur R (1995) Evaluation of daily ET estimates from instantaneous measurements. *Agric For Meteorol* 74:139–154.

CHAPTER 2  
REMOTE SENSING AND GIS TECHNIQUES FOR MANAGING  
IRRIGATION SCHEMES: A CASE STUDY  
IN SOUTHERN CALIFORNIA

**Abstract**

This paper presents the potential of remotely-sensed data in managing irrigation schemes, as well as in addressing spatially distributed irrigation equity, adequacy, and sustainability. The “Surface Energy Balance Algorithm for Land (SEBAL)” was implemented over an irrigation district along the Lower Colorado River in southern California. Satellite and ground-based data were combined in an ArcGIS environment to estimate daily components of water balance. On an annual basis, the water balance closure error was less than 1%. Out of 2,266 mm of applied water (diverted water minus canal spills, plus precipitation), 1,286 mm was used in evapotranspiration processes. This amount of agricultural consumptive use was about 52% of the total diverted water, and 7% of the annual flow in the Colorado River above the diversion dam. Evaluating several irrigation and drainage performance indicators revealed that, overall, irrigation practice was adequate and highly uniform. The extensive network of deep open drains was also found to be functioning at an optimal level. In addition, the application of two commonly used methods in estimating spatially-distributed potential evapotranspiration under advective conditions was studied and suggestions were made to avoid the error introduced by ignoring the effect of horizontally-transported energy on enhancing/suppressing water consumption.



## Introduction

Historically, the western US has been known for its arid climate, low precipitation, and long droughts, which have made water management a very complex issue in this part of the world. Water governance in the western US must be performed in such a way as to not only provide for increasing human and agricultural demands, but also to protect ecosystems and critical habitat for flora and fauna. In addition, new concerns on the possible consequences of climate change have added to the complexity of this already challenging task.

Accounting for about 65% of total water withdrawals, irrigation has been the largest use of fresh water in the United States since 1950. Not surprisingly, the majority of agricultural withdrawals (86%) and irrigated area (75%) were in the seventeen contiguous western states (Hutson et al. 2004). Therefore, it is of great importance to accurately determine how much water needs to be diverted for irrigation and how it is partitioned into different consumptive and non-consumptive uses. Quantifying water balance components at irrigation scheme scales has a wide variety of applications, including but not limited to: initiating and evaluating water conservation practices, improving irrigation scheduling (Santos et al. 2008), developing irrigation modernization scenarios (Isidoro et al. 2004), assessing biophysical and economical water productivities (Teixeira et al. 2008), and managing soil salinization (Faci et al. 1985; Khan et al. 2006; Marlet et al. 2009).

In irrigated agriculture, the most significant water balance components are crop transpiration and soil evaporation. These two processes are usually treated as the

combined process of evapotranspiration (ET), not only due to the fact that separating them is difficult in practice, but also because both have the same effect in transforming the state of water from liquid into gas, which makes it unrecoverable, at least within the area in which it was lost. Although accurate point measurements of ET have been extensively used in managing agricultural water resources, recently developed remote sensing techniques also have acceptable levels of accuracies (above 94% on seasonal scales: Gowda et al. 2008). In addition, these techniques provide spatially-distributed data that enables researchers to enhance the scale of their analysis from the entire irrigation scheme to a pixel that could be only a few square meters in size. Another advantage of air- or space-borne remote sensing data is their objectiveness; an important characteristic that can revolutionize developing and standardizing benchmarks for comparing irrigation schemes from around the world.

When combined with water balance information, remotely-sensed ET can also be utilized in evaluating the performance of irrigation and drainage systems. Irrigation performance is traditionally evaluated based on point measurements. A major caveat of this approach is that the results can only provide one average value representing the entire study area. Considering that water application and management are highly variable from field to field, the results of traditional methods are less useful as the scale of the study increases from field to district and basin. Recent developments in remote sensing and GIS techniques have made it possible to assess scheme-wide performance on a pixel-by-pixel basis (Bastiaanssen and Bos 1999).

Although remote sensing techniques have been successfully applied in improving irrigation management, there is still a gap between research projects and practical

application of these techniques in real world (Ambast et al. 2002). Bastiaanssen and Bos (1999) and Bastiaanssen et al. (2000) stated that more demonstration projects are needed to increase the level of awareness among water managers about the potential of air- and space-borne imagery. The study presented herein was carried out over an irrigation district in semi-arid southern California in order to map evapotranspiration of agricultural crops, as well as several new and existing irrigation and drainage performance indicators. To achieve this objective, the results of a satellite-based energy balance model were integrated in an ArcGIS environment with ground measurements of agro-hydrological parameters to identify water balance components for the entire irrigation scheme over different temporal scales.

## **Methods and materials**

### **Study area**

Palo Verde Irrigation District (PVID) is located in Imperial and Riverside counties, California, on the west bank of the Colorado River. With about 500 km<sup>2</sup> of territory, PVID was privately developed in 1925 to serve local water users. Colorado River water is diverted into the PVID main canal at Palo Verde diversion dam on the Northeast side of the district. The most common irrigation method is gravity-fed surface irrigation (laser-graded borders and furrows), supported by an extensive network of 400 km of irrigation canals and 230 km of open drains. The alluvial soils in the PVID were deposited over the years by Colorado River floods. The medium texture of PVID soils allows them to hold a considerable amount of water, and to be easily drained. The main

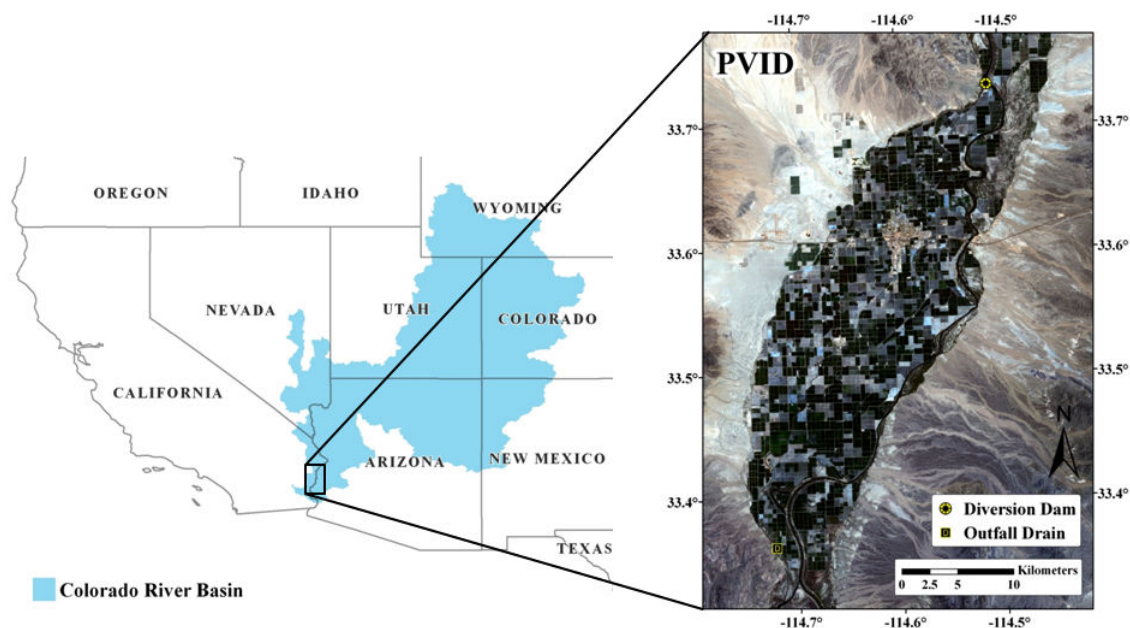


**Fig. 2.1** Palo Verde Irrigation District (PVID) in southern California, within the Colorado River basin

crops are alfalfa, cotton, small grains, and winter vegetables, with a year-round growing season facilitated by the favorable climate of southern California (warm summers and mild winters). Figure 2.1 shows the location of the study area.

#### Water balance components

Water balance analysis over irrigated areas can be summarized by the following equation:

$$I + P + WT = ET + DP + RO + \Delta S \quad (2.1)$$

where  $I$  is applied irrigation water,  $P$  is precipitation,  $WT$  is water table contribution (e.g. sub-surface irrigation),  $ET$  is evapotranspiration,  $DP$  is deep percolation,  $RO$  is surface runoff, and  $\Delta S$  is the change in soil water content over the study period. The  $RO$  and  $\Delta S$

terms may be positive, negative, or zero. Due to the great extent of heterogeneity in agroecosystems, accurate estimation of scheme-wide  $\Delta S$  is usually very difficult. One solution is to select a study period over which the net change in soil moisture is negligible. Therefore, the first step in this study was to define an appropriate time-frame based on groundwater fluctuations. Groundwater data were obtained once a month from more than 260 piezometers, scattered over the whole PVID area on approximately one-mile by one-mile grids.

### *Precipitation*

PVID benefits from a network of 32 rain gages installed on major hydraulic structures of irrigation canals (about 7 rain gages per every 100 km<sup>2</sup> of PVID's cultivated land). These point measurements were imported into an ArcGIS environment and maps of precipitation depth were generated using simple interpolation methods.

### *Water inflow/outflow*

Colorado River water is diverted into PVID's main canal using a small diversion dam. Since the valley is relatively flat and the fields are mostly blocked-end furrows and borders, the surface runoff is not significant, and any possible runoff is directed toward the drains. Therefore, water outflow from PVID consists of only two components, namely drainage and canal spills. The high density of deep open drains (about 0.5 km<sup>-1</sup>) along with the medium texture of PVID's alluvial soils significantly enhances the movement of water from the root zone toward the drains. All of the drains merge and discharge into a main outfall drain at the downstream end of PVID. The United States Geological Survey (hereafter USGS) measures the flow rates of water diversion, drain

discharge, and all canal spills on a daily basis and reports them on-line. These data were downloaded from USGS web portal at: <http://az.water.usgs.gov/pubs/yuma.htm>

### *Evapotranspiration*

The “Surface Energy Balance Algorithm for Land (SEBAL)” was implemented in this study to estimate spatially distributed evapotranspiration (Bastiaanssen et al. 1998a). Having been applied in more than thirty countries, SEBAL estimates of ET have been validated against ground measurements (Bastiaanssen et al. 1998b; Ramos et al. 2009), showing a high accuracy at field and catchment scales (Bastiaanssen et al. 2005). In SEBAL, net radiation ( $R_n$ ) is estimated through quantifying all of the incoming and outgoing short- and long-wave radiation components. Once  $R_n$  is determined, soil heat flux ( $G$ ) is modeled as a ratio of net radiation and a function of surface temperature and fraction of vegetation cover.

SEBAL utilizes an innovative approach for modeling sensible heat flux ( $H$ ). This approach is based on the assumption that over a well-watered vegetation at full cover, the transfer of water between land and atmosphere is solely controlled by atmospheric demand. In other words, since there is no shortage of water, most of the available energy is used in evaporating water, leaving a negligible amount of energy to be used in generating a temperature gradient. In contrast, since there is little or no water to evaporate over a dry surface (e.g. a bare agricultural soil), the vapor pressure gradient and latent heat flux would approach zero. Spatially anchoring these two extreme limits makes it possible to interpolate  $H$  over all other surfaces in between, using the remotely sensed surface temperature. After  $R_n$ ,  $H$ , and  $G$  are identified, latent heat flux ( $LE$ ) can

be calculated as the residual of the energy balance equation, assuming that the energy consumed in photosynthesis and the canopy storage of energy are both insignificant (equation 2.2).

$$LE = R_n - G - H \quad (2.2)$$

Space or airborne imagery – as input data to models such as SEBAL – provide only a snapshot of LE at the time of overpass. As a result, remote sensing techniques offer only an instantaneous estimate of ET that needs to be scaled up to longer periods (daily and seasonal) for most practical purposes. In the earlier versions of SEBAL, instantaneous ET was extrapolated to daily values using the Evaporative Fraction (EF or  $\Lambda$ ). This concept is based on the assumption that the ratio of instantaneous ET to instantaneous available energy ( $R_n - G$ ) is constant during the day (Brutsaert and Sugita 1992; Crago 2000), especially under cloud-free conditions (Zhang and Lemeur 1995). Once this ratio is determined, daily ET could be calculated by multiplying the EF ratio and the daily value of available energy. Although the EF technique has provided reliable results in many studies (Gowda et al. 2008), its accuracy decreases in arid regions due to the occurrence of afternoon advection. Trezza (2002) modified the EF ratio by replacing available energy with alfalfa reference evapotranspiration ( $ET_r$ ), which encompasses the effect of any energy imported from dry neighboring areas. Up-scaled daily ET estimates using this new method (ET<sub>r</sub>F method) have shown to be significantly improved (Romero 2004; Allen et al. 2007 a, 2007b). Alternatively, grass-based reference ET ( $ET_o$ ) could also be used in extrapolating instantaneous ET values (ET<sub>o</sub>F method). Colaizzi et al. (2006) compared estimates of five different up-scaling techniques with measurements of precision weighing lysimeters at Bushland, Texas, where strong advection of heat is

common. For cropped surfaces, the EToF method worked better than ETrF and EF methods. Chavez et al. (2008) also indicated that under advective condition, the performance of EToF is better than ETrF and EF approaches.

Since PVID is surrounded by dry desert regions, EToF was selected as the up-scaling method in this study. Daily  $ET_o$  estimates and other weather parameters required in running SEBAL were downloaded from the website of the California Irrigation Management Information System (CIMIS), for a weather station located in the middle of PVID (CIMIS # 135). The input satellite data to the SEBAL model consisted of all cloud-free Landsat TM5 imagery acquire between January 2008 and January 2009. PVID is located on the overlap zone of two Landsat paths (38 and 39; row 37). This enabled the authors to acquire 6 extra scenes from path 39 in addition to 15 scenes from path 38 (total of 21 scenes). All the images were obtained from the website of the USGS Global Visualization Viewer (GLOVIS), <http://glovis.usgs.gov/>. GLOVIS provides Landsat scenes that are processed using the LPGS processing system, which results in 60-m resolution for the thermal band and 30-m resolution for other bands.

#### Irrigation and drainage performance

Several performance indicators (PI) were studied at different spatio-temporal resolutions. These PIs can be arranged in three groups based on the aspect of the system that they address:

1. equity: Water Consumption Uniformity (WCU),
2. adequacy: Relative ET (RET) and Depleted Fraction (DF), and;



3. sustainability: Drainage Ratio (DR), Drainage Distribution Uniformity (DDU), Relative Groundwater Depth (RGD).

#### *Water consumption uniformity (WCU)*

A great advantage of estimating spatially distributed ET is that such information can be used as a simple performance indicator by itself. For example, the variability of ET within and among agricultural fields is a measure of irrigation equity (Bastiaanssen and Bos 1999). ET variability is estimated as the Coefficient of Variation at two levels, namely within an irrigation unit ( $CV_w$ ) and among irrigation units ( $CV_s$ ). In order to extract required statistical parameters for each field in PVID, a crop classification layer was used in ArcGIS as a mask layer. Developed from Landsat TM5 imagery by the US Bureau of Reclamation (USBR), this classification layer defines field boundaries and provides information on the cropping pattern in 2008. However, since the thermal band of Landsat TM5 has a coarser resolution than the other six bands, an inner buffer zone of 60 m was defined for each field boundary to avoid any edge effects. The mean and standard deviation of ET were obtained for every field that had a remaining area larger than 4 ha after applying the buffer. This reduced the number of studied fields from a total of over 2,000 to 1,485 fields.

#### *Relative evapotranspiration (RET)*

Relative evapotranspiration is defined as the ratio of actual ET ( $ET_a$ ) to potential ET ( $ET_p$ ). This indicator is used as a measure of irrigation adequacy to investigate any water shortage and its severity. But before evaluating RET over irrigated areas, an exact definition of  $ET_p$  should be provided, along with an accurate method for estimating this

parameter. As the name implies,  $ET_p$  is the level of water consumption that a specific crop could potentially reach. It is similar to reference ET ( $ET_o$ ) in that both of them are estimated for stress-less conditions, when no environmental factor (e.g. water shortage, disease, etc.) is limiting the ability of the crop to consume water. However, the difference between  $ET_p$  and  $ET_o$  is in accounting for the actual growth stage of the crop. While  $ET_o$  is estimated over a reference surface (grass or alfalfa) that is maintained at a certain height,  $ET_p$  is a crop-specific parameter that could vary between zero (right after sowing) to a value equal to or sometimes higher than  $ET_o$  (Droogers and Bastiaanssen 2002). From a crop coefficient perspective,  $ET_p$  can be estimated by multiplying  $ET_o$  and a locally-developed crop coefficient ( $K_c$ ), setting the stress coefficient ( $K_s$ ) to unity.

To the best of our knowledge, two distributed  $ET_p$  estimation methods have been used in evaluating RET over large and heterogeneous irrigation schemes: available energy ( $R_n - G$ ) method, implemented by Roerink et al. (1997) and Bastiaanssen et al. (1996); and the Priestley-Taylor approach (Priestley and Taylor 1972), utilized by Bastiaanssen et al. (2001), Bandara (2003), and Karatas et al. (2009). A major concern in applying these methods is that, in both of them, only radiative energy is considered and advection of heat is neglected (Glenn et al. 2007). However, irrigated areas located in arid/semi-arid regions of the world frequently experience an oasis effect. If water is available, the effect of advection on enhancing ET in these regions is large enough that neglecting it would result in significant underestimation of  $ET_p$ . Another important factor that deserves extra attention is the fact that available energy (from either radiation or horizontal transport) would be converted to latent heat flux only if crops are present to transpire or if the soil surface is wet to evaporate. Therefore, the application of these

methods over agricultural fields with exposed dry soil would result in an ET overestimation error. The underestimation error of ignoring advection may partially compensate the overestimation error of including bare soils in analysis, resulting in an average RET value that is “right for the wrong reasons.”

In this study,  $ET_p$  is estimated on a pixel-by-pixel basis using Priestly-Taylor (PT) equation (Priestly and Taylor 1972):

$$LE = \alpha^{\Delta / (\Delta + \gamma)} \times (R_n - G) \quad (2.3)$$

where  $\alpha$  is the Priestley-Taylor parameter,  $\Delta$  is the slope of the water vapor saturation curve,  $\gamma$  is a psychrometric constant, and other terms are defined previously. However, to account for the effect of advection, the above equation was calibrated for the local condition of PVID through a process similar to what is implemented by Diaz-Espejo et al. (2005). In this process the original  $\alpha$  value of 1.26 was modified in a fashion that would force PT equation to estimate ET rates similar to what was estimated over a reference grass surface, using Penman-Monteith equation (Allen et al. 1998). To avoid the effect of exposed soil, all the fields that were not close to full-cover were eliminated from analyzing RET. Based on expert knowledge and spectral characteristics of the fields, a SAVI (Soil Adjusted Vegetation Index, Huete 1988) value of 0.65 was defined as the threshold. All the fields with an average SAVI less than this threshold were excluded from the analysis.

#### *Depleted fraction (DF)*

In essence, DF is a rather new term for an old concept that has been given several names such as irrigation efficiency, water efficiency, water application efficiency, and

consumptive use coefficient. All of these terms provide information on the fraction of water that has been depleted from available resources (Jensen 2007). According to Bos et al. (2005), DF is defined as:

$$DF = ET_a / (P_g + V) \quad (2.4)$$

where  $P_g$  is the gross precipitation over the study area; and,  $V$  is the volume of applied ( $V_a$ ) or diverted ( $V_d$ ) water. For the sake of developing benchmarks and comparing irrigation schemes, it is important to differentiate between applied and diverted water, because operational and maintenance constraints might impose a large variation in the amount of canal spills. Estimated DF would be gross ( $DF_g$ ) or net ( $DF_n$ ), if  $V_d$  or  $V_a$  is used in the above equation, respectively.

#### *Drainage ratio (DR)*

The drainage ratio is another performance indicator that provides information on what portion of applied water has left the study area in the form of drainage. DR is inversely related to  $DF_n$  (Bos et al. 2005):

$$DR = 1 - DF_n \quad (2.5)$$

The leaching fraction (LF) necessary for maintaining a favorable salt balance can be taken as a critical value of DR. If estimated DR is less than required LF, soil salinisation may become problematic in the future. A DR value greater than LF means that applied water can be reduced without affecting the current level of agricultural production. If this is the case, irrigation managers may want to reduce the amount of applied water to preserve its quality, even though it is not lost to the system and will be available somewhere downstream.

### *Drainage distribution uniformity (DDU)*

This indicator that evaluates drainage performance is introduced in this study for the first time. DDU is assessed by evaluating among and within field coefficient of variation ( $CV_s$  and  $CV_w$ ) of the depth to groundwater. A low DDU is only an indication of uniform depth to groundwater and it does not necessarily mean that water is at a depth that allows an adequate root respiration. Therefore, this indicator should be studied along with other drainage performance indicators, such as relative groundwater depth (explained below). In areas where crop water requirement is met by controlling the level of groundwater, DDU could serve as a measure of traditional irrigation distribution uniformity (commonly abbreviated as DU).

### *Relative Groundwater Depth (RGD)*

Bos (1997) proposed RGD as the ratio of Actual Groundwater Depth ( $GWD_a$ ) to Critical Groundwater Depth ( $GWD_c$ ). Although defined over a decade ago, RGD has never been actually estimated over any irrigated area, to the best of our knowledge. Since for most crops, groundwater should be kept at levels below the root zone to avoid any negative effects caused by water-logging and/or soil salinisation, it is assumed that  $GWD_c$  is equal to the effective root depth for every crop group. Table 22 Allen et al. (1998) suggest a range of effective depths for each crop. In this study, the upper limit of this range is selected as the  $GWD_c$ . Selected  $GWD_c$  is assigned to each field in PVID, using the crop classification layer. Then, the minimum  $GWD_a$  is obtained for each field from the interpolated maps of depth to groundwater for the months of February and September, when groundwater is furthest from and closest to the surface, respectively.

RGD estimates based on minimum  $GWD_a$  and maximum  $GWD_c$  represent the portion of the field that has the worst drainage conditions. Values less than unity indicate that the water table is within the crop root zone, a situation that irrigation managers should avoid for most crop types.

## Results and discussion

### Groundwater fluctuations

Figure 2.2 summarizes the groundwater dynamics of PVID, monitored at 260 piezometers on a monthly basis during 2008. In Fig. 2.2a, monthly averaged measurements from all 260 piezometers are presented to provide a general idea of the overall groundwater dynamics and the influence of irrigation on it. PVID groundwater levels reach their highest elevation in September and October, after irrigation has been extensively practiced for several months.

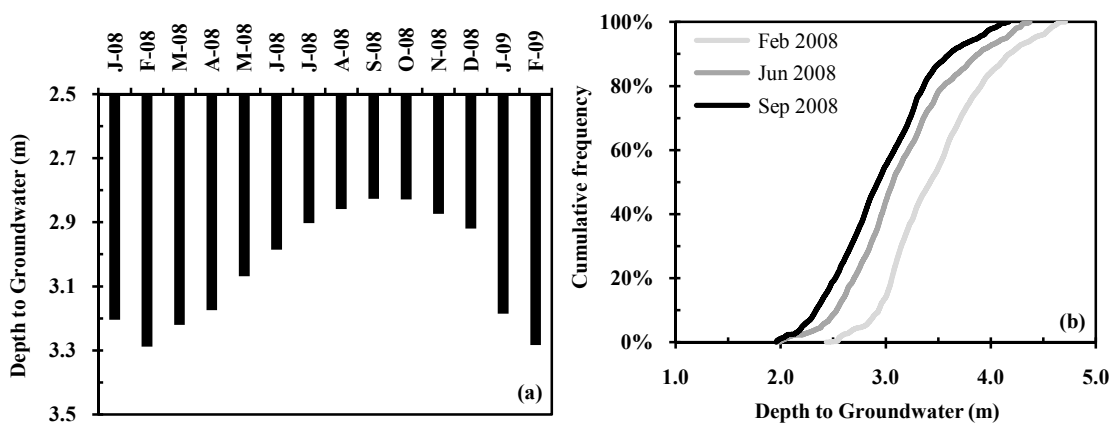


**Fig. 2.2** (a) Monthly average of all piezometer readings and (b) Cumulative frequency distribution of depth to groundwater for three months: February, June, and September 2008

In November, when the irrigation of agricultural fields decreases, groundwater levels began to decline and eventually returned to the same level as a year before. Figure 2.2a clearly shows that the closing water balance for the irrigation season (March to November), rather than for the whole year, would introduce a significant underestimation error in water outflow. Based on this information, the study period was defined from mid-January 2008 to mid-January 2009, when PVID usually discontinues diversions to perform maintenance on the main canal.

Point measurements of piezometers were interpolated in ArcGIS in order to generate depth to groundwater maps. The results were analyzed on a pixel-by-pixel basis and cumulative frequency curves are developed for the three months of February, September, and December 2008 (Fig. 2.2 b). These months are selected to show three different levels of groundwater, namely the lowest, the highest, and an intermediate position. According to Fig. 2.2 b, nowhere in PVID groundwater level raises higher than 2 m below the soil surface, an indication of a successfully functioning drainage system. The idea of using spatially distributed depth to groundwater data for evaluating the performance of drainage network is further investigated in the drainage performance section.

Water balance components

### *Precipitation*

During the study period, a total of 25 precipitation events happened (all in forms of rain). Point measurements of precipitation depth were interpolated in ArcGIS environment to develop precipitation maps. Out of all the rain events, only two had an

average cumulative depth of over 10 mm. The total annual precipitation depth was about 71 mm, underscoring the aridity of this region.

#### *Water inflow/outflow*

According to USGS flow measurements, the volume of the Colorado River water diverted into PVID main canal between January 2008 and January 2009 was 1,088 Mm<sup>3</sup>. This amount of water is equal to 0.9 million ac-ft, or 2,480 mm of water depth over the whole PVID cultivated area (about 440 km<sup>2</sup>). Considering that the diversion to the main canal was shut down for maintenance purposes during the first week of January, the monthly average flow rates ranged between 14.5 and 49.3 (m<sup>3</sup>/s) in January and June, respectively.

With a volume of about 125 Mm<sup>3</sup>, canal operational spills accounted for about 11.5% of the total annual water diversion. Monthly average canal spills measured at discharge structures varied from 2.3 to 4.5 m<sup>3</sup>/s in January and June, respectively. It is very important to take the amount of canal spills into account when evaluating system performance since this water is never applied and therefore returns to the river with (most probably) an unchanged quality. Monthly average flow rates of drainage discharge measured at downstream end of outfall drain ranged between 10.2 m<sup>3</sup>/s in January and 16.2 m<sup>3</sup>/s in July, which shows a lag in comparison with the peak flow rate of diversion. With a volume of about 438 million m<sup>3</sup>, the total annual amount of drainage was 40% of diversion. This portion increases to over 45% if only applied water (diverted minus spills) is considered.



*Evapotranspiration*

The SEBAL model was applied over all cloud-free Landsat TM5 images acquired during the study period. Figure 2.3 presents a SEBAL-derived ET map on July 29<sup>th</sup>, 2008 as an example of one of the 21 processed images.

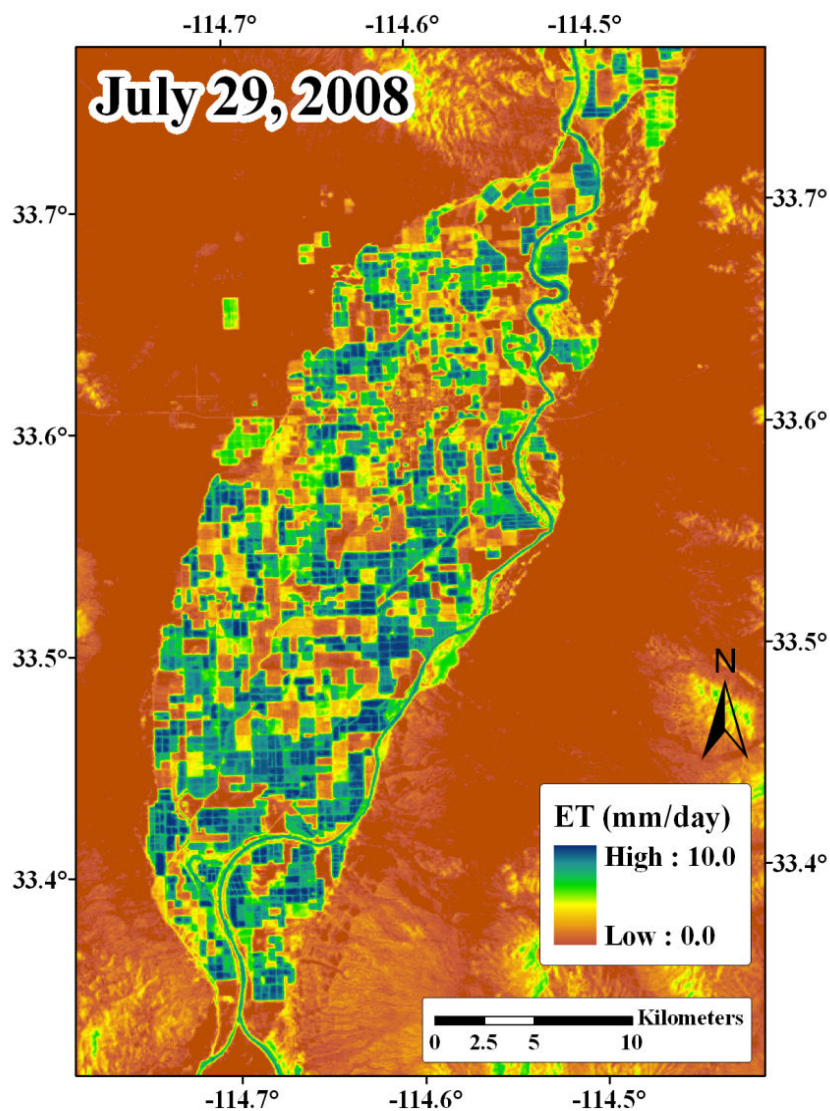


**Fig. 2.3** SEBAL-derived spatially distributed daily ET on July 29<sup>th</sup>, 2008 (DOY: 211)

On this date, 19% of all pixels had a modeled ET rate higher than grass-based  $ET_o$  for the same date (8.4 mm). By using three separate GIS layers, namely crop classification, SAVI, and surface temperature, it was found that these pixels belong to recently-irrigated alfalfa and cotton fields at full cover.

Spatially distributed ET estimates were linearly interpolated for all the dates between satellite overpasses and summed over the study period to obtain the total water consumption of every pixel. On average, the annual  $ET_a$  over 440 km<sup>2</sup> of PVID cultivated land was 1,286 mm. Annual field-level  $ET_a$  ranged from less than 70 mm for fallow fields to more than 2,000 mm for alfalfa fields. Evapotranspiration from the fields under other dominant crops was less than alfalfa and about 905, 1063, and 1320 mm for small grains, Sudan grass, and cotton, respectively. It should be noted that the growing seasons and conditions are different for each crop. For example, Sudan grass is planted in March and harvested in August, a period which usually has no rainfall; while small grains (wheat, barley, oats, and millet) are planted in November and harvested in June of the next year, a period with cooler temperatures and almost all the annual precipitation events.

Crop coefficients ( $K_c$ ) were also determined by dividing SEBAL-derived ET by the grass-based reference ET estimated at a standard weather station in a central location at PVID. The frequency distribution and cumulative frequency of  $K_c$  values over PVID are demonstrated in Fig. 2.4a and b, for the same two satellite overpass dates in 2008 (April 8<sup>th</sup> and July 13<sup>th</sup>).

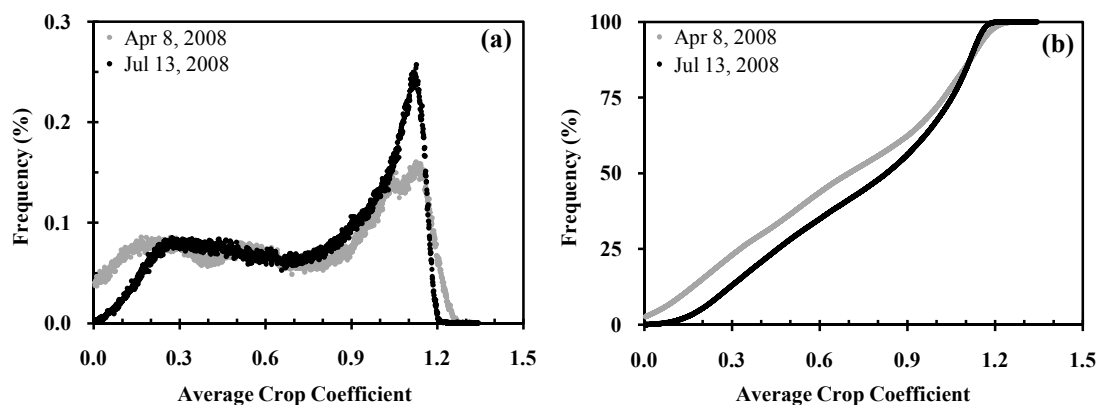


**Fig. 2.4 (a)** Frequency distribution of  $K_c$  on a pixel-by-pixel basis for two dates in 2008: April 8th (DOY: 99) and July 13th (DOY: 195) and **(b)** the cumulative frequency of  $K_c$  for the same dates

As depicted in Fig. 2.4a, the general distributions of  $K_c$  frequencies follow the same pattern. On both dates the most frequent  $K_c$  occurs at values about 1.1, which is the peak  $K_c$  of alfalfa, the most dominant crop in PVID. There is a middle range of  $K_c$ , from 0.25 to 1.0, over which frequencies are stable for enclosed values and on both dates. This range represents small grains and alfalfa and grass fields that are not at full cover. Since alfalfa has a year-round growing season, early-April curve represents a  $K_c$  distribution that is mainly controlled by alfalfa. The divergence from this base curve on July 13<sup>th</sup> can be attributed to cotton, which is the second major crop of PVID. Cotton is planted in mid-March, so its water consumption is still negligible on April 8<sup>th</sup> ( $K_c$  values less than 0.25). By mid-July, however, most of the cotton fields are at full cover, consuming water at the highest rates. As a result, the low- $K_c$  frequencies moved to a range between 1.0 and 1.15. The areas between the two curves over these two intervals ( $K_c$  smaller than 0.25 and between 1.0 and 1.15) are roughly equal, reaffirming that the observed difference between the two dates is a result of the contribution by cotton. On April 8<sup>th</sup>,

slightly higher frequencies for  $K_c$  values higher than 1.17 are from a few large cotton fields that had their first heavy irrigation on that date.

### *Closing water balance*

Daily water balance components estimated in previous steps are used to close water balance for the period from mid-January 2008 to mid-January 2009. Since reporting water balance components in depth units are more common among irrigation engineers, volumes are divided by the total cultivated area of PVID (about 440 km<sup>2</sup>). Figure 2.5 shows the daily magnitude of water inputs and outputs. Several sudden decreases in water diversion coincided with the occurrence of precipitation events.

Annual water inputs consisted of 2,479 mm of surface inflow and 71 mm of precipitation. Water outputs included 284 mm of canal spills, 998 mm of drainage, and 1,286 mm of ET. Based on these data, water balance closure error was only 18 mm, which is less than one percent of the water inputs (Table 2.1).

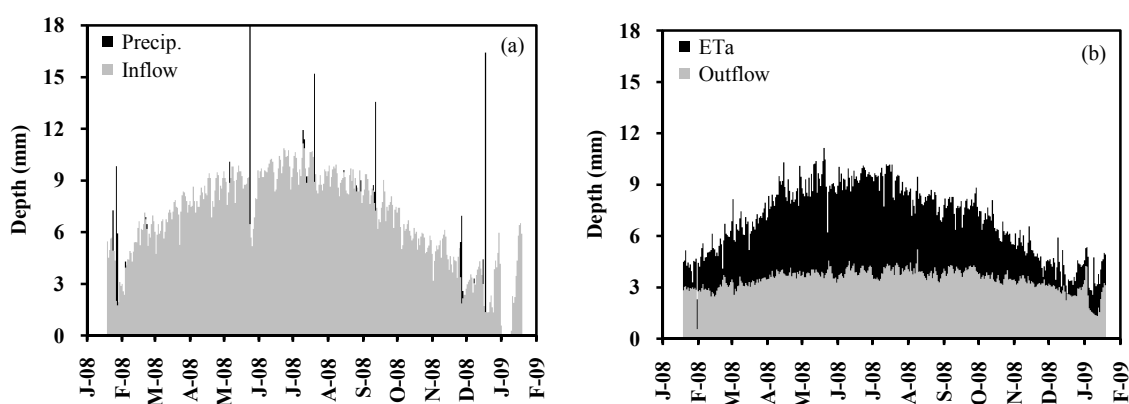


**Fig. 2.5** Stacked bars of daily depths of **(a)** water inputs and **(b)** outputs

**Table 2.1** Total annual amounts of water balance components and associated percentages

	Depth (mm)	Percentage
Precipitation	71	3
Surface inflow	2479	97
$\Sigma$ Inputs	2550	100
Canal Spills	284	11
Drainage	998	39
Evapotranspiration	1286	50
$\Sigma$ Outputs	2568	100
$\Sigma$ Inputs – $\Sigma$ Outputs	-18	-0.7

Over PVID and for the same study period, Murray et al. (2009) used a simple linear equation that relates  $ET_a$  to  $ET_o$  and MODIS-derived Enhanced Vegetation Index (EVI). They estimated annual ET of 1,962 mm, which is more than 50% greater than our result. The authors of this paper have more confidence in the estimate of 1,286 mm, not only because it is supported by an accurate water balance closure, but also because the empirical EVI approach was developed using ground measurements taken over a well-irrigated alfalfa field. As a result, the ET of any crop is assumed to be equal to the ET of alfalfa with a similar EVI. But SEBAL is a physically-based energy balance model that takes advantage of satellite imagery in all bands, including thermal. In addition, the results presented herein are based on high-resolution images of Landsat TM5 which can capture surface heterogeneity much better than low-resolution MODIS imagery.

## Irrigation and drainage performance

### *Water consumption uniformity (WCU)*

Within field variability ( $CV_w$ ) of annual  $ET_a$  ranged from 1 to 80%, with an average and median of 7.0 and 3.4%, respectively. Although variabilities as high as 80% were detected, 85% of the fields had a  $CV_w$  lower than 10%. Using maps of  $CV_w$ , PVID irrigation managers can easily locate the remaining 15% of the fields with  $CV_w$  values higher than 10% and focus their attention only to these flagged fields rather than all the fields. This is a great example of how the distributed nature of remotely sensed data can save a lot of time and energy. The low values of average  $CV_w$  suggest that, overall, water application at the field level is uniform in PVID. A primary reason behind such a high uniformity is that almost all of PVID fields are precisely leveled, using modern laser grade-control systems. Among field variation ( $CV_s$ ) for PVID fields was about 38.2%, but this high value does not translate into poor irrigation equity, since PVID fields are diverse in crop type, growing season, water requirement, etc. Table A.1 in Appendix compares the CV estimates found in this study with reported values in the literature.

Crop-specific ET variability was also studied over cotton and alfalfa fields in PVID. For 22 large cotton fields,  $CV_s$  and  $CV_w$  were 8.5 and 3.2%, respectively. Santos et al. (2008) reported slightly higher variability for 13 cotton fields in Genil–Cabra Irrigation Scheme (GCIS) in southern Spain ( $CV_s = 12\%$  and  $CV_w = 5\%$ ). It is worth mentioning that GCIS fields are under a modern pressurized system with an on-demand delivering regime, while PVID fields are under surface irrigation and a modified-demand water delivery. Evapotranspiration variability for 45 large alfalfa fields in PVID was also

promising, with  $CV_s$  and  $CV_w$  values of 9.4 and 3.1%, respectively. According to Molden and Gates (1990), a  $CV_s$  of less than 10% is considered a good uniformity.

#### *Relative evapotranspiration (RET)*

Priestly-Taylor (PT) equation (Priestly and Taylor 1972) is applied to map potential ET over PVID. Instead of using the traditional PT parameter ( $\alpha$ ) of 1.26,  $\alpha$  is adjusted to include the effect of advective energy on enhancing/suppressing water consumption. New values are estimated by dividing Penman-Monteith  $ET_o$  (Allen et al. 1998) to equilibrium ET ( $\Delta/(\Delta+\gamma) \times (R_n-G)$ ). The analyses were limited to the period from the first of March to the first of October, a time frame that is more representative of a usual agricultural growing season. Figure 2.6 shows adjusted daily  $\alpha$  values for the mentioned period. According to this figure, out of 215 days of analyzed data, only one day had a PT parameter less than the traditional value of 1.26.

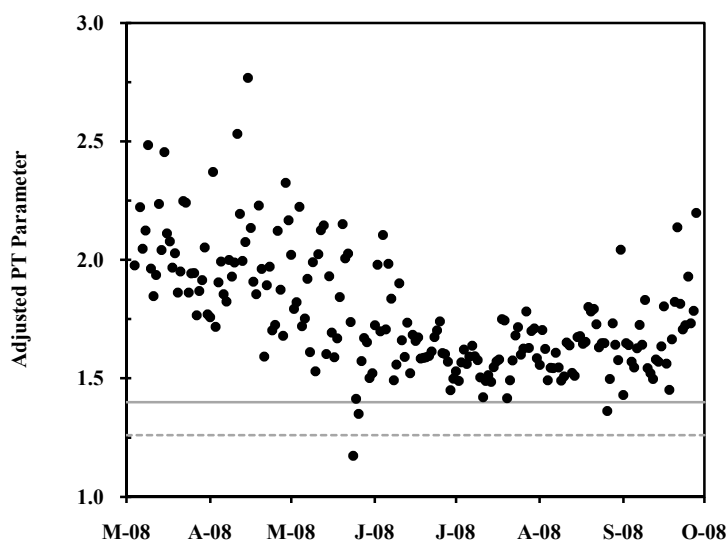


**Fig. 2.6** Adjusted values of daily PT parameter ( $\alpha$ ). Dashed and solid gray lines represent 1.26 and 1.4, respectively

This date (May 24th) is the day on which PVID rain gages recorded an average precipitation depth of 14.4 mm, the most intensive rainfall in this period. Therefore, it is highly probable that moist and cool air from surrounding desert lands was converged over PVID, resulting in water consumption lower than predicted by the available energy.

Several research studies conducted at different locations (e.g. Davis, CA; Campinas, Brazil; China Plains, etc.) have found that  $\alpha$  value greater than 1.4 (Diaz-Espejo et al. 2005; Pereira and Nova 1992) and 1.5 (Li and Yu 2007) indicate the occurrence of enhanced advective conditions. The fact that, except for three days, adjusted  $\alpha$  values were all above 1.4 suggests that advection is a major contributor to water consumption of PVID crops. Thus, utilizing a simple available energy approach or the original PT method for PVID would result in an underestimation of  $ET_p$ , and consequently overestimation of RET (Fig. 2.7).

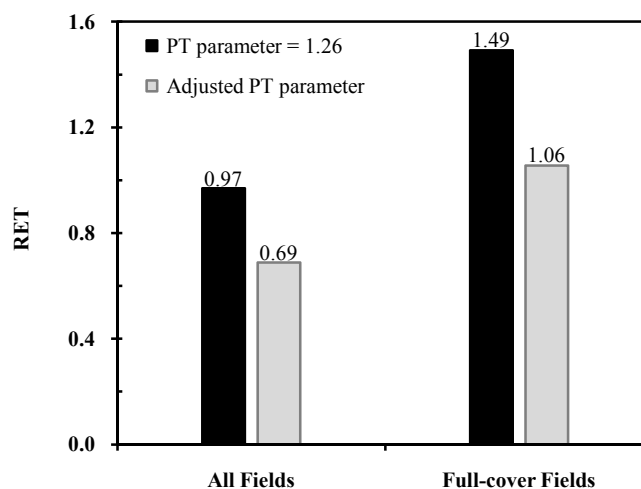


**Fig. 2.7** Average RET over all and full-cover fields of PVID, under hypothetical non-advective and actual advective conditions



Average RET for all PVID fields was 0.97 when an original  $\alpha$  value of 1.26 was used. Adjusting the PT parameter for actual advective condition reduced the average RET to 0.69. However, performing the analysis only over full-cover fields significantly increased RET from 0.69 to 1.06, meaning that full-cover fields of PVID are consuming water at a rate which is 6% higher than their potential rate. This extra 6% is detected because PT parameter was calibrated with grass-based  $ET_o$ , while ET of alfalfa (the most dominant crop in PVID) is usually about 20% higher than grass under the same agro-climatological conditions. Ignoring advection over full-cover fields resulted in  $ET_p$  estimates that were 49% smaller than actual crop ET. Subtracting this 49% from the 6% estimated under actual advective condition results in a value of 43%, which is the average underestimation error of  $ET_p$  introduced by not accounting for the horizontally transported energy. When all fields are considered in analysis,  $ET_p$  underestimation over full-cover fields is compensated by  $ET_p$  overestimation over fallow fields and those with exposed dry soil, resulting in an average RET value of 0.97.

Assuming that  $ET_p$  is simply equal to available radiative energy ( $R_n - G$ ), Roerink et al. (1997) reported average RET values of about 0.6 for several secondary and tertiary irrigation units in Rio Tunuyan irrigation scheme in Argentina. The authors also suggested that RET values of 0.75 and higher are acceptable for irrigated agriculture. Using traditional PT approach, Karatas et al. (2009) estimated an average RET of 0.7 for the period of May until September over irrigated area of the Lower Gediz Basin (LGB) in Turkey, which is similar to PVID in terms of irrigation method (surface) and main crops. It may seem appropriate to compare RET estimates of LGB with RET estimate of PVID before adjusting PT parameter ( $\alpha = 1.26$ ). Such a comparison would give credit to PVID,

with an average RET of 0.97. For LGB, however, the effect of advection on enhancing ET is not known. Although the amount of precipitation during the study period was very similar for both regions (about 30 mm), advective conditions may be different under the Mediterranean climate of LGB. If that is the case, comparing average RET of LGB with average RET of PVID after adjusting  $\alpha$  may be more reasonable (0.7 vs. 0.69). The same logic applies in comparing PVID results with average RET of 0.76 over Nilo Coelho, a pressurized irrigation scheme in Brazil (Bastiaanssen et al. 2001).

#### *Depleted fraction (DF)*

Gross and net DF were estimated on a daily basis and averaged for each month in 2008.  $DF_g$  ranged between 0.33 in December and 0.58 in May, with annual average of 0.49. As expected,  $DF_n$  values were higher from 0.41 in December to 0.64 in May, with annual average of 0.55. Figure 2.8 demonstrates the inter-monthly variation of  $DF_g$  and  $DF_n$  in 2008. For the Nilo Coelho irrigation scheme in Brazil, Bastiaanssen et al. (2001) reported  $DF_n$  values ranging between 0.4 in April and 0.85 in November with annual average of 0.61. For the condition of this irrigation scheme (perennial orchards under pressurized irrigation), DF values beyond the operational range of 0.7 to 1.0 were found to result in at least 10% reduction in the yield. Over the semi-arid Lower Gediz Basin Karatas et al. (2009) estimated  $DF_g$  values higher than 3.0 in May and September. The authors claimed that a depletion which was 300% greater than diverted water was probably provided from the soil moisture stored in the root zone.  $DF_g$  values dropped to as low as 0.28 in July, resulting in an average  $DF_g$  of 0.69 for the whole study period (May to September).

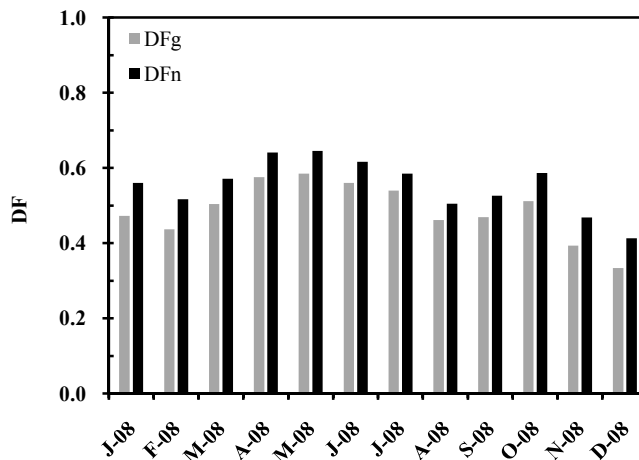


**Fig. 2.8** Average  $DF_g$  and  $DF_n$  for each month in 2008

#### *Drainage ratio (DR)*

Average annual DR over PVID was 0.45, ranging from 0.36 in May to 0.59 in December. Since no soil salinity study has been carried out in PVID, there is no information on leaching requirement to be used as target value for DR. If the PVID leaching requirement is similar to the typical values of irrigated areas in arid/semi-arid regions (about 5 to 10%), the fact that drainage is 45% of applied water may be an indication of over-irrigation in this area. Reducing the amount of applied water may not be in the farmers' interest, but it is important from a riparian management standpoint, especially since elevated levels of salts in irrigation return flow can significantly foster the replacement of native phreatophytes by invasive riparian species (Glenn et al. 1998).

#### *Drainage distribution uniformity (DDU)*

The among field and within field coefficients of variability ( $CV_s$  and  $CV_w$ ) of the depth to groundwater were estimated for large PVID fields for the two months of

February and September, representing the conditions when groundwater is furthest from and closest to the soil surface.  $CV_s$  was 13.4 and 15.5% in February and September, respectively.  $CV_w$  was significantly smaller, with average values of 0.9 and 1.1% for February and September, respectively.

#### *Relative Groundwater Depth (RGD)*

RGD was also estimated for the two months of February and September. In both months there was not a single field in PVID with a RGD value less than unity, meaning that the saturated zone is always kept below the maximum depth that crop roots could reach. However, the distribution of RGD values was different between two months (Fig. 2.9). For example in February only 2.5% of the fields had RGD between 1.0 and 1.5, but this frequency increased to about 27% in September.

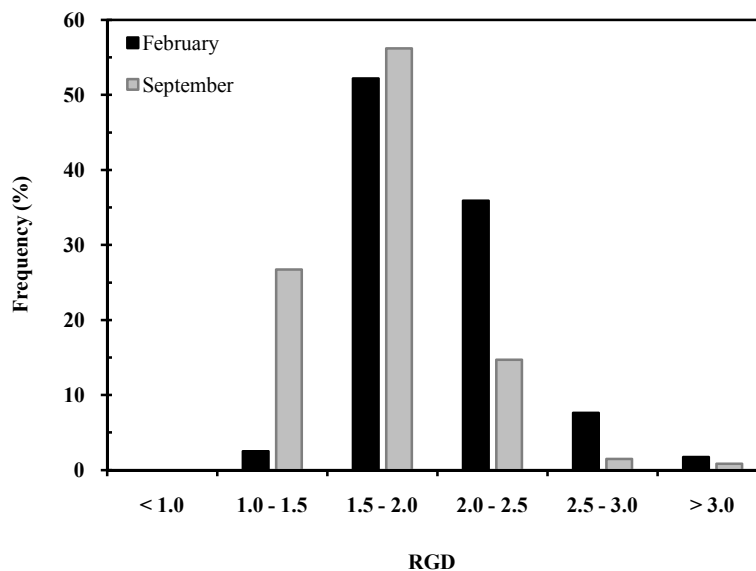


**Fig. 2.9** Frequency distribution of RGD of all PVID fields for February and September

Spatially distributed information on drainage performance generated by GIS techniques can significantly assist irrigation managers to locate the fields that are at higher sustainability risk (Fig. 2.10). Focusing only on these fields would result in a significant saving of money and human resources. In order to examine the effect of drain proximity on RGD, the distance between the centroid of each field and the closest drain was estimated in ArcGIS. But there was no correlation between distance to drain and RGD. This means that even the most distant fields from drains are still close enough to prevent groundwater from entering the root zone.

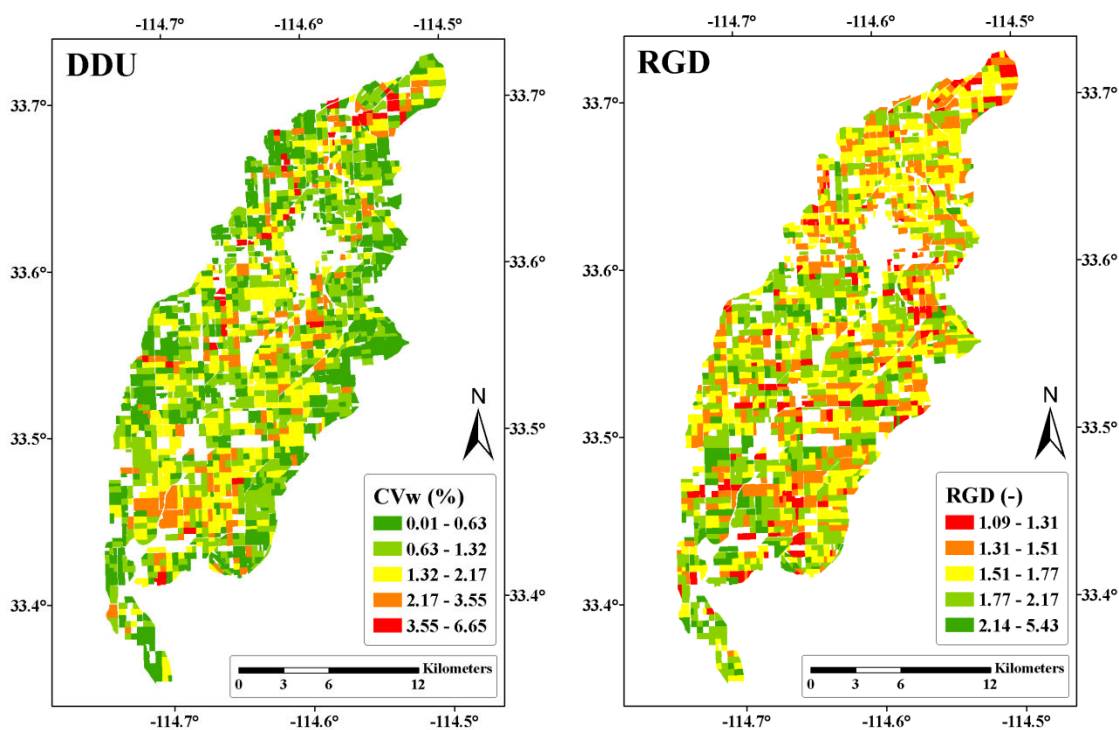


**Fig. 2.10** Field-specific DDU (left) and RGD (right) of larger PVID fields in September 2008

### Summary and conclusions

All available cloud-free Landsat TM5 imagery acquired from January 2008 through January 2009 (21 images) were collected and processed using the “Surface Energy Balance Algorithm for Lands (SEBAL)” to estimate spatially distributed evapotranspiration over Palo Verde Irrigation District in Southern California. The results were then combined with ground measurements of precipitation, water diversion, operational canal spills, and drainage. Monitoring groundwater fluctuations showed that on average groundwater level was at its lowest position in February 2008 (about 3.3 m from the surface). This is after a period of several months with reduced irrigation. The groundwater level rose gradually as the irrigation applications became more intensive until it reached its peak of about 2.9 m from the surface in September and October. As irrigation decreased during the winter months, groundwater dropped to the same level in February of the next year.

The detailed study of groundwater dynamics showed that over irrigation schemes, neglecting the “soil water storage” component of the water balance is only valid if the appropriate study period is selected based on sufficient groundwater measurements. As an example, closing water balance over PVID for the usual agricultural growing season (March to November) would fail to account for a significant amount of water that is still stored in the soil and has not reached the drains. This unaccounted water would introduce error in the analysis, especially if one of water balance components (e.g. ET) is estimated as the residual of water balance closure.

The annual water balance closure error was less than 1%, suggesting that all the water balance components were accurately quantified or estimated. During the study period, precipitation accounted for only 3% of water inputs (71 mm). The rest (2,479 mm) was diverted from the Colorado River, using the Palo Verde diversion dam on the river. Canal operational spills, drainage, and ET were 11, 39, and 50% of total water outputs from the system, respectively. However, decision makers are usually more interested to know what portion of manageable diverted water (excluding precipitation) is consumed. Consumptive use of water by PVID crops in 2008 was about 52% of diverted water and 7% of the Colorado River discharge (7,815 Mm<sup>3</sup>) upstream of the Palo Verde diversion dam.

Several irrigation and drainage performance indicators were also estimated. Field water consumption was very uniform (7% variability on average). Such a high uniformity most probably resulted from a precise grading of PVID fields, using laser leveling equipment. However, 15% of the fields had variability higher than 10%. Using the distributed information of ET variability, PVID irrigation managers can easily locate these fields and focus their attention specifically on them to investigate possible reasons behind the observed low uniformity in those fields.

In this study, the Priestley-Taylor method (Priestley and Taylor 1972) was applied to map potential ET, a parameter that is required in estimating several performance indicators. To account for the advective condition of PVID, the Priestley-Taylor (PT) parameter was adjusted using  $ET_o$ , from the data measured at a standard grass-based weather station. On some days, adjusted values were up to two times greater than the original value of 1.26, meaning that neglecting advective enhancements could result in

significant underestimation of potential ET in arid/semi-arid regions like southern California. However, there is another source of error that is acting in the opposite direction (overestimation of  $ET_p$ ). This error is generated by including  $ET_p$  estimates over fallow fields and fields with soil exposure in analyses. If soil surface is dry, no water consumption would occur, even if energy is provided by either radiation and/or advection. Therefore the analyses were limited to those fields that were at full cover. Using adjusted  $ET_p$  values, SEBAL-derived actual water consumption of full-cover fields was 6% greater than their potential rate estimated by the PT method. This higher rate of water consumption is detected because the PT parameter was calibrated using ET estimates over a full-cover grass patch, while most of PVID fields are under alfalfa, with one of the highest water consumption rates among all agricultural crops. A relative ET of 1.06 indicates that, on average, PVID fields are provided with adequate water.

Three drainage performance indicators were also estimated over PVID to investigate irrigation sustainability. The drainage ratio was 0.45, a value much higher than the typical leaching requirements of irrigation schemes (0.05 to 0.10). This high amount of drained water would prevent any salt accumulation in the crop root zone. Assuming that the leaching requirement in PVID is not greater than 0.15, water application can be reduced by about 30% without negatively affecting agricultural production. Overirrigating always raises concerns about waterlogging problems. However, the depth to the water table was not only uniformly distributed over PVID, but it was also below the maximum range of crop effective root depth at all times. This means that PVID drains are successfully functioning, and water logging is not an issue.



## References

- Ahmad MD, Turrall H, Nazeer A (2009) Diagnosing irrigation performance and water productivity through satellite remote sensing and secondary data in a large irrigation system of Pakistan. *Agric Water Manage* 96:551–564.
- Allen RG, Pereira LS, Raes D, Smith M (1998) Crop evapotranspiration: Guidelines for computing crop requirements. Irrigation and Drainage Paper No. 56, FAO, Rome, Italy.
- Allen RG, Tasumi M, Morse A, Trezza A, Wright JL, Bastiaanssen W, Kramber W, Lorite-Torres I, Robison CW (2007a) Satellite-based energy balance for Mapping Evapotranspiration with Internalized Calibration (METRIC)-Applications. *Irrig Drain Eng* 133(4):395–406.
- Allen RG, Tasumi M, Trezza R (2007b) Satellite-based energy balance for mapping evapotranspiration with internalized calibration (METRIC)-model. *Irrig Drain Eng* 133(4):380–394.
- Ambast SK, Keshari AK, Gosain AK (2002) Satellite remote sensing to support management of irrigation systems: concepts and approaches. *Irrig Drain* 51:25–39.
- Bandara KMPS (2003) Monitoring irrigation performance in Sri Lanka with high-frequency satellite measurements during the dry season. *Agric Water Manage* 58:159–170.
- Bastiaanssen WGM, Van Der Wal T, Visser TNM. (1996) Diagnosis of regional evaporation by remote sensing to support irrigation performance assessment. *Irrig Drain Sys* 10:1–23.
- Bastiaanssen WGM, Menenti M, Feddes RA, Holtslang AA (1998a) A remote sensing surface energy balance algorithm for land (SEBAL): 1. Formulation. *J Hydrol* 212–213:198–212.
- Bastiaanssen WGM, Pelgrum H, Wang J, Ma Y, Moreno JF, Roerink GJ, van der Wal T (1998b) A remote sensing surface energy balance algorithm for land (SEBAL): 2. Validation. *J Hydrol* 212–213:213–229.
- Bastiaanssen WGM, Bos MG (1999) Irrigation performance indicators based on remotely sensed data: a review of literature. *Irrig Drain Sys* 13:291–311.
- Bastiaanssen WGM, Molden DJ, Makin IW. (2000) remote sensing for irrigated agriculture: examples from research and possible applications. *Agric Water Manage* 46:137–155.

- Bastiaanssen WGM, Brito RAL, Bos MG, Souza RA, Cavalcanti EB, Bakker MM (2001) Low cost satellite data for monthly irrigation performance monitoring: benchmarks from Nilo Coelho, Brazil. *Irrig Drain Sys* 15:53–79.
- Bastiaanssen WGM, Noordman EJM, Pelgrum H, Davids G, Thoreson BP, Allen RG (2005) SEBAL model with remotely sensed data to improve water-resources management under actual field conditions. *Irrig Drain Eng* 131(1):85–93.
- Bos MG (1997) Performance indicators for irrigation and drainage. *Irrig Drain Sys* 11:119–137.
- Bos MG, Burton MAS, Molden DJ (2005) *Irrigation and Drainage Performance Assessment: Practical Guidelines*. CABI Publishing, Cambridge, MA, USA. 158 Pp.
- Brutsaert W, Sugita M (1992) Application of self-preservation in the diurnal evolution of the surface energy budget to determine daily evaporation. *J Geophys Res* 97:18377–18382.
- Chavez JL, Neale CMU, Prueger JH, Kustas WP (2008) Daily evapotranspiration estimates from extrapolating instantaneous airborne remote sensing ET values. *Irrig Sci* 27:67–81.
- Colaizzi PD, Evett SR, Howell TA, Tolck JA (2006) Comparison of five models to scale daily evapotranspiration from one-time-of-day measurements. *Trans ASABE* 49(5):1409–1417.
- Crago RD (2000) Conservation and variability of the evaporative fraction during the daytime. *J Hydrol* 180(1–4):173–194.
- Diaz-Espejo A, Verhoef A, Knight R (2005) Illustration of micro-scale advection using grid-pattern mini-lysimeters. *Agric For Meteorol* 129:39–52.
- Droogers P, Bastiaanssen WGM (2002) Irrigation Performance using Hydrological and Remote Sensing Modeling. *Irrig Drain Eng* 128(1):11–18.
- Faci J, Aragues R, Alberto F, Quilez D, Machin J, Arrue JL (1985) Water and salt balance in an irrigated area of the Ebro River Basin (Spain). *Irrig Sci* 6:29–37.
- Glenn EP, Tanner R, Mendez S, Kehret T, Moore D, Garcia J, Valdes C (1998) Growth rates, salt tolerance and water use characteristics of native and invasive riparian plants from the delta of the Colorado River, Mexico. *J Arid Environ* 40:281–294.

- Glenn EP, Huete AR, Nagler PL, Hirschboeck KK, Brown P. (2007) Integrating remote sensing and ground methods to estimate evapotranspiration. *Critic Rev Plant Sci* 26(3):139–168.
- Gowda PH, Chavez JL, Colaizzi PD, Evett SR, Howell TA, Tolk JA (2008) ET mapping for agricultural water management: present status and challenges. *Irrig Sci* 26:223–237.
- Huete AR (1988) A soil-adjusted vegetation index (SAVI). *Remote Sens Environ* 25:295–309.
- Hutson SS, Barber NL, Kenny JF, Linsey KS, Lumia DS, Maupin MA (2004) Estimated use of water in the United States in 2000. U.S. Geological Survey Circular 1268, Reston, VA.
- Isidoro D, Quilez D, Aragues R. 2004. Water balance and irrigation performance analysis: La Violada irrigation district (Spain) as a case study. *Agric Water Manage* 64(2):123–142.
- Jensen M (2007) Beyond irrigation efficiency. *Irrig Sci* 25:233–245.
- Karatas BS, Akkuzu E, Unal HB, Asik S, Avci M (2009) Using satellite remote sensing to assess irrigation performance in water user associations in the Lower Gediz Basin, Turkey. *Agric Water Manage* 96:982–990.
- Khan S, Tariq R, Yuanlai C, Blackwell J (2006) Can irrigation be sustainable? *Agric Water Manage* 80(1–3):87–99.
- Li L, Yu Q (2007) Quantifying the effects of advection on canopy energy budgets and water use efficiency in an irrigated wheat field in the North China Plain. *Agric Water Manage* 89(1–2):116–122.
- Marlet S, Bouksila F, Bahri A. 2009. Water and salt balance at irrigation scheme scale: a comprehensive approach for salinity assessment in a Saharan oasis. *Agric Water Manage* 96 (9):1311–1322.
- Molden DJ, Gates TK. (1990) Performance measures for evaluation of irrigation-water-delivery systems. *Irrig Drain Eng* 116(6):804–823.
- Murray RS, Nagler PL, Morino K, Glenn EP (2009) An empirical algorithm for estimating agricultural and riparian evapotranspiration using MODIS enhanced vegetation index and ground measurements of ET. II. Application to the Lower Colorado River, U.S. *Remote Sens* 1:1125–1138.

- Pereira AR, Nova NAV. (1992) Analysis of the Priestley–Taylor parameter. *Agric For Meteorol* 61:1–9.
- Priestley CHB, Taylor RJ (1972) On the assessment of surface heat flux and evaporation using large-scale parameters. *Month Weather Rev* 100: 81–92.
- Ramos JG, Cratchley CR, Kay JA, Casterad MA, Martinez-Cob A, Dominguez R (2009) Evaluation of satellite evapotranspiration estimates using ground-meteorological data available for the Flumen District into the Ebro Valley of N.E. Spain. *Agric Water Manage* 96:638–652.
- Roerink GJ, Bastiaanssen WGM, Chambouleyron J, Menenti M (1997) Relating crop water consumption to irrigation water supply by remote sensing. *Water Resour Manage* 11(6):445–465.
- Romero MG (2004) Daily Evapotranspiration estimation by means of evaporative fraction and reference evapotranspiration fraction. Dissertation, Utah State University, Logan, UT.
- Santos C, Lorite IJ, Tasumi M, Allen RG, Fereres E (2008) Integrating satellite-based evapotranspiration with simulation models for irrigation management at the scheme level. *Irrig Sci* 26:277–288.
- Teixeira AH de C, Bastiaanssen WGM, Moura MSB, Soares JM, Ahmad MD, Bos MG. 2008. Energy and water balance measurements for water productivity analysis in irrigated mango trees, Northeast Brazil. *Agric For Meteorol* 148(10):1524–1537.
- Trezza R (2002) Evapotranspiration using a satellite-based surface energy balance with standardized ground control. Dissertation, Utah State University, Logan, UT.
- Zhang L, Lemeur R (1995) Evaluation of daily ET estimates from instantaneous measurements. *Agric For Meteorol* 74:139–154.
- Zwart SJ, Leclert LMC (2010) A remote sensing-based irrigation performance assessment: a case study of the Office du Niger in Mali. *Irrig Sci* 28:371–385.

CHAPTER 3  
REMOTE SENSING OF CROP COEFFICIENTS AND WATER  
REQUIREMENTS OF IRRIGATED COTTON

**Abstract**

The crop coefficient of cotton (*Gossypium* spp.) was estimated using a remotely-sensed energy balance model and a reflectance-based crop coefficient method. The results were compared with tabulated crop coefficients presented in the FAO-56 paper, as well as the values that are developed by the U.S. Bureau of Reclamation to be used in the “Lower Colorado River Accounting System.” Remote sensing methods detected a longer growing season in comparison with tabulated values. In addition, a heavy pre-planting irrigation event was correctly detected by the implemented energy balance model. In order to modify tabulated crop coefficient values that are currently used in the management of water deliveries on the Lower Colorado River, remotely-sensed estimates were averaged over the traditional four stages of crop growth. Piece-wise crop coefficients from all four sources were analyzed to estimate daily and seasonal water consumption of cotton during the 2008. Total seasonal water use of cotton was largest using the energy balance model at 1,364 mm, which was 78% of the total reference ET during the same period. Since the application of energy balance models is complicated and time-consuming, a simple linear model that can be easily used in irrigation scheduling was developed to approximate cotton basal crop coefficient from the satellite estimates of Soil Adjusted Vegetation Index (SAVI).

## Introduction

As one of the major crops in the western US, accurately identifying the water consumption of cotton (*Gossypium* spp.) can significantly assist decision makers with managing the limited water resources in this semi-arid region. Although traditional point measurements can be very accurate, they provide only one value, which has limited application over large irrigation schemes with considerable variations in agro-hydrological conditions. Remote sensing techniques have proved to be reliable in estimating spatially-distributed evapotranspiration (ET) at different temporal and spatial scales (Gowda et al. 2008). These methods can fall into two main categories, namely the reflectance-based crop coefficient approach and the surface energy balance modelling.

In the first approach, a regression function is developed relating the crop coefficients of bare soil and effective cover to remotely-sensed vegetation indices (VI's) at the same point in time. The resulting spatially-distributed crop coefficients can then be multiplied by the reference ET to generate maps of actual crop ET. Depending on the methods used for estimating regression parameters, developed functions may approximate either the single ( $K_c$ ) or the basal ( $K_{cb}$ ) crop coefficient. The difference between these two coefficients is that the  $K_c$  includes evaporation from soil surface, while the  $K_{cb}$  represents mostly plant transpiration, a dry soil surface, and well-water conditions in the root zone. As a result, VI- $K_{cb}$  relations are more robust when they are transferred to other areas, as irrigation method, frequency, and application depth are highly variable among irrigation schemes. For example, soil evaporation under a high-frequency sprinkler irrigation that applies small amount of water is probably larger

compared to a low-frequency, heavy surface irrigation, and both are lower than subsurface drip irrigation systems.

Several previous studies have developed VI- $K_c$  and/or VI- $K_{cb}$  relationships for cotton. Over an arid irrigated area in China, Shuhua et al. (2003) related the Normalized Difference Vegetation Index (NDVI), obtained from a single Landsat ETM+ image, to cotton  $K_c$ , estimated using Penman-Monteith equation. Hunsaker et al. (2003) observed that for the period between planting and full-cover, cotton  $K_{cb}$  and NDVI had similar evolutions, but  $K_{cb}$  started to decline shortly after reaching the full-cover point, while NDVI remained nearly constant. Therefore, they developed two separate relationships: a linear regression equation for the pre-full-cover stage, and a bi-parameter equation for the post-full-cover period. This model was applied a few years later in order to schedule cotton irrigation, but it resulted in a significant underestimation of water requirement and consequently a lower yield (Hunsaker et al. 2005). To overcome this issue, a new set of non-linear NDVI- $K_{cb}$  relationships were developed for early and late season periods. Applying the new equations for irrigation scheduling of the following year was very successful and the entire crop water requirement was met (Hunsaker et al. 2005).

As Hunsaker et al. (2005) correctly noted, a major factor that hampers the transferability of NDVI-based models is the sensitivity of this VI to the soil background effects. Therefore, other researchers have proposed the implementation of the Soil Adjusted Vegetation Index (SAVI), which is less sensitive to the soil surface wetness conditions compared to the NDVI (Huete 1988). For irrigated cotton in southern Spain, González-Dugo and Mateos (2006) developed a power function that estimated “fraction of cover ( $f_c$ )” from SAVI. Estimated  $f_c$  values were then used to obtain  $K_{cb}$  over the

entire growing season of cotton. Neale and González-Dugo (2011, personal communication) also developed a linear SAVI- $K_{cb}$  regression model for the cotton planted in southern Spain. Table A.2 in the Appendix presents the previously developed VI equations for estimating cotton crop coefficient, along with the methods used in obtaining each parameter and the location of the study site.

Unlike the empirical VI-based approach, energy balance models are physically-based. In these models, net radiation ( $R_n$ ), sensible heat flux ( $H$ ), and soil heat flux ( $G$ ) are quantified on a distributed basis, using aerial or satellite imagery. Latent heat flux ( $LE$ ) is then estimated as the residual of energy balance equation. One of the main parameters used in the estimation of  $H$  is the radiometric land surface temperature. Any increase in the value of this parameter translates into higher values of  $H$  and consequently lower estimates of  $LE$ . Hence, energy balance models have the advantage of being able to detect stress development sooner than the VI approach, since canopy temperature is one of the first bio-physical parameters that reacts to the presence of stress factors. Vegetation indices are not affected by the sub-optimal conditions, unless the presence of stress factors prolongs enough to cause wilting or detectable changes in crop foliage.

In this study, a remotely-sensed energy balance model was applied to estimate the spatially-distributed  $ET$  and  $K_c$  of cotton fields in an irrigation scheme in southern California. The results were then compared with the estimates of a previously developed SAVI- $K_{cb}$  model, and with tabulated  $K_c$  values presented in the FAO-56 publication and the Lower Colorado River Accounting System (LCRAS) report. Finally, a new equation was developed to approximate the basal crop coefficient of cotton, using satellite-based SAVI.



## Methods and materials

### Study Area

Palo Verde Irrigation District (PVID) is located in Imperial and Riverside counties, California, on the west bank of the Lower Colorado River. The river water is diverted into the PVID main canal using a small diversion dam at the upstream end of the district. The most common irrigation method is the gravity-fed surface irrigation supported by an extensive network of 400 km of irrigation canals and 230 km of open drains. The medium texture of PVID alluvial soils allows them to hold a considerable amount of water, and to be easily drained. The main crops are alfalfa and cotton, with a year-round growing season facilitated by the favorable climate of southern California.

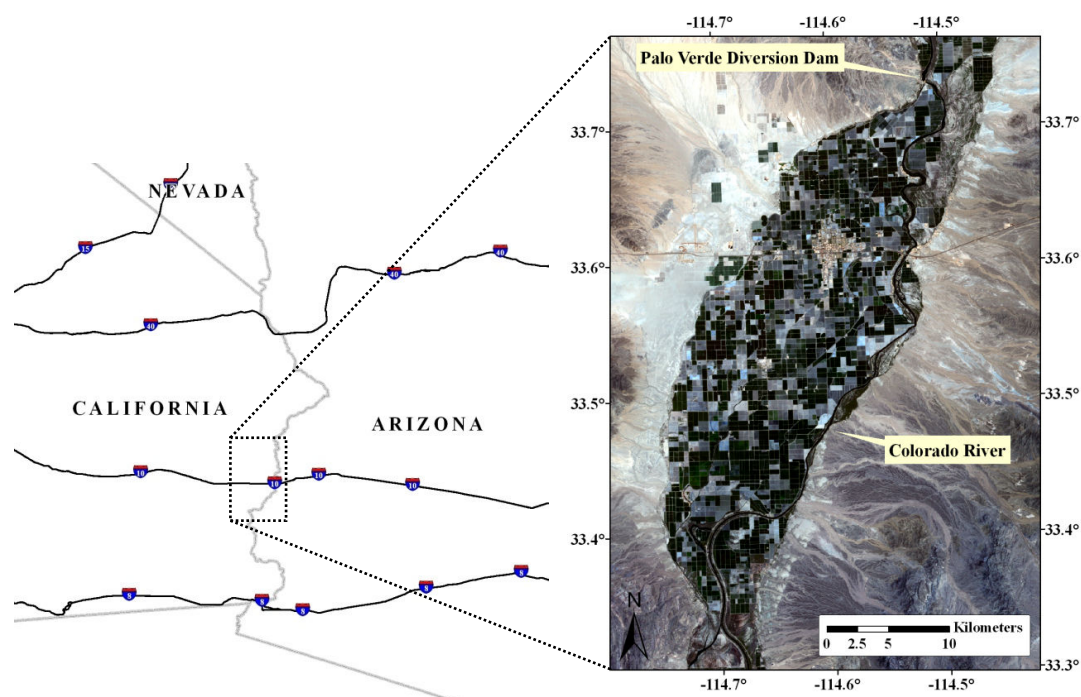


**Fig. 3.1** Palo Verde Irrigation District (PVID) in southern California

## Cotton agricultural practices in PVID

The legal planting and plowing dates of cotton at PVID are March 15<sup>th</sup> and January 1<sup>st</sup>, respectively. However, the actual sowing may happen two to three weeks before or after the legal date, depending on farmer's plan for the harvest. Regardless of the planting date, a rest period of two months or more should be considered between plowing the fields and the planting. There are two methods of planting cotton in the region, namely wet-bed and dry-bed planting. In case of wet-bed planting, which is the more common method, a heavy pre-planting irrigation (250 mm of water) is applied about three weeks before sowing. This irrigation provides the water requirement for cotton seeds to germinate and usually no further irrigation is needed until early May (Henning 2010, personal communication).

Finishing boll development is achieved using either of the two different methods. If the farmer wants to turn fields around quickly, cotton would be sprayed by growth regulators during the season to stop the vegetative growth and promote boll development. Growth regulators may be also applied earlier in the season to prevent the plant from growing taller than about 1.2 m. Alternatively, finishing boll development can be accomplished by stopping irrigation. Harvest date depends on when crop has developed bolls for maximum yield and how fast the cotton gin can process products. Generally, the first cotton bales are harvested around October 1<sup>st</sup>, depending on weather conditions. Harvesting continues into January or February with cotton being stacked in dry areas so that when the gin is ready, it can be picked up and hauled for processing (Henning 2010, personal communication).

## Energy balance model

The “Surface Energy Balance Algorithm for Land” (SEBAL) is one of the better performing energy balance models in irrigated areas, which has been applied and validated in more than 30 countries worldwide (Bastiaanssen et al. 1998a, 1998b). In this study, the SEBAL model was implemented to map spatially-distributed instantaneous ET over the entire PVID, using all available and cloud-free Landsat TM5 images acquired between January 2008 and January 2009. A detailed explanation on methods, results, and results’ validation based on water balance analysis is presented in Chapter 2. In order to estimate spatially-distributed  $K_c$ , the modelled instantaneous ET was divided by the instantaneous grass-based reference ET ( $ET_o$ ), estimated at a local standard weather station in the middle of PVID, close to the city of Blythe, CA. This weather station was owned and operated by the California Irrigation Management Information System (CIMIS). Instantaneous  $ET_o$  values were estimated based on the FAO-56 Penman-Monteith equation (Allen et al. 1998) and reported on the CIMIS web portal at <http://wwwcimis.water.ca.gov/cimis/welcome.jsp>.

## Field selection

PVID cotton fields were selected using a crop classification map developed by the US Bureau of Reclamation (USBR). Classification of crop types was carried out based on surface spectral signature retrieved from Landsat imagery (Fig 3.2).

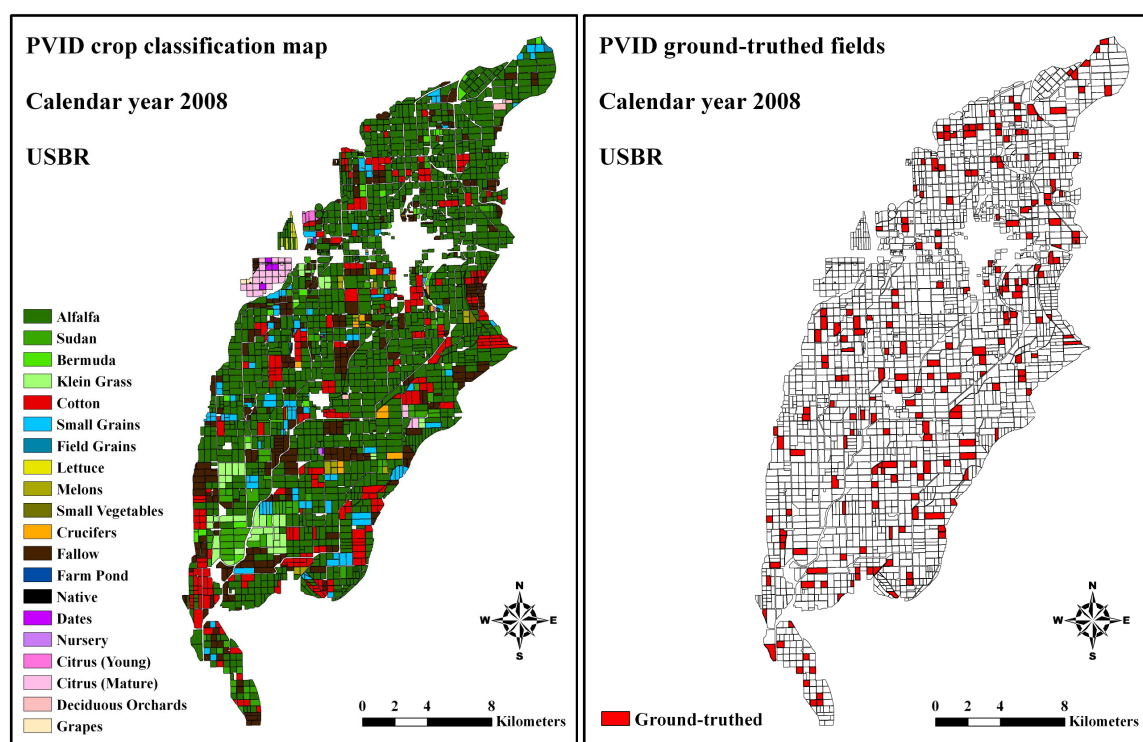


**Fig. 3.2** 2008 crop classification layer of PVID fields (left) and ground-truthed fields (right)

However, Stehman and Milliken (2007) showed that although ground-truthing can enhance the accuracy of the results, classification error could still be significant (from 7% for alfalfa to 67% for small vegetables in 2002). In this study, only ground-truthed cotton fields were considered in analyses in order to avoid any classification error. This resulted in the selection of 22 cotton fields, with the total area of about 350 ha. In addition, an inner buffer zone of 60 m was defined for each of the 22 studied fields to eliminate any edge effect. The new buffered, ground-truthed cotton field layer was finally used as a mask in ArcGIS to obtain field statistics from the SEBAL-derived  $K_c$  maps.

### Comparing crop coefficients

Remotely-sensed  $K_c$  estimates of SEBAL were compared with the results of three other independent methods. The first method was an empirical VI approach developed by Neale and Gonzalez-Dugo (2011, personal communication), in which  $K_{cb}$  was related to SAVI through the following equation:

$$K_{cb} = 1.587 \times \text{SAVI} + 0.007 \quad (3.1)$$

This relationship was developed over an irrigated cotton field within a semi-arid area in southern Spain, which is similar to the southern California in terms of agro-climatological conditions. Equation (3.1) was applied to the same 21 Landsat images used in running SEBAL model. As mentioned before, SAVI-based  $K_{cb}$  estimates are expected to be lower than the SEBAL results, since SAVI is not sensitive to the soil surface wetness.

Besides the VI approach, SEBAL- $K_c$  was also compared against tabulated values presented in two sources, namely the FAO-56 publication and the LCRAS report. Since FAO-56 values are developed for sub-humid climatic condition, they were adjusted to represent the semi-arid climate of PVID (Allen et al. 1998). The adjustment was made based on the FAO-56 guidelines, using the relative humidity and wind speed data (measured at the CIMIS weather station), as well as irrigation frequency information collected by interviewing PVID farmers. LCRAS values are also based on FAO-56 recommendations, but they have been modified for the specific agro-climatological conditions of the Lower Colorado River Basin (Jensen 2002).

Since  $K_c$  values from both FAO-56 and LCRAS reports assume a four-stage crop growth, SEBAL-derived and SAVI-based crop coefficients were averaged over each of

the growth stages in order to generate piece-wise functions comparable with FAO-56 and LCRAS curves. Daily and seasonal water consumption of cotton were also determined through multiplying the piece-wise crop coefficients by the grass-based reference ET, estimated at the local CIMIS weather station.

## **Results and discussion**

### Remotely-sensed crop coefficients

The average SEBAL- $K_c$  values for all of the studied cotton fields ranged from 0.25 before emergence to 1.12 in summer. Among-field variation in  $K_c$  was large before reaching the full-cover and after the onset of senescence with a maximum standard deviation of 0.39, but it was significantly lower during the mid-season, with a standard deviation of 0.03. Tasumi et al. (2005) also observed large variation in remotely-sensed  $K_c$  of several agricultural crops during early and late season periods. The SAVI- $K_{cb}$  values followed a pattern very similar to the SEBAL- $K_c$ , ranging between 0.18 and 1.11, but always less than or equal to the SEBAL- $K_c$ . The smaller peak of ET detected by SEBAL in the initial stage of cotton growth is due to the heavy pre-planting irrigation event that usually occurs between late February and late March (Fig. 3.3).

According to Fig. 3, cotton at PVID has a growing season of about 9 months (270 days), which is longer than the 225 and 214 days reported in FAO-56 and LCRAS, respectively. To allow for the comparison of SEBAL and SAVI results with the FAO-56 and LCRAS, the traditional four stages of crop growth, namely the initial, development, mid-season, and late-season were identified using the remotely-sensed data, as well as the

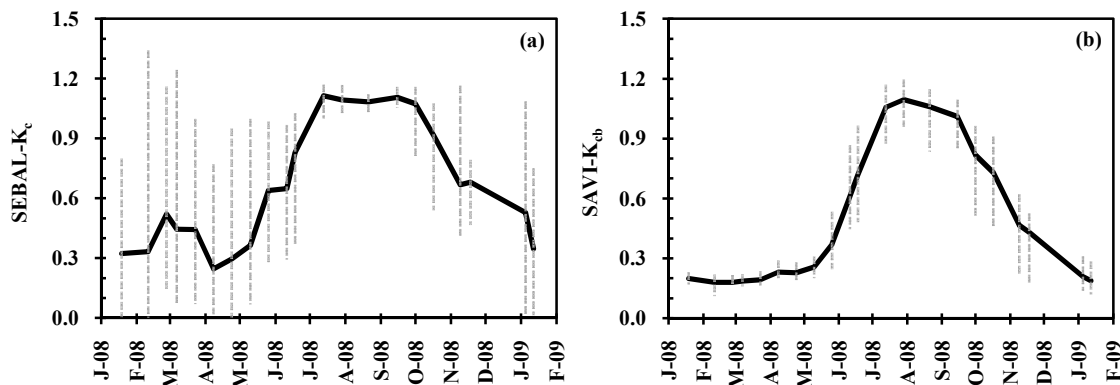


**Fig. 3.3** Average cotton crop coefficient during the 2008, estimated by (a) the SEBAL model and (b) the SAVI method. Vertical dashed lines represent the range of values for all 22 studied fields

information obtained by interviewing the local farmers. March 10<sup>th</sup> and December 1<sup>st</sup> were assumed to represent the average cotton planting and harvest dates, respectively.

While the length of the initial stage was similar among all approaches (45 to 51 days), the length of the development stage based on the remotely-sensed data was 75 days, significantly shorter than the 90 days, recommended by the FAO-56 and LCRAS. Contrarily, the remotely-sensed mid-season period was 65 days, longer than the FAO-56 and LCRAS assumptions of 45 and 35 days, respectively. The length of the remotely-sensed late-season stage (77 days) was also longer than the FAO-56 and LCRAS by 32 and 38 days, respectively.

Both SEBAL- $K_c$  and SAVI- $K_{cb}$  estimates were then averaged over each of the growth stages (Fig. 4). During the initial growth stage, SEBAL detected a  $K_c$  value of 0.37, which was higher than FAO-56 and LCRAS suggestions of 0.25 and 0.26, respectively.

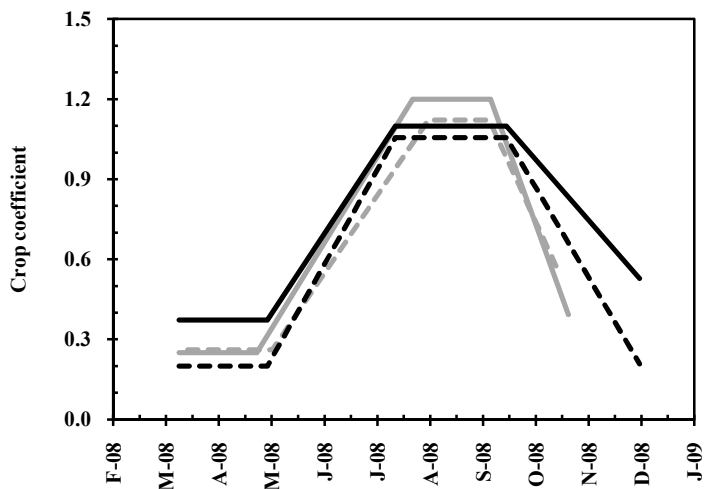


**Fig. 3.4** Piece-wise crop coefficients: SEBAL- $K_c$  (solid black line), SAVI- $K_{cb}$  (dashed black line), FAO-56- $K_c$  (solid gray line), and LCRAS- $K_c$  (dashed gray line)

The high initial SEBAL- $K_c$  was mainly a result of the heavy pre-planting irrigation, which is not accounted for in the tabulated methods. As expected, SAVI- $K_{cb}$  was lower than the  $K_c$  estimates, with a value of 0.20.

Over the mid-season period, FAO-56 predicted a  $K_c$  of 1.20, which was 9% higher than the  $K_c$  estimate from SEBAL (1.10). For a 20-ha, flood-irrigated cotton field in western Turkey, Allen (2000) also found that FAO-56 crop coefficient was higher than SEBAL estimates by 30 and 20% on June 26<sup>th</sup> and August 29<sup>th</sup> of 1998, respectively. SEBAL-  $K_c$  of 1.10 is equal to the mid-season cotton  $K_c$ , estimated by Karam et al. (2006) over eastern Lebanon. Mid-season crop coefficient was 1.12 and 1.06 from LCRAS and SAVI, respectively. The negligible difference between the estimates of SEBAL and SAVI (1.10 vs. 1.06) implies that although the SAVI model was developed in Spain, it is efficient in estimating  $K_{cb}$  under the conditions of southern California.



The late-season estimates of SEBAL and LCRAS were similar at 0.53 and 0.57, respectively. The FAO-56 value was lower at 0.39, while the SAVI- $K_{cb}$  had the lowest value (0.21), very close to the  $K_{cb}$  estimate during the initial stage (0.20).

#### Water consumptions

Piece-wise crop coefficients were multiplied by the daily  $ET_o$ , calculated at the CIMIS weather station (CIMIS # 135), in order to estimate cotton water use. SEBAL estimates were higher than other methods during the initial and late season stages. But the maximum rate of daily water use resulted from the FAO-56, with a value of 10.6 mm/day in late July. Maximum daily ET was 9.7, 9.4, and 9.5 from SEBAL, SAVI, and LCRAS approaches, respectively (Fig. 3.5).

Daily ET rates were then summed over the entire growing season of cotton. The cumulative water use of cotton based on SEBAL model was 1,364 mm, higher than both FAO-56 and LCRAS with estimates of 1,216 and 1,064 mm, respectively. The reflectance-based crop coefficient approach resulted in seasonal water transpiration of 1,167 mm, lower than SEBAL and FAO-56, but higher than LCRAS. As mentioned before, the difference between SEBAL and SAVI estimates represents soil surface evaporation, which was 196 mm (14% of the total ET) over the entire growing season. For a cotton field in western Turkey, Allen (2000) reported that the contribution of soil evaporation to the total ET was 29 and 6% during annual and growing season periods, respectively.

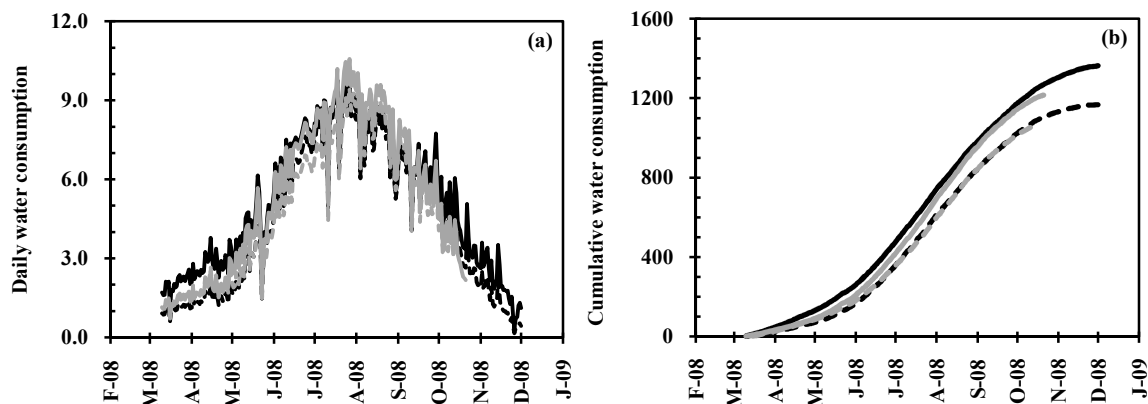


**Fig. 3.5** (a) Daily and (b) seasonal cotton water use: SEBAL-K<sub>c</sub> (solid black line), SAVI-K<sub>cb</sub> (dashed black line), FAO-56-K<sub>c</sub> (solid gray line), and LCRAS-K<sub>c</sub> (dashed gray line)

Remotely-sensed seasonal ET estimates of this study were not only greater than the tabulated values, but they were also greater than most of the cotton water use estimates reported in the literature. Allen (2000) used FAO-56 method and estimated 800 mm of cotton water consumption. Using a soil water balance approach, Tennakoon and Milroy (2003) showed that seasonal water consumption of six largest cotton production areas in eastern Australia vary between 600 to 1000 mm. Karam et al. (2006) measured only 642 mm of ET in the Bekaa Valley of Lebanon, using drainage lysimeters.

It seems that the main reason behind the high water consumption of PVID cotton fields is the significantly longer growing season in this irrigation scheme. For example, cotton planting date was in early May in both Lebanon and Turkey study sites, which is about two months later than the usual planting date in PVID (early March). Compared to PVID, the harvest also happened sooner in these two studies, around mid-October. This resulted in a growing-season length of 134 and 164 days in Lebanon and Turkey, respectively, which is about half of the growing season in PVID.

Bulletin 113-3 of the California Department of Water Resources also reported the results of a cotton water use study that was conducted in the Imperial Irrigation District (IID). Since IID is located downstream of PVID in southern California, the agro-climatological conditions of these two irrigation schemes are very similar. In addition, both schemes divert the Colorado River water for irrigation purposes. The study was carried out between 1967 and 1969, using a hydraulic ET tank. The length of the growing season was 213 and 210 days in 1967 and 1968, respectively, longer than the growing season in both Lebanon and Turkey study sites and closer to the PVID condition. Measured ET was 998 and 1021 mm in 1967 and 1968, respectively. Growing season was longer in 1969 (238 days) and resulted in a seasonal ET estimate of 1067 mm (California DWR 1975).

According to PVID cotton growers, the total application depth of irrigation water is approximately between 1450 and 1650 mm, depending on the agro-climatological conditions of each growing season. This is similar to the previously reported values of 1524 and 1646 mm in Coachella Valley and IID, respectively (California DWR 1975). Since most of PVID fields are blocked-end borders and furrows, it is reasonable to assume that no run-off is generated from irrigation events and all the applied water percolates through the root zone. Therefore, the application efficiency of cotton irrigation could be estimated by dividing the actual ET (from SEBAL) with the depth of applied water. This resulted in an application efficiency ranging from 83 to 94%, which is high for surface irrigation systems. This high efficiency is most probably achieved because PVID fields are precisely leveled using laser-leveling technology.

### SAVI- $K_{cb}$ relationship

Cotton is one of the more dominant crops in the arid/semi-arid western US. Developing a locally-calibrated and easy-to-use method for estimating cotton water use from remotely-sensed VIs can significantly assist irrigation managers. Therefore, SEBAL- $K_c$  was plotted against satellite SAVI to determine their relationship. This resulted in a triangular distribution of SAVI- $K_c$  pairs, where the range of modelled SEBAL- $K_c$  decreased with the value of SAVI (Fig. 3.6). The high variation in  $K_c$  for lower SAVI values was a result of evaporation from soil surfaces after irrigation and/or precipitation events.

Tasumi et al. (2005) also plotted SEBAL- $K_c$  versus NDVI and observed a similar triangular pattern for several hundred potato and sugar beet fields in Idaho. They suggested that the lower envelop to the triangular distribution of all points could serve as the VI- $K_{cb}$  relationship.

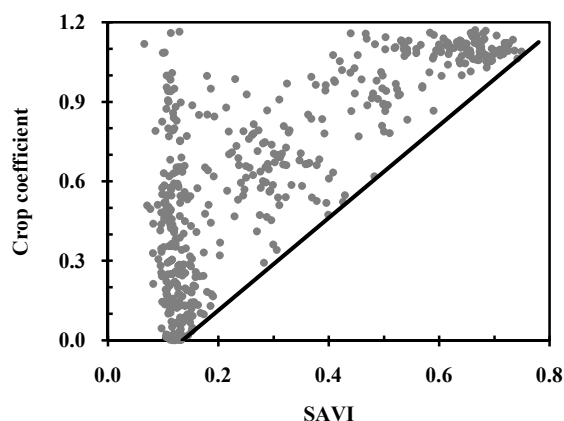


**Fig. 3.6** SEBAL- $K_c$  versus SAVI. Each point represents one Landsat TM5 overpass and one field. A total of 21 satellite scenes were used to study 22 cotton fields. The solid black line represents the lower envelop to the estimated  $K_c$ -SAVI pairs

Applying this assumption to the SAVI- $K_c$  point cloud of this study resulted in the following linear equation:

$$K_{cb} = 1.745 \times \text{SAVI} - 0.235 \quad (3.2)$$

The slope of this model is 10% larger than the slope of the model developed by Neale and Gonzalez-Dugo (2011, personal communication). It should be noted that the lower envelop approach would provide an estimate of basal crop coefficient, only if the lower values in the SAVI- $K_c$  point cloud are due to a negligible soil evaporation and not the presence of stress factors such as disease or water shortage. For the studied fields, visiting the fields and the results of a previous study (see Chapter 2) suggested that stress factors were absent.

### **Summary and conclusions**

Two remotely-sensed methods were used to monitor the timing and duration of different growth stages, as well as water consumption of cotton, grown in southern California. The results suggest that tabular crop coefficients (FAO-56 and LCRAS) underestimate the length of the growing season. The energy balance model implemented herein was also able to detect a heavy pre-planting irrigation event that is not accounted for in FAO-56 and LCRAS. The growth length underestimation along with neglecting the pre-planting irrigation event resulted in lower estimates of cotton seasonal water consumption by FAO-56 and LCRAS. Based on the energy balance model, seasonal cotton water use was 1,364 mm, which was about 78% of the total reference ET during the same period (1,736 mm). Of the total cotton water use, 14% was evaporated from the soil surfaces and the rest was crop transpiration. The remotely-sensed information was

used to modify current tabulated values used in the management of water deliveries on the Lower Colorado River. In addition, to provide irrigation managers with a simple and efficient method in scheduling cotton irrigation, a linear model was developed to calculate cotton basal crop coefficient from satellite-detected SAVI estimates. The slope of this model was 10% larger than the slope of a similar model developed in southern Spain. Since the developed model is only based on SAVI, it can be easily applied to satellite imagery as soon as they become available, which results in a near real time approximation of cotton water requirement.

### References

- Allen RG, Pereira LS, Raes D, Smith M (1998) Crop evapotranspiration: Guidelines for computing crop requirements. Irrigation and Drainage Paper No. 56, FAO, Rome, Italy.
- Allen RG (2000) Using the FAO-56 dual crop coefficient method over an irrigated region as part of an evapotranspiration intercomparison study. *J Hydrol* 229(1–2):27–41.
- Bastiaanssen WGM, Menenti M, Feddes RA, Holtslang AA (1998a) A remote sensing surface energy balance algorithm for land (SEBAL): 1. Formulation. *J Hydrol* 212–213:198–212.
- Bastiaanssen WGM, Pelgrum H, Wang J, Ma Y, Moreno JF, Roerink GJ, van der Wal T (1998b) A remote sensing surface energy balance algorithm for land (SEBAL): 2. Validation. *J Hydrol* 212–213:213–229.
- California Department of Water Resources (1975) Bulletin No. 113-3: Vegetative Water Use in California, 1974. State of California, Resources Agency, Department of Water Resources, Sacramento, CA.
- González-Dugo MP, Mateos L (2006) Spectral vegetation indices for benchmarking water productivity of irrigated cotton and sugarbeet crops. *Agric Water Manage* 95(1):48–58.

- Gowda PH, Chavez JL, Colaizzi PD, Evett SR, Howell TA, Tolk JA (2008) ET mapping for agricultural water management: present status and challenges. *Irrig Sci* 26:223–237.
- Huete AR (1988) A soil-adjusted vegetation index (SAVI). *Remote Sens Environ* 25:295–309.
- Hunsaker DJ, Pinter Jr. PJ, Barnes EM, Kimball BA (2003) Estimating cotton evapotranspiration crop coefficients with a multispectral vegetation index. *Irrig Sci* 22:95–104.
- Hunsaker DJ, Barnes EM, Clarke TR, Fitzgerald GJ, Pinter Jr. PJ (2005) Cotton irrigation scheduling using remotely sensed and FAO-56 basal crop coefficients. *Trans ASAE* 48(4):1395–1407.
- Jensen ME (2002) Coefficients for vegetative evapotranspiration and open water evaporation for the lower colorado river accounting system (LCRAS) addendum to the 1998 report prepared for the Bureau of Reclamation. (Available from the Bureau of Reclamation Boulder Canyon Operations Office in Boulder City, Nevada).
- Karam F, Lahoud R, Masaad R, Daccache A, Mounzer O, Roupheal Y (2006) Water use and lint yield response of drip irrigated cotton to the length of irrigation season. *Agric Water Manage* 85(3):287–295.
- Shuhua Q, Changyao W, Zheng N, Chunyan Y (2003) Retrieving the crop coefficient spatial distribution for cotton under different growth status with Landsat ETM+ image. *Geoscience and Remote Sensing Symposium*, 21-25 July 2003. *IGARSS '03. Proceedings*. 2003 IEEE International 4:2212–2214.
- Stehman SV, Milliken JA (2007) Estimating the effect of crop classification error on evapotranspiration derived from remote sensing in the Lower Colorado River basin, USA. *Remote Sens Environ* 106:217–227.
- Tasumi M, Allen RG, Trezza R, Wright JL (2005) Satellite-based energy balance to assess within-population variance of crop coefficient curves. *Irrig Eng*. 131:94–109.
- Tennakoon SB, Milroy SP (2003) Crop water use and water use efficiency on irrigated cotton farms in Australia. *Agric Water Manage* 61(3):179–194.

CHAPTER 4  
WATER CONSUMPTION AND STREAM-AQUIFER-PHREATOPHYTE  
INTERACTION ALONG A TAMARISK-DOMINATED  
SEGMENT OF THE LOWER COLORADO RIVER

**Abstract**

Spatially-distributed evapotranspiration was modelled over the Tamarisk-dominated riparian forest along the Lower Colorado River by implementing a modified remotely-sensed energy balance approach. Water consumption estimates were validated using an independent method based on diurnal groundwater fluctuations. In addition, point measurements of groundwater elevation and electrical conductivity were analyzed in conjunction with the Colorado River stage measurements in order to study stream-aquifer interaction and the effect of water availability on riparian evapotranspiration. In general, Tamarisk evapotranspiration and aquifer depth were strongly coupled and the onset of water use coincided with the fall of water table. The Colorado River always acted as a source to the riparian ecosystem, with hydraulic gradients being largest in summer and smallest in winter and spring, during Tamarisk dormancy. The annual Tamarisk water consumption was 913 mm, which was significantly lower than the Tamarisk water use approximation that is currently used in the management of the Lower Colorado River. Projecting these estimates over the entire Tamarisk monocultures along the Lower Colorado River resulted in 166.2 Mm<sup>3</sup> of annual evaporative losses, which was 1.4% of the total annual release from the Davis dam.



## Introduction

Invasive vegetation species such as Tamarisk (*Tamarix* spp.) and Russian olive (*Eleagnus angustifolia*) have spread throughout the Western US water systems and rivers, out-competing and replacing native species such as Cottonwoods (*Populus* spp.) and Willows (*Salix* spp.) in the Upper Colorado Basin and Mesquite (*Prosopis* spp.) and other desert trees and scrubs in the floodplains of the Lower Colorado Basin. Tamarisk in particular is one of the most dominant invasive species in the Lower Colorado Basin that has a high tolerance to drought (Cleverly et al. 1997) and salinity (Glenn et al. 1998; Vandersande et al. 2001) and grows in medium to dense stands covering large areas of the generally wider floodplains. For decision makers in the semi-arid western US with scarce water resources, it is of crucial importance to accurately estimate Tamarisk evapotranspiration (ET) and the amount of water that can be salvaged by its removal. However, Tamarisk ET rates reported in the literature are inconsistent, covering a wide range from very low to unrealistically high values (Owens and Moore 2007). For example, in estimating riparian water consumption along the Lower Colorado River, US Bureau of Reclamation (USBR) applies a coefficient of 0.86 as the ratio of annual Tamarisk ET to reference ET, while Murray et al. (2009) estimated a value of only 0.42 over the same area. Such differences have resulted in contrasting opinions on the effectiveness of Tamarisk control efforts for water salvage purposes. Fostering an aggressive eradication program, Zavaleta (2000) reported that the negative effects of Tamarisk water consumption on agricultural and municipal water supplies, hydropower generation, and flood control reach an annual value as high as 285 million USD. On the

other hand, Vandersande et al. (2001) found that water use of Tamarisk is similar to other native species while Murray et al. (2009) concluded that water salvage from Tamarisk removal in the Lower Colorado River would not be negligible.

Most of the methods that have been developed for quantifying Tamarisk water use are based on point measurements, representing the very local condition of the site where measurements take place. Given the high level of heterogeneity in hydro-climatological conditions of riparian communities, extrapolating the results of point measurements to catchment and basin scales may fail to provide a comprehensive picture of actual riparian water consumption. Air and space-borne imagery provide spatially-distributed information that can significantly improve the approximation of Tamarisk ET. In addition, since the same aerial or satellite image is provided to all researchers, a huge source of error introduced during collecting and processing of ground measurements is avoided. Over the past few decades, many ET estimation methods have been developed based on remotely-sensed data, with the accuracies ranging from 67 to 97%, and above 94% for daily and seasonal temporal scales, respectively (Gowda et al. 2008). Existing remotely-sensed ET methods fall into two main categories: empirical approaches based on vegetation indices (VI) and physically-based models for quantifying surface energy balance components.

In the first category (VI approach), several methods have been proposed for estimating ET over riparian thickets. Nagler et al. (2005) developed a bi-parameter regression equation that related ET measurements of energy-flux towers (Bowen-ratio and eddy-covariance) to the point measurement of air temperature and remotely-sensed Enhanced Vegetation Index (EVI: Huete et al. 2002), obtained from the MODIS

instrument. Applying this method over a Tamarisk-dominated corridor in Upper Colorado River Basin resulted in annual ET of about 700 mm (Dennison et al. 2009), while Hultine et al. (2010) measured only 260 to 270 mm over the same area, using sap-flux sensors that were specifically calibrated for Tamarisk studies. This significant difference between the methods was attributed to the fact that in developing ET-EVI relationship, ET measurements from energy-flux towers were plotted against EVI of the single MODIS pixel containing that tower. However, tower footprints are highly variable in size and direction and sometimes fall over surfaces other than narrow riparian corridors (Hultine et al. 2010). Likewise the spatial resolution of the MODIS pixels (250 m for red and near-infrared bands) is coarse for the narrow riparian zones of the Upper Colorado River system.

Later, Nagler et al. (2009a) modified the EVI method by making two adjustments. The first adjustment was the replacement of air temperature with grass-based reference ET ( $ET_o$ ), estimated at a standard weather station. The second adjustment was the use of sap-flux technique rather than energy balance towers in estimating actual ET rates. Both EVI approaches (original and modified) were applied over the Cibola National Wildlife Refuge (the same site in this study), where original equation produced 20% higher estimates than the modified one. The authors claimed that since energy-flux towers measure evapotranspiration but sap-flux sensors measure only transpiration, the extra 20% detected by original method represents evaporation from soil surface. However, such a contribution from soil evaporation seems to be too high for a semi-arid area with annual precipitation of less than 100 mm and average depth to groundwater of more than

2 meters. In addition, most of rainfall events in this area happen during winter, while the data were collected over summer months (June to September).

A major drawback of the VI approach is that vegetation indices are not effective in capturing stress development, unless stress factors prolong enough to cause detectable changes in plants vegetative conditions (Nagler et al. 2005; Nagler et al. 2009a). In addition, the inherent empiricism in VI approach limits its extrapolation to sites other than the one it is developed over (Scott et al. 2008). In case of EVI, another limitation arises from the fact that high temporal resolution of MODIS imagery comes at the cost of a spatial resolution (250 m for visible bands) that is rather coarse for mapping ET of heterogeneous riparian communities. This could be problematic especially in differentiating between water consumption of different species in mixed stands, as well as in estimating ET along the edges of riparian corridors, where MODIS pixels may partially cover water bodies or bare soils. Pixel contamination could have significant effects, given that many riparian corridors along western rivers are only few hundred meters wide. Scott et al. (2008) improved EVI method by incorporating MODIS-derived nighttime land surface temperature (LST) maps. Although new model was successfully validated over the same area it was developed, it should be noted that the pixel size of the MODIS thermal band is four times greater than its visible bands (1 km). Groeneveld et al. (2007) also developed a linear regression equation that approximated the ratio of actual to reference ET based on scaled NDVI estimates derived from Landsat imagery. High spatial resolution of Landsat visible bands was a great advantage in capturing riparian heterogeneity (64 Landsat pixels can easily fit in one MODIS pixel), but the

mismatch between highly variable footprint of energy-flux towers – used in model parameterization – and fixed pixels used in NDVI extraction was a major source of error.

Unlike the VI approach, energy balance (EB) models take advantage of the ability of air- and space-borne imagery to estimate net radiation, sensible, and soil heat fluxes. Latent heat flux is then estimated as the residual of the energy balance equation. Although recent improvements in estimating sensible heat flux (Norman et al. 1995; Bastiaanssen et al. 1998a) have significantly enhanced the accuracy of EB models, it should be noted that these models are originally developed to be applied over agricultural ecosystems. Therefore, modifications are required before applying these models over riparian ecosystems, where biophysical characteristics of surface vegetation are significantly different compared to agricultural crops. To the best of our knowledge, only one riparian application of remotely sensed energy balance models has been reported so far, and it is the research carried out by Bawazir et al. (2009) over the Middle Rio Grande Basin in New Mexico.

The implemented energy balance approach in this study is very similar to the “Surface Energy Balance Algorithm for Land (SEBAL),” developed by Bastiaanssen et al. (1998a). The only modification made is in selection of the wet pixel, which is used in interpolating sensible heat flux between two known extremes. In newer versions of SEBAL, a well-irrigated alfalfa field at full-cover is selected as the wet pixel and it is assumed that temperature gradient and consequently sensible heat flux over this pixel is negligible. In the study by Bawazir et al. (2009), however, wet pixel was selected from the footprint of an eddy-covariance tower over a dense Tamarisk canopy. Instead of assuming a negligible value, associated temperature gradients were obtained from the

measurements of the same tower. Although this modified EB model was successful in accurately estimating ET over Tamarisk and cottonwood communities of the Middle Rio Grande Basin, its general application is limited to areas where energy-flux towers are available. Since installing such towers over the large river systems of the western US and collecting/correcting their measured fluxes are time- and expense-extensive, applying this modified model to manage large watercourse systems is not feasible.

The goal of this study is to provide water managers with new sources of information on highly-debated Tamarisk water consumption. However, although such information is extremely needed, it does not provide a comprehensive understanding on the mechanisms that control Tamarisk water use; unless it is supported by a detailed investigation of stream-aquifer-phreatophytes interaction (Devitt et al. 1997). Therefore, another objective of this study is to study the complicated interaction between the river stage, water table fluctuations, and Tamarisk ET. In order to achieve these objectives, SEBAL model is implemented over a riparian ecosystem, located in southern California along the Lower Colorado River. Remotely sensed ET estimates are further analyzed using an independent method based on diel groundwater fluctuations. Possible sources of error in applying SEBAL over riparian communities are identified and appropriate modifications are also suggested. Finally, a water balance analysis is performed over a 75-km stretch of the Colorado River containing the studied riparian and a large irrigated agricultural area: the Palo Verde Irrigation District.

A major factor that adds to the importance of conducting this research study is the release of saltcedar leaf beetle (*Diorhabda carinulata*) in a few locations along the Upper Colorado River. Recent studies have shown that the spread rate of beetle is rather fast

(Hultine et al. 2009) and it is very likely that they would travel southward to the Lower Colorado River in search for more food. Since the effect of beetle release on Tamarisk water consumption is largely unknown (Hultine et al. 2010), it is critical to accurately identify current ET rates, so the water salvage from future beetle defoliation could be estimated by comparison with existing estimates.

### **Methods and materials**

#### Study area

The study area is within the Cibola National Wildlife Refuge (CNWR) located downstream from the Palo Verde Irrigation District (PVID) in southern California. Established in 1964, CNWR occupies about 70 km<sup>2</sup> of floodplains on the west bank of the Lower Colorado River. Figure 1 demonstrates a stretch of the river between Palo Verde diversion dam and a river flow measurement gage at Cibola and its location within the Colorado River Basin. A water balance analysis was performed over this river reach, which includes both PVID (at north) and CNWR (at south).

Ground elevation at CNWR ranges from 66 m at the east (the river) to about 70 m at west (desert hills). CNWR is the home of more than 280 bird species and several phreatophytes. Over 90% of the area is covered by Tamarisk (Nagler et al. 2009b) with an average age of about 20 years (Godaire and Klinger 2007). Mesquite (*Prosopis velutina*) and arrowweed (*Pluchea sericea*) are the next dominant species.

Three specific measurement stations within the lower CNWR were selected for performing the analyses of this study. These stations were called Slitherin, Diablo, and Swamp with far, medium, and close proximities from the river, respectively.

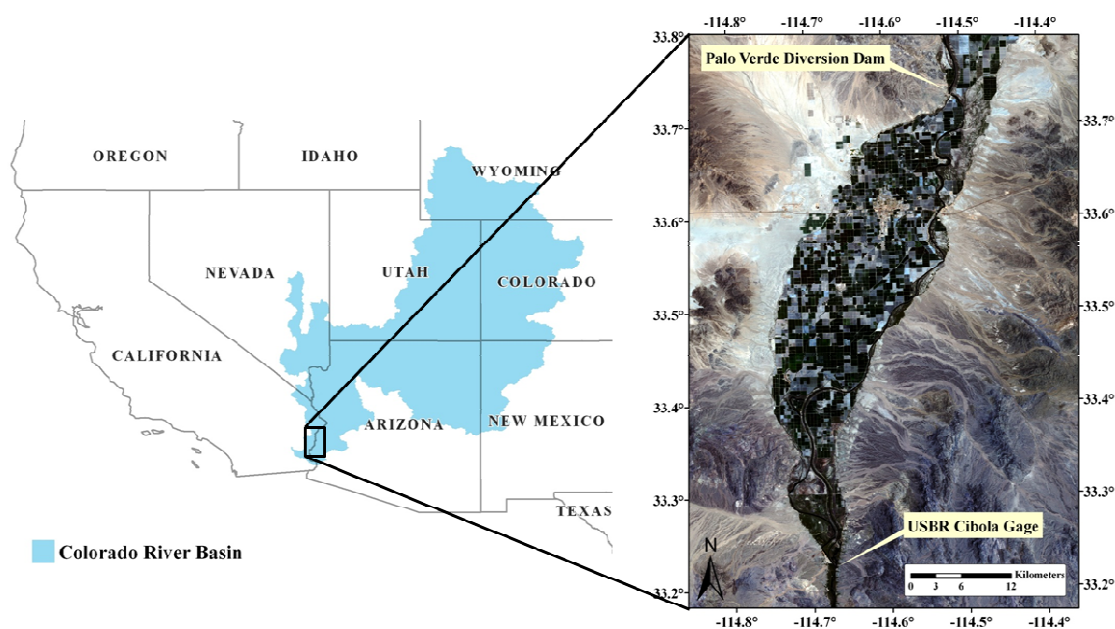


**Fig. 4.1** The stretch of the Lower Colorado River between Palo Verde diversion dam and USBR gaging station at Cibola

The locations of these sites were selected in a fashion to capture the variability in Tamarisk density and groundwater availability and quality. Table 4.1 summarizes different characteristics of these sites (geo-hydrological parameters are averaged for the 2008).

Figure 4.2 shows two high-resolution airborne images of the lower CNWR, acquired in summer of 2008 by Utah State University aircraft. The false-color image (left plot) shows the location of each measuring station, with five groundwater observation wells at each site. Part of the new, engineered channel of the Colorado River is captured on the east side of the image. Further to the west is the old river channel that carries small flow rates just to protect the flora and fauna of this riparian ecosystem.



Other features of this image are: abandoned agricultural fields at north, desert hills at the western boundaries and interspaced bare soil represented with blue/green tones, and the “Three Fingers” lake at the south-central part of the image.

The 1-m airborne LiDAR image (right plot) illustrates the variability in canopy height, ranging from zero over bare soil and water to more than eight meters over dense Tamarisk stands at Slitherin. To generate this canopy height layer, a bare earth elevation layer was first generated from the classification of LiDAR point cloud data. Then, the laser beam returns from the top of vegetation (first returns) were converted into a top of canopy elevation layer. Finally, the bare earth elevation layer was subtracted from the top of canopy elevation layer in ArcGIS environment to obtain pixel-wise canopy height.

**Table 4.1** Characteristics of measuring stations

	<b>Swamp</b>	<b>Slitherin</b>	<b>Diablo</b>
Tamarisk density	Medium-low	High	Medium-high
Distance from old river channel (m)	100	650	1500
Distance from existing river channel (m)	850	2900	2400
Groundwater temperature (°C)	22.2	21.7	22.3
Depth to groundwater (m)	2.9	3.5	3.4
Groundwater electrical conductivity (dS/m)	4.1	8.0	17.0

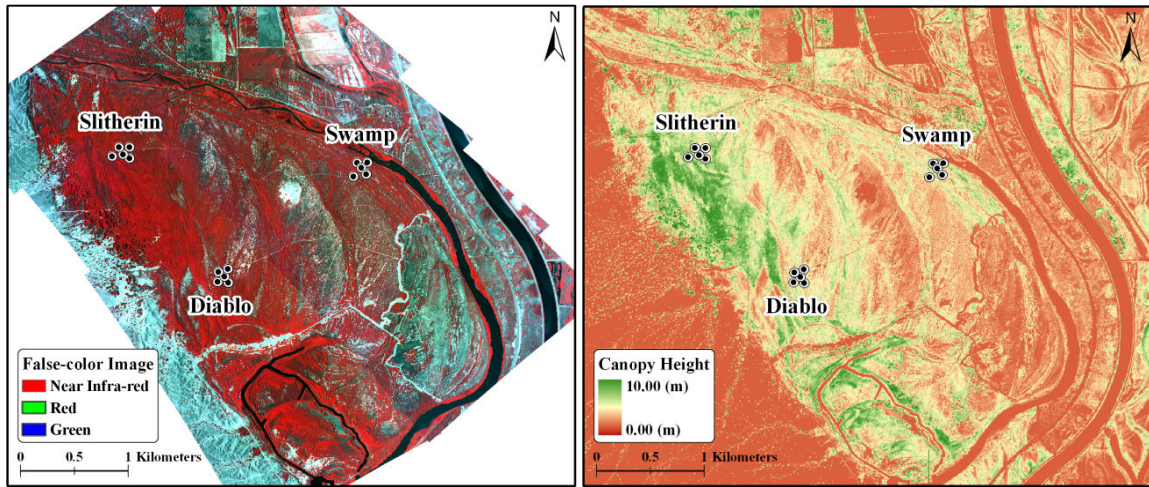


**Fig. 4.2** The lower Cibola National Wildlife Refuge (CNWR) and the location of study sites. Left: False-color multispectral airborne image and Right: LiDAR-derived canopy height, both at 1 m resolution

#### Groundwater characteristics

As mentioned above, five observation wells were drilled near each measuring station (total of 15 wells) to monitor groundwater dynamics. One well was in a central position and the rest of the wells were located at about 80 m from the central well in all four directions. A hand-held EC-meter was used to measure groundwater electrical conductivity of each well on a monthly basis. In addition, submerged HOB0 water level data loggers (Onset Computer Corporation, Bourne, MA, USA) were used to monitor groundwater head and temperature at 15 min intervals. Besides these submerged loggers, a HOB0 barometric sensor was also installed above groundwater level at a Slitherin well to monitor changes in atmospheric pressure. Recorded atmospheric pressure was subtracted from all water pressure measurements of submerged sensors to obtain the pressure that is exerted only by water column above the sensors. Water head data were

then converted to depth to groundwater, using the measured distance between HOBO loggers and ground surface at each observation well. Daily and seasonal patterns in depth to groundwater data were used in studying the effect of water availability on Tamarisk ET. However, the depth to groundwater needs to be converted to groundwater elevation before any analysis of groundwater flow and stream-aquifer interaction can be performed. In order to do so, soil surface elevation at each observation well was extracted from LiDAR data at 1-m resolution. Depth to groundwater was subtracted from the associated soil surface elevation to estimate groundwater elevation.

One of the most important aspects of studying stream-aquifer interaction is the direction of groundwater flow to determine if the river is acting as a source or a sink. In this study, groundwater elevation data were analyzed in conjunction with river stage data. USBR owns and operates two stage gages within few kilometers of CNWR, where river stage is measured on an hourly basis. These sites are “Taylor Ferry” and “Cibola” gages, located upstream and downstream of CNWR, respectively. However, it was only necessary to select one point on the river to be able to compare river stage data with groundwater elevation at each site. Therefore, a line passing through the Swamp site and perpendicular to the river was drawn in ArcGIS and the intersection of this line and the river was selected as the river stage reference point. This point was about 24 river km downstream of the Taylor Ferry gage and 7 km upstream of the Cibola gage. It was assumed that the river stage varies between these two gages in a linear fashion, so the stage value at the reference point was interpolated between the two measurements, proportional to the distances.

## Tamarisk evapotranspiration

Tamarisk ET was estimated using two independent methods. The first method is based on high-frequency point measurements of groundwater diel fluctuations (White method), while the second method is a remotely sensed energy balance modeling approach (SEBAL).

### *White method*

After a comprehensive study of groundwater dynamics in the Escalante Valley in southeastern Utah, White (1932) proposed a method for estimating riparian evapotranspiration from water table fluctuations:

$$ET = S_y (24r \pm s) \quad (4.1)$$

where ET is daily evapotranspiration (mm),  $S_y$  is the specific yield of the aquifer (dimensionless),  $r$  is the average rate of groundwater recharge between midnight and 4:00 AM (mm/hr), and  $s$  is the net change in water table over a 24-hour period (mm). The White method is based on several key assumptions. The first assumption is that  $r$  represents daily average rate of groundwater flux. Another important assumption is that diurnal decline and the following nocturnal incline in groundwater level is a result of presence and absence of water extraction by tapping roots of phreatophytes, respectively. However, other factors such as barometric pressure changes, freeze-thaw processes, tropical rainfall, and anthropogenic factors may also induce groundwater fluctuation (Gribovszki et al. 2010). In this study the first factor is accounted for by measuring atmospheric pressure on a same time scale, using the same type of sensors. Measured values are subtracted from groundwater pressure measurements to obtain a pressure that

is exerted only by the head of water above sensors. The next two factors are also ruled out, since CNWR is located in a semi-arid environment with annual precipitation of less than 100 mm and minimum air temperatures that rarely fall below zero. Diablo and Slitherin sites are also far enough from any anthropogenic activity, so the third factor is not an issue either. However, the Swamp site was close to the old Colorado River channel that currently carries agricultural drainage water from the upstream PVID and some regulated flow rates for supporting riparian ecosystem. It is also directly influenced by the fluctuating river stages. Therefore, this site was excluded from ET estimation by White method.

The White method is particularly sensitive to the value of specific yield. Previous studies have shown that except for clean sand, laboratory-derived values of this parameter result in a significant overestimation error by White method (Gribovszki et al. 2010). This is chiefly due to the fact that unlike laboratory conditions, water table rise or fall in a real situation does not happen instantaneously. To avoid this source of error, Meyboom (1966) suggested a 50% reduction in  $S_y$  values and called it “readily available specific yield.” In this study we used adjusted specific yield values developed by Loheide et al. (2005) for structure-less loam to sandy-loam soils of Diablo and Slitherin.

Since the White method is solely based on diel fluctuations in groundwater, any water extraction by phreatophytes from the vadose zone is neglected. Therefore, the results are usually considered to represent only that part of the total daily ET that is provided by the aquifer. Consequently, White estimates are usually referred to as “groundwater consumption” rather than “ET.” Over CNWR, however, annual precipitation rarely exceeds 100 mm, with usually less than a quarter of the annual

amount falling during the growing season of Tamarisk. Due to such a low precipitation and the aridity of this region, the contribution of vadose zone water content to ET from precipitation is negligible and almost all of the riparian water consumption is provided by the aquifer.

### *SEBAL*

The “Surface Energy Balance Algorithm for Land (SEBAL)” is a remotely sensed energy balance model that was developed by Bastiaanssen et al. (1998a). This model has been successfully applied over agricultural ecosystems in more than thirty countries, producing accurate estimates of crop ET (Bastiaanssen et al. 1998b, 2005; Ramos et al. 2009). In SEBAL, net radiation ( $R_n$ ) is estimated through quantifying all of the incoming and outgoing short- and long-wave radiation. Soil heat flux ( $G$ ) is also modeled as a ratio of net radiation. Finally, sensible heat flux ( $H$ ) is mapped using an innovative approach that interpolates  $H$  between two extreme conditions, representing minimum and maximum sensible heat flux. For the minimum condition, a cold, well-irrigated agricultural field at full cover is selected. Over such a surface, the available energy is used in changing the state of water from liquid to gas, resulting in a negligible temperature gradient. The maximum- $H$  pixel is selected over a dry agricultural bare soil, where there is little or no water to evaporate and the available energy is used in heating the soil and the air. As a result, vapor pressure gradient and latent heat flux approach zero. After identifying these two extreme limits,  $H$  is interpolated over all other pixels using Monin-Obukhov similarity theory. Knowing  $R_n$ ,  $H$ , and  $G$ , latent heat flux ( $LE$ )

can be calculated as the residual of the energy balance equation, assuming that the energy consumed in photosynthesis and the canopy storage of energy are both insignificant:

$$LE = R_n - G - H \quad (4.2)$$

Latent heat flux estimated from equation (4.2) is only an instantaneous estimate at the time of overpass, which has limited application for practical purposes such as managing water resources. Several methods have been proposed in literature for scaling instantaneous values up to longer periods (daily and seasonal). The original up-scaling method of SEBAL is based on the Evaporative Fraction (EF or  $\Lambda$ ) which is the ratio of instantaneous ET to instantaneous available energy ( $R_n - G$ ). Assuming that EF remains constant during the day (Brutsaert and Sugita 1992; Zhang and Lemeur 1995; Crago 2000), daily ET is calculated by multiplying EF and daily available energy. Although this technique has provided reliable results in many studies (Gowda et al. 2008), its accuracy is hampered over arid/semi-arid irrigated areas, where afternoon advection can substantially enhance the ET.

Trezza (2002) modified EF method by using the ratio of instantaneous ET to instantaneous alfalfa-based reference ET ( $ET_r$ ), estimated at a standard weather station. Extrapolated daily ET estimates of irrigated crops using this new method ( $ET_rF$  method) have shown to be improved (Allen et al. 2007 a, 2007b), since the effect of converged energy is detected by  $ET_r$  estimates. Similar to  $ET_r$ , grass-based reference ET ( $ET_o$ ) could also be used in up-scaling instantaneous ET values ( $ET_oF$  method). Colaizzi et al. (2006) and Chavez et al. (2008) reported that under advective condition,  $ET_oF$  method works better than  $ET_rF$  and EF methods. In present study, both EF and  $ET_oF$  methods

were implemented in extrapolating instantaneous ET of Tamarisk. The performance of each of these methods was evaluated by using expert knowledge and by comparing the results with White approach approximations and water balance closure. In the absence of any other extrapolation method, suggestions are made on how to modify current methods to attend to the specific hydro-climatological conditions of phreatophytes.

Daily  $ET_0$  estimates and other required weather parameters were obtained from a nearby weather station located in Blythe, California and operated by The California Irrigation Management Information System (CIMIS). In addition, all cloud-free satellite imagery acquired by Landsat TM5 between January 2008 and January 2009 were downloaded from the website of USGS Global Visualization Viewer, GLOVIS (<http://glovis.usgs.gov/>). This resulted in a total number of 21 scenes (path/row: 38/37 and 39/37).

#### Closing water balance

A water balance analysis was performed over a 75-km stretch of the Lower Colorado River between Palo Verde diversion dam and Cibola flow measuring gage. In addition to CNWR and the riparian corridor, this stretch of the river also contains Palo Verde irrigation district (PVID). Closing the water balance was used not only to validate the results of spatially-distributed ET, but also to provide water managers with unique information on the consumptive use of water over this river reach. Following equation was the basis of water balance analysis in this study:

$$Q_{in} + P = ET + Q_{out} + \Delta S \quad (4.3)$$



where  $Q_{in}$  is the river flow at the upstream end of the study area,  $P$  is precipitation,  $ET$  is evapotranspiration,  $Q_{out}$  is the river flow at the downstream end, and  $\Delta S$  is the change in soil water content over the study period. Since accurate approximation of  $\Delta S$  is very difficult, study period is usually selected in a fashion that would result in a negligible net change in soil moisture. A detailed investigation of the readings from 260 piezometer revealed that between January 2008 and January 2009, net change in water table over the PVID is negligible (see Chapter 2). A similar study over CNWR also showed that fluctuations in riparian aquifer is also negligible over the same time frame (refer to results and discussion section).

Besides  $ET$ , which was modeled using a remotely-sensed  $EB$  approach, other components of water balance were measured. For every rainfall event, point measurements of 32 rain gages located over the study area were imported into ArcGIS environment and rainfall maps were generated, using simple interpolation methods. Pixel-wise interpolated estimates were then summed over the entire river reach to obtain the total annual volume of water input from precipitation. In addition, USBR measures river discharges at upstream and downstream ends of the studied river reach. These data were acquired and analyzed to estimate the volume of surface inflow and outflow through the boundaries of the studied control volume.

## **Results and discussion**

### Groundwater characteristics

Groundwater electrical conductivity ( $EC$ ) was measured at every observation well and then averaged over all the five wells of each station.  $EC$  increased with distance

from the closest source of water (old river channel), with annual averages of 4.1, 8.1, and 17.0 dS/m at Swamp, Slitherin, and Diablo, respectively (Fig. 4.3). The trend in observed groundwater EC could be an indication that aquifer is being recharged only by the river and no other source, because groundwater quality is best at the closest station to the river and degrades substantially as denser Tamarisk canopies of middle and west CNWR extract water and leave the salts behind. In addition, groundwater EC at Diablo may be high enough to impose adverse effects on water consumption. Glenn et al. (1998) conducted a greenhouse experiment and observed 50% reduction in Tamarisk transpiration rates when the salinity of soil extract was higher than 16 dS/m. For Diablo, the average EC of the five observation wells ranged from 16.2 to 18.0 dS/m during the 2008, always higher than the threshold value found by Glenn et al. (1998).

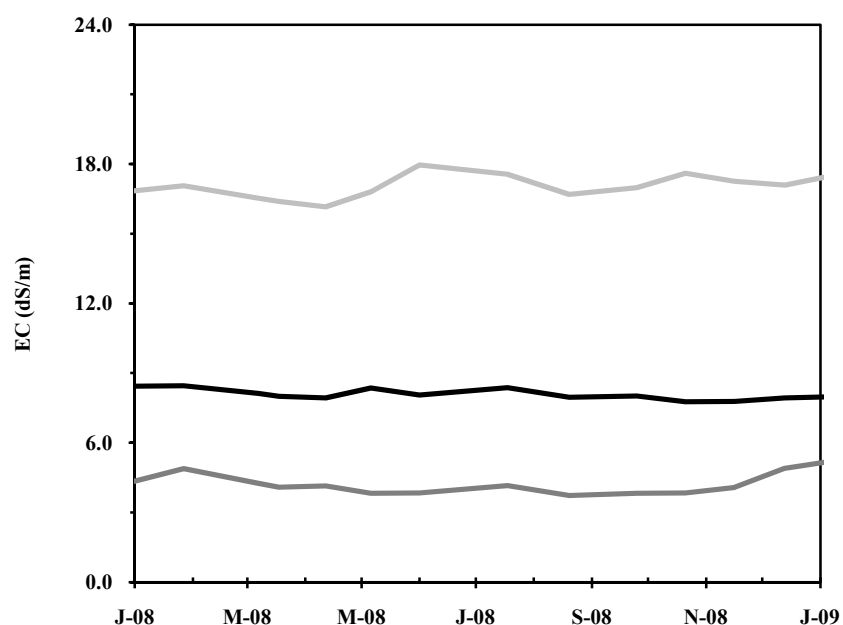


**Fig. 4.3** Average groundwater EC during 2008 at Diablo (light gray), Swamp (dark gray), and Slitherin (black)

Depth to groundwater was greatest over Slitherin and smallest over Swamp, with annual average values of 3.5 and 2.9 m from soil surface, respectively. Water table at Diablo was slightly higher than Slitherin at 3.4 m on average. This means that overall; Tamarisk individuals at Swamp have a better access to groundwater, most probably due to the close distance between this station and the river. Deeper levels at Slitherin and Diablo may be another indication that the direction of groundwater flow is away from the river, but this can be verified after examining groundwater elevation, as soil surface elevation is also higher at these two stations. Although groundwater depth was largest at Slitherin, groundwater EC was at this station was significantly lower than Diablo, which is most probably due to the proximity of Slitherin to the old river channel. Seasonal pattern of groundwater fluctuation was also studied over all three stations (Fig. 4.4).

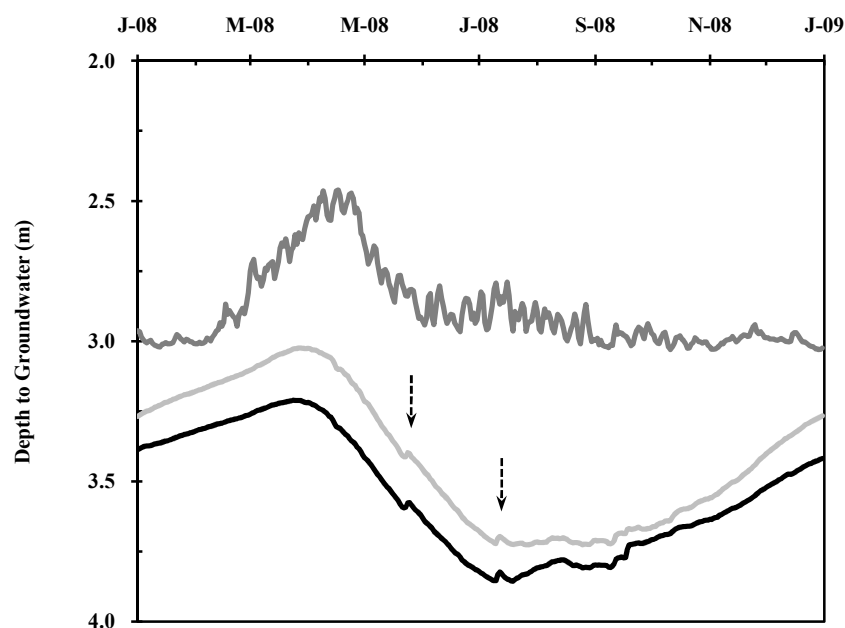


**Fig. 4.4** Average daily depths to groundwater during 2008 at Diablo (light gray), Swamp (dark gray), and Slitherin (black)

For all three sites, groundwater returned to the same level over a period of one year. This confirms that assuming a negligible change in soil water storage over the selected study period (January 2008 to January 2009) is valid. Groundwater level had an obvious seasonal fluctuation pattern over Slitherin and Diablo with the deepest level in mid to late summer, when atmospheric demand and riparian water consumption are substantially high. As the air temperature decreases in October and Tamarisk start senescing, aquifer recharge rate becomes greater than water extraction by phreatophytes and groundwater starts to rise until it reaches the shallowest level in April. Water table at Swamp had a different behavior, with a peak in spring and an approximately constant level of about 3.0 m from the surface during the rest of the year. Higher frequency fluctuations observed at this station are most probably a result of stage variations in both old and new Colorado River channels. The annual magnitude of water level variation was 0.56, 0.64, and 0.70 m over Swamp, Slitherin, and Diablo, respectively.

The two indents in the depth to groundwater curves of Slitherin and Diablo (pointed by dashed arrows) coincided with two monsoon rain events in late May and mid July with average cumulative depth of 12.2 and 8.6 mm, respectively. These two events together consisted 29% of the total annual rainfall (71 mm). The rest of precipitation happened during the period when groundwater was gradually rising, therefore no effect on water table is observed. In the following sections, groundwater depth data are further analyzed to determine any possible effect of water availability on Tamarisk ET. LiDAR-derived high-resolution map of ground surface elevation was used to extract the elevation of each observation well for converting groundwater depth to groundwater elevation data. Interestingly, this conversion removed almost all of the observed

variability in measured groundwater depth between the five closely-located wells at each station. As an example, Fig. 4.5 shows before and after conversion values for the five wells at Diablo station. Daily groundwater elevation data were then averaged over all five wells at each station and compared with the interpolated river stage to study the stream-aquifer interaction (Fig. 4.6).

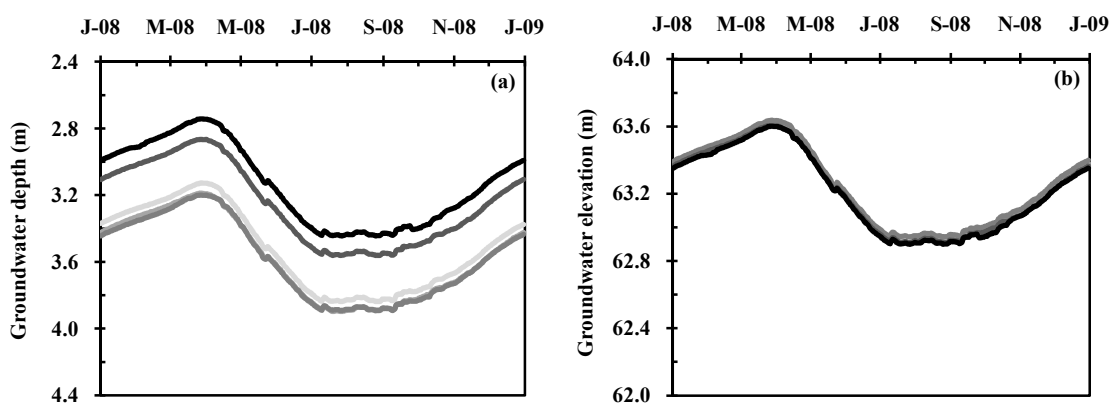


**Fig. 4.5** Daily average (a) depths to groundwater and (b) groundwater elevation, at five observation wells of the Diablo station

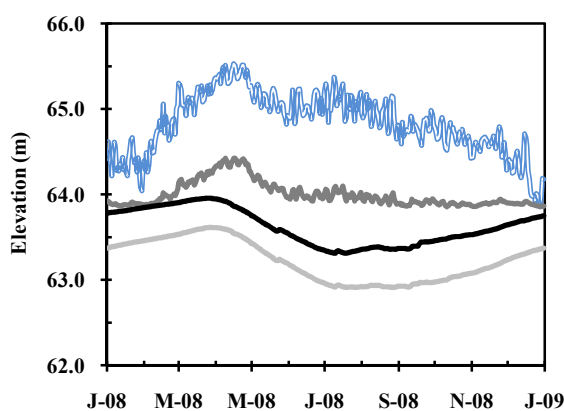


**Fig. 4.6** Daily average groundwater elevation (m) at Diablo (light gray), Swamp (dark gray), and Slitherin (black), along with the river stage (double blue line). All elevations are based on the same datum

Water table elevation had a seasonal fluctuation pattern over Slitherin and Diablo. However, fluctuations at Swamp were clearly different, following a pattern similar to the Colorado River stage fluctuations. Diablo groundwater elevation was always lower than the two other stations and the river stage, ranging from 62.9 m in late summer to 63.6 m in April. The fact that water level at Diablo was the deepest confirms the hypothesis that the direction of sub-surface flow is from water bodies toward the heart of CNWR. On average, water table at Slitherin was 0.4 m higher than Diablo, with a minimum level of 63.3 m and a maximum of 64.0 m, occurring at roughly the same times as Diablo.

The Colorado River reached a high stage of 65.5 m in mid-April and a low of 63.9 m in late December. Over the entire 2008 calendar year, the river stage was at a higher level than the CNWR aquifer, except for one date (12/28/2008), when it was equal to the aquifer level at Swamp. This indicates that the hydrologic interaction between the Colorado River and the CNWR aquifer is a one-way, source-sink interaction, where water is always flowing from the river toward the riparian forest. Based on measured aquifer and river elevations, the hydraulic gradients were also estimated. The hydraulic gradient between the river and Swamp varied from zero to a maximum of about 0.14% (1.4 mm/m) in July, reaffirming the presence of a westward subsurface flow. Compared to the River-Swamp gradient, inter-station gradients were lower (Fig. 4.7a).

Swamp-Diablo and Swamp-Slitherin gradients had similar patterns, following the greening and senescence of Tamarisk, which occur in March and November in CNWR (Nagler et al. 2009b). However, Slitherin-Diablo gradient did not pose a significant seasonal pattern, suggesting the existence of a rather constant southward flow in addition to the westward flow.

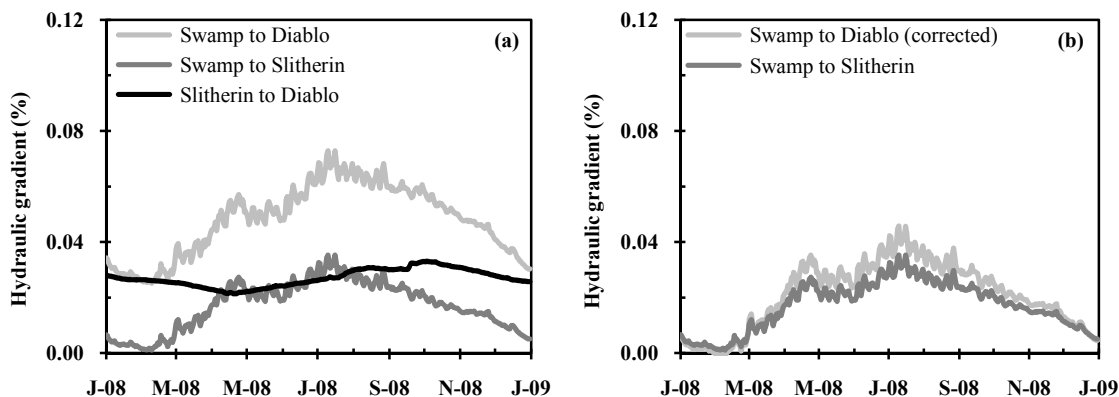


**Fig. 4.7** Daily average inter-station hydraulic gradient expressed in percentage **(a)** before and **(b)** after correcting for the effect of southward flow

This southward flow is most probably fed by the old river channel on the north boundary of CNWR, which carries a significant amount of drainage water from the upstream PVID, as well as a fraction of the river flow. Unlike the Swamp-Slitherin path which is west-east, the Swamp-Diablo path has a southwest direction. Therefore, observed Swamp-Diablo gradient may be enhanced by the southward subsurface flow. To examine the effect of this, the Slitherin-Diablo gradient was subtracted from Swamp-Diablo gradient (Fig. 4.7b). Interestingly, the subtraction eliminated almost all the differences between hydraulic gradients toward the Diablo and toward the Slitherin.

Tamarisk evapotranspiration

#### *White method*

Monitoring the aquifer fluctuations revealed that water table at Swamp is strongly affected by the heavily-regularized fluctuations in river stage. Therefore, the five observation wells of this station were not included in applying White method. Figure 4.8

presents the average daily groundwater consumption estimates for Slitherin and Diablo. The White method estimates confirmed the 240-day growing season of Tamarisk in CNWR, with emerging new leaves in mid-March and dropping them in mid-November. Since diurnal water table fluctuations were not significant during the Tamarisk dormancy, a small decline in the water level between midnight and 4:00 AM resulted in several dates with negative estimates over this period.

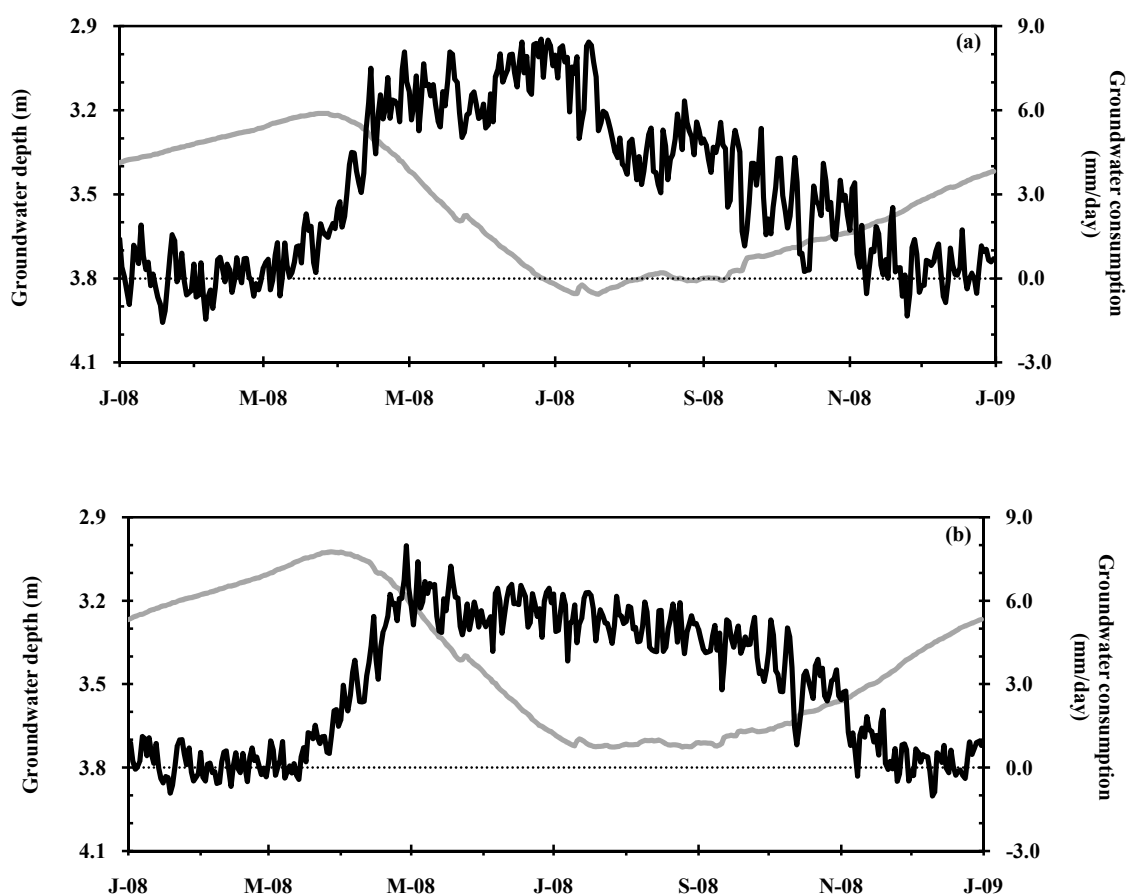


**Fig. 4.8** 2008 daily groundwater consumption estimated by White method (black), overlaid by the measured depth to groundwater (gray), average for all the five observation wells at **(a)** Slitherin and **(b)** Diablo



Groundwater depth and Tamarisk ET were strongly coupled. The rather sharp increase in Tamarisk water consumption happened at the same time as the aquifer level started to decline. For Slitherin, ET rates remained high at about 8 mm/day until early July, when water table fell to its deepest level of 3.85 m from the soil surface. It seems that the rapid 50% reduction in Tamarisk ET at the same time is a result of this deep water level. The reduced ET caused an increase in water level for about a month until mid-August, but the feed-back effect of the elevated water level was increased ET which again caused a slower response in the water table rise. Aquifer level remained approximately constant for another month and then it started increasing as the Tamarisk ET decreased due to the lower atmospheric demand. Over Diablo, however, such a distinct water stress was not recognizable, probably because groundwater at this station was always higher compared to Slitherin.

According to these data, a groundwater depth of 3.85 is the water availability threshold for Tamarisk individuals at Slitherin. Dropping water table to levels below this threshold would significantly suppress Tamarisk water consumption. This is contradictory to the general belief that Tamarisk has the ability to extract large amounts of water from deep aquifers. A few other research projects (e.g. Devitt et al. 1997) have also shown that Tamarisk transpiration has an inverse relationship with water table depth. Over Hassayampa River in Arizona; Horton et al. (2001) observed canopy dieback in Tamarisk when depth to groundwater was beyond the range of 2 – 3 m.

*SEBAL*

Since remotely-sensed energy balance models have not been applied over riparian ecosystems before, their limitations and potentials in estimating riparian ET are not known. An important unanswered question in implementing these models is how to extrapolate instantaneous ET estimates to longer periods (e.g. daily). In this study, instantaneous ET was estimated over the CNWR on a pixel-by-pixel basis, using SEBAL model applied to 21 Landsat TM5 images. Both of the two existing up-scaling methods, namely EF and  $ET_oF$  were used to obtain daily estimates of Tamarisk ET (Fig. 4.9).

For a short period of few days in late May, advection of cold air preceded by over 12 mm of rainfall resulted in an ET increase to more than 10 mm followed by a sudden decrease to 3.0 mm. Except for this period, Slitherin daily ET reached values as high as 8.0, and occasionally higher than 9.0 mm. As depicted in Fig. 9, ET rates from the  $ET_oF$  techniques were always higher than the EF. The difference ranged from almost zero in May and June to about 2 mm/day during Tamarisk dormancy.

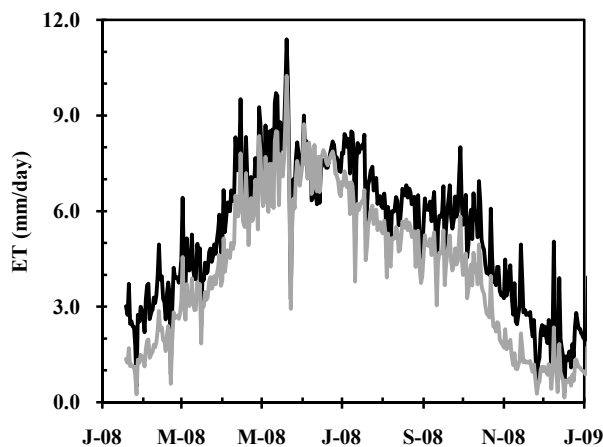


**Fig. 4.9** Daily ET rates over Slitherin station, estimated by SEBAL model and two different extrapolation techniques:  $ET_oF$  (black) and EF (gray)

In general, SEBAL estimates over Diablo were lower than Slitherin, but they showed the same behavior ( $ET_oF$  being higher than  $EF$ ). The observed difference between the two extrapolating methods is chiefly due to the fact that  $ET_oF$  method is based on the ground measurements of air temperature and vapor deficit. Therefore, some effect of horizontally-transported energy under advective conditions is taken into account in this method. For well-irrigated agricultural crops that have enough access to water, advective enhancement translates into  $ET$  rates higher than what is predicted by the  $EF$  technique. However, riparian  $ET$  is mainly water-limited rather than energy-limited. Devitt et al. (1997) observed that when water table that was about 3.0 m from soil surface, Tamarisk individuals were not able to meet increased atmospheric demand of advective condition. Hence,  $EF$  seems to be a more appropriate up-scaling technique, since it does not assume that all the converged energy is used in transforming the state of water from liquid to gas.

Another major concern in extrapolating instantaneous  $ET$  is the validity of a key assumption that is made in both techniques. According to this assumption, the instantaneous  $ET_oF$  and/or  $EF$  ratio at the time of satellite overpass remains constant throughout the day. This may not be the case if phreatophytes experience afternoon depression. However, Nagler et al. (2009a) found that Tamarisk individuals at Slitherin station had a rather constant diurnal  $EF$ . Over Diablo, however, signs of midday depression were observed, but it was compensated by nocturnal transpiration, resulting in the validity of assuming a generally constant  $EF$  ratio. Figure 4.10 illustrates the map of  $ET$  modeled by SEBAL- $EF$  method on July 29<sup>th</sup>, 2008, as one example of the 21 processed Landsat scenes.

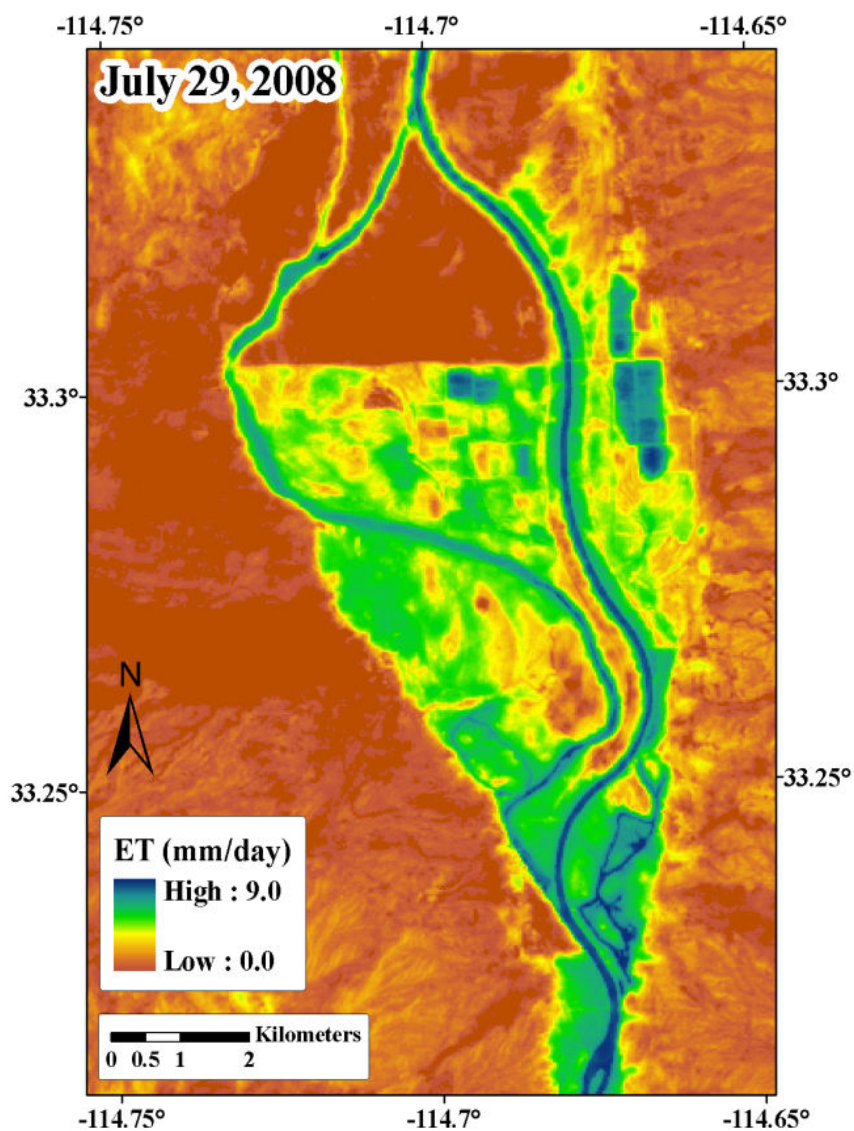


**Fig. 4.10** Spatially-distributed ET rates modeled by the SEBAL-EF methods over CNWR

#### *SEBAL-White comparison*

Remotely-sensed estimates of Tamarisk ET from SEBAL-EF model were plotted along with the groundwater consumption estimates of the White method. Both methods resulted in similar ET rates during the growing season over both stations. However, the

estimates were significantly different during the first few months of 2008 (Fig. 4.11). For example, while White method estimated no significant ET in early March, SEBAL-EF estimates were about 3.0 and 2.0 mm for Slitherin and Diablo, respectively. These ET rates seem to be overpredicted as Tamarisk was still at the end of its dormancy period in early March and not transpiring. In addition, no measurable precipitation event had happened in more than a month prior to this date, so the remotely-sensed ET cannot be attributed to soil evaporation. During the entire Tamarisk dormancy period, SEBAL-EF estimated ET of 188 and 142 mm for Slitherin and Diablo, respectively, much higher than the total precipitation during the same period (50 mm).

One hypothesis to explain this overestimation was that empirical equations in SEBAL model for estimating surface roughness length are calibrated against measurements over agricultural crops, with a relatively short and homogeneous height compared to Tamarisk trees that could be as tall as 10 m (over Slitherin).

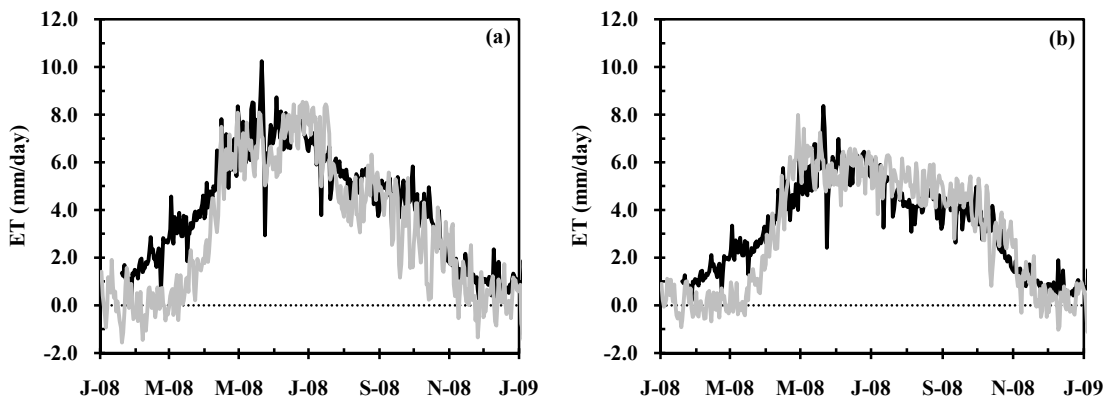


**Fig. 4.11** A comparison of daily ET rates estimated by SEBAL-EF method (black) with the White method (gray) over (a) Slitherin and (b) Diablo

To investigate this hypothesis, a high-resolution, LiDAR-derived map of Tamarisk canopy height was used to estimate actual roughness length (based on Prueger and Kustas 2005). A comparison of ET estimates using the actual roughness length layer with the estimates using original empirical equations showed no significant difference (results not presented here). This was not surprising as any effect from an underestimated canopy height would have been projected over the entire study period, not only the first few months of the year. In addition, Wang et al. (2009) evaluated the sensitivity of SEBAL estimates over pecan orchards in New Mexico. Changing the value of roughness length from zero to 2.5 (representing vegetation heights from zero to 20.8 m) did not have a significant effect on the modeled ET, especially when canopy cover was higher than 50%. Tasumi (2005) also reported that METRIC (an energy balance model based on SEBAL) was not sensitive to the value of this parameter.

Further investigation of all the steps in running SEBAL model revealed that the main reason behind overestimation of ET is the dominant presence of shadows in the Tamarisk forest that contaminate and lowers the canopy temperatures detected by satellite sensors. The overpass times for all of the Landsat scenes used in this study were within 7 minutes of 18:00 Greenwich Mean Time, which is about 10:00 Pacific Standard Time (PST = GMT – 8:00). This fixed overpass time resulted in a sun elevation angle that varied between 30.8 degrees on January 19<sup>th</sup> and 66.2 degrees on June 11<sup>th</sup>, 2008. The values of sun elevation and azimuth angles reported in the header file of the Landsat imagery and the LiDAR-derived map of top-of-canopy elevation were used as input data to the “Hill-shade” function in ArcGIS. Analyzing the generated maps showed that the percentage of the shadow pixels (shaded relief value of zero) ranged from 33.4% on

January 19<sup>th</sup> to 2.5% on May 26<sup>th</sup>, 2008. This extensive presence of shadows lowered the canopy temperature in the 60-m by 60-m pixel of Landsat thermal band. Contaminated pixels tended to shift more toward the selected cold extreme in the image, resulting in a lower assigned sensible heat flux, and consequently a higher latent heat flux.

### *Modified SEBAL*

The evolution of vegetation indices had a typical pattern opposite of the changes in shaded area, so a pixel-wise normalized SAVI (Huete 1988) was used as the adjusting coefficient to correct for the overestimation error introduced by pixel contamination. The normalized SAVI was estimated by dividing the SAVI of each pixel in every satellite image by the maximum SAVI of the same pixel among all 21 images. This coefficient was finally multiplied by the ET from SEBAL-EF to develop new maps of ET. Applying the correction coefficient reduced the remotely-sensed Tamarisk ET during non-growing season to levels similar to what was predicted by White method (Fig. 4.12).

The modified ET rates were close to zero in January and December, but rose rather rapidly in mid to late March as Tamarisk transpiration initiated with the green up of the vegetation. The annual RMSD of adjusted SEBAL estimates and White results were 1.1 and 1.0 mm/day over Slitherin and Diablo, respectively. Figure 4.12 also shows the daily ET rates measured by Bowen-ratio (BR) towers located at the center of each station. At Slitherin, Bowen-ratio measurements were very close to the adjusted SEBAL and White estimates, with RMSDs of 0.9 and 1.2 mm/day, respectively, for the 251 days of available BR data for this station. At Diablo, however, measured ET rates were

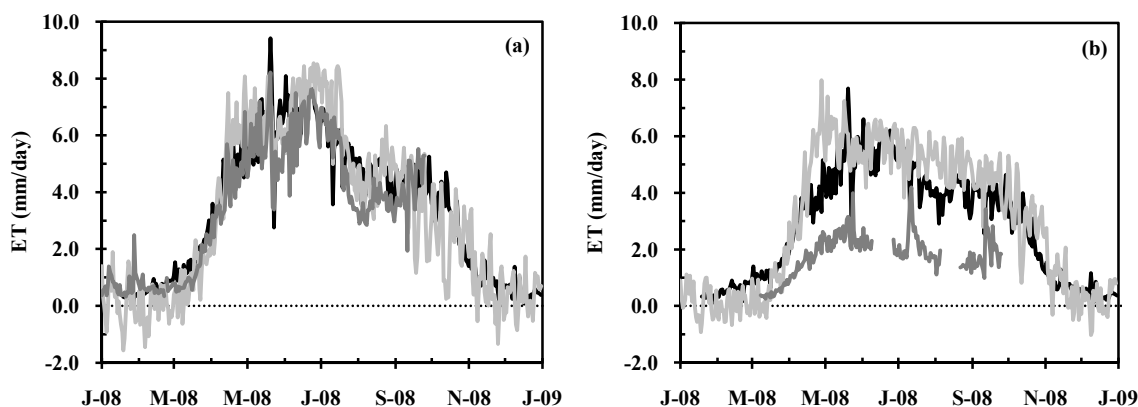


**Fig. 4.12** A comparison of daily ET rates estimated by SAVI-adjusted SEBAL-EF method (black), the White method (light gray), and measured by the Bowen-Ratio tower (dark gray) over (a) Slitherin and (b) Diablo

significantly lower than both SEBAL and White approaches, with RMSDs of 2.3 and 3.0 mm/day, respectively, for the 169 days of available BR data. The low values of measured ET over Diablo may be a result of poor groundwater quality at this station and possibly the fact that the ET in the upwind footprint to the tower is not representative of the vegetation immediately around the tower where the wells are located.

In managing water deliveries on the Lower Colorado River, USBR utilizes an approach that is known as the “Lower Colorado River Accounting System (LCRAS).” LCRAS is based on the crop coefficient ( $K_c$ ) concept in which, the daily ET rates of agricultural and riparian species are expressed as a fraction of reference ET on the same day. To make the results of this study more useful for the river managers, daily  $K_c$  was estimated based on both adjusted SEBAL-EF and White method, then piece-wise linear curves were fitted to the data in order to be consistent with the traditional 4-stage  $K_c$  curves of LCRAS (Figure 4.13).



As depicted in Fig. 4.13, the lengths of different Tamarisk growth stages were similar among all presented approaches. However,  $K_c$  values currently used by USBR were significantly higher than the estimates of both adjusted-SEBAL and White methods. For example,  $K_c$  estimates over Slitherin station during the mid-season period (mid-May to late-September) were 0.74 and 0.76 based on SEBAL and White methods, respectively. These values are similar to the Tamarisk  $K_c$  of 0.76, estimated using the measurements of the Bowen-ratio flux towers at the Havasu National Wildlife Refuge, which is located upstream of the CNWR (Westenburg et al. 2006). But LCRAS assumes a mid-season  $K_c$  of 1.10, about 45% higher than estimated and measured Tamarisk  $K_c$ . Except for the month of December, LCRAS assumptions were higher than SEBAL and White method estimates over both Diablo and Slitherin stations during the entire 2008. Such a high  $K_c$  approximation can result in water releases in excess of actual demand.

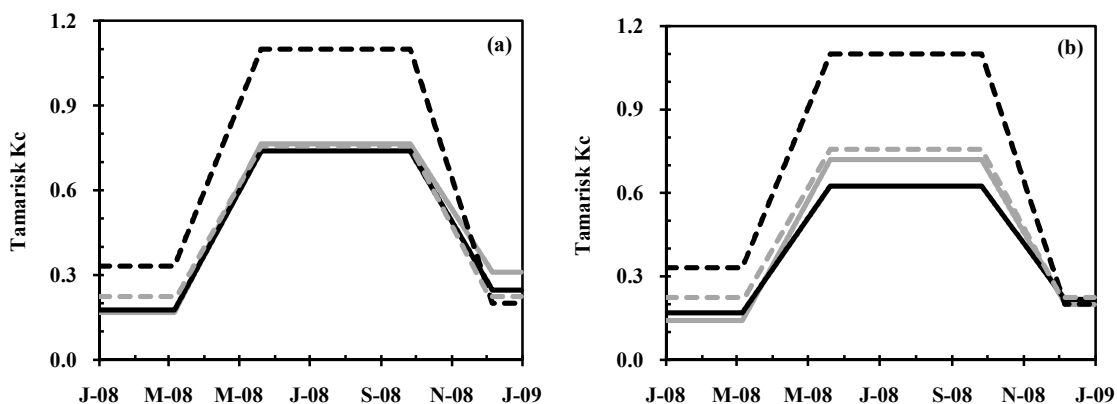


**Fig. 4.13** Piece-wise  $K_c$  curves over (a) Slitherin and (b) Diablo, using the following methods: adjusted SEBAL-EF (solid black), White (solid gray), LCRAS (dashed black), and LCRAS modified by Westenburg et al. (2006) (dashed gray)

*Annual and seasonal Tamarisk ET*

Adjusted EF technique resulted in ET estimates lower than EF and both were lower than  $ET_oF$  on annual and growing-season basis. In general, seasonal ET estimates were lower than annual estimates for both Diablo and Slitherin, but the situation was opposite for the fraction of  $ET_o$ . Lower annual  $ET_o$  fractions were a result of insignificant Tamarisk ET during its dormancy, while grass surface was consuming water at the same time (Table 4.2). Adjusted remotely-sensed and White estimates for Slitherin are consistent with the findings of Nagler et al. (2008). They applied the MODIS-derived EVI approach and estimated an annual Slitherin ET of 1,300 mm, averaged over a period of six years (2000 – 2006).

**Table 4.2** Annual and seasonal water consumption in mm over Slitherin and Diablo. Values in parentheses are the percentage of the corresponding (annual or seasonal) grass-based reference ET

Time scale	Method	Slitherin	Diablo
Annual	SEBAL- $ET_oF$	1,889 (94%)	1,444 (72%)
	SEBAL-EF	1,478 (73%)	1,178 (58%)
	SEBAL-EF (Adj)	1,211 (60%)	999 (50%)
	White	1,191 (59%)	1,119 (56%)
Growing season	SEBAL- $ET_oF$	1,551 (93%)	1,183 (71%)
	SEBAL-EF	1,290 (77%)	1,036 (62%)
	SEBAL-EF (Adj)	1,137 (68%)	933 (56%)
	White	1,142 (68%)	1,077 (64%)

However, their estimate over Diablo was higher at 1,430 mm, 43 and 28% larger than the results of SEBAL-EF (Adj) and White methods in this study, respectively.

A later publication by Nagler et al. (2009b) reported that annual CNWR ET ranges from 800 to 1400 mm and it is about half of the reference ET. At Havasu National Wildlife Refuge, AZ (about 250 river km upstream of CNWR), Westenburg et al. (2006) used Bowen-ratio towers and estimated an annual Tamarisk ET of 1,076 mm which was 60% of the annual  $ET_o$  for the same year (2003) and very similar to the findings of this study. The footprint of this tower was located over a dense Tamarisk site at roughly the same height as Diablo.

For Slitherin, the adjusted SEBAL-EF method produced ET estimates that were very close to White estimates (both on annual and seasonal scales). However, remotely sensed estimates over Diablo were lower than the predictions of White method. This could be an effect of possible mismatch between the footprints of SEBAL and White methods. To extract SEBAL averages for each station, a circular footprint encompassing all five observation wells at each station was used. The center of this circle was located on the central well, and its radius was 230 m (approximate area of  $0.17 \text{ km}^2$ ). Since other four wells are about 80 m from the central well, the boundary of this circular footprint was roughly 150 m from the closest well. However, groundwater fluctuations at each well may be under the influence of Tamarisk individuals at farther or closer distances. The mismatch of footprints is less problematic over Slitherin, where Tamarisk canopy is more homogeneous and at full cover. Over Diablo, not only the canopy is shorter and interspaced with bare soil and arrowweed, the groundwater quality is also inferior.

*Wide-area evapotranspiration*

The annual evaporative water loss from the lower CNWR (978 ha) was 913 mm for the 2008 (45% of  $ET_o$ ), with daily ET rates ranging from 0.3 mm in January to 5.5 mm in June. This peak daily ET is lower than the rates reported by Nagler et al. (2009b) over the same area. Based on their EVI approach, average daily ET rates had reached a maximum of about 8.0 mm in every year during 2000 to 2007. The total annual volume of ET from the lower CNWR was about  $9.1 \text{ Mm}^3$ , only 0.1% of the river discharge above Palo Verde diversion dam. Along the Lower Colorado River below Davis dam to the US-Mexico border, the total area of Tamarisk monocultures (more than 90% of the vegetation being Tamarisk) is about 18,200 ha (Nagler et al. 2008). Assuming that these regions are similar to CNWR in terms of water consumption, total volume of annual water loss by Tamarisk for the Lower Colorado Basin adds up to about  $166.2 \text{ Mm}^3$ , which is about 7% lower than the  $178.4 \text{ Mm}^3$  estimated by Nagler et al. (2008).

It is generally believed that Tamarisk ET is equal or higher than other phreatophytes. If this is true, an upper limit of water consumption can be estimated for the Lower Colorado Basin by assuming that ET rates over the entire riparian ecosystem is similar to what was estimated over CNWR. Based on a total riparian area of 34,000 ha, total riparian water use would be about  $310.4 \text{ Mm}^3$ , which is again 7% lower than the  $333.2 \text{ Mm}^3$  estimated by Nagler et al. (2008) and less than half of the  $748.1 \text{ Mm}^3$  reported in the 2008 LCRAS for the same region (USBR 2009b). The estimates of this study and the study by Nagler et al. (2008) are 2.56 and 2.75% of the total volume of water released from the Davis dam in 2008, respectively (USBR 2009a).

### Closing water balance on the river

In order to close water balance over the specified segment of the Lower Colorado River, spatially distributed ET was also modeled over the irrigated fields (PVID) and the riparian corridor. For the riparian corridor the same adjusted SEBAL-EF method that has proved to produce reliable estimates was used. Over PVID, SEBAL-ET<sub>oF</sub> was applied since this method is more appropriate for irrigated regions in arid/semi-arid climates. The annual water consumption averaged over the 75-km stretch of the river that includes PVID, CNWR, water bodies, and bare soil was 968 mm in 2008.

### *Other water balance components*

The total volume of annual precipitation from all 25 rainfall events was 52.8 Mm<sup>3</sup>, which is an average of about 71 mm over the whole area. According to USBR, annual average Colorado River daily flow rates at upstream of the PVID diversion dam and at Cibola gage were 246.5 and 230.6 m<sup>3</sup>/sec, respectively. The daily flow rates were converted to the volume of water to close the water balance (Table 4.3). Over the whole period of study, precipitation was less than 1% of water inputs into the control volume under study. Evaporative losses accounted for 9% of the river discharge at upstream of the Palo Verde diversion dam. This amount of evapotranspiration was equal to 968 mm of water depth over the studied stretch of the river. In general, the error of closing water balance over a stretch of the river is expected to be higher than when the analyses are performed over catchments and watersheds. This is mainly due to the mismatch between hydrologic and study area boundaries, as well as difficulties in identifying all the components of water inputs and outputs to the studied control volume.

**Table 4.3** Total annual amounts of water balance components. Depth values are estimated by dividing the volume of water by the total studied area (73,862 ha)

	Volume (Mm <sup>3</sup> )	Depth (mm)
Precipitation	52.77	71
River US flow	7,815.07	10,581
$\Sigma$ Inputs	7,867.84	10,652
River DS flow	7,312.63	9,900
Evapotranspiration	714.71	968
$\Sigma$ Outputs	8,027.34	10,868
$\Sigma$ Inputs – $\Sigma$ Outputs	-159.5	-216

Goodrich et al. (2000) studied water balance of a riparian-dominated segment of the San Pedro River in AZ. Closure error for this 10-km-long segment of the river was 5.2% of the input volume over a period of 90 days. In this study, water balance closure over a 75-km stretch of the river was only two percent of the river discharge above the Palo Verde dam. Over PVID, which consists 60% of the surface area of the considered river reach, Chapter 2 results validated the SEBAL estimates of ET against water balance closure and found an error of 0.7%. So it was expected that the closure over the whole stretch of the river would not be less than 0.7%.

The observed 2% error is well within the range of accuracies reported for remotely-sensed energy balance models, as well as precipitation and river flow measuring devices. The slightly higher values of water outputs is partly a result of ignoring

precipitation that fall on the hills east of the river. Natural drains and gullies direct any rainfall-generated runoff toward the river, but since no precipitation data is available over this area, it was not included in the analysis. Assuming that average precipitation was the same 71 mm over this area, a volume of about 50 Mm<sup>3</sup> should be added to water inputs from precipitation. This would reduce the difference between water inputs and outputs by about one third.

### **Summary and conclusions**

The poorly-understood connection between river flows and water levels with fluxes into the floodplain groundwater system resulting from riparian water demands poses operational challenges for the management of the western rivers. The results of this study showed that water table depths at two sites that were further located from the river (Slitherin and Diablo) were strongly affected by Tamarisk water extraction, with a peak in April (before Tamarisk greening) and a minimum level in July and August. But aquifer fluctuations at a site close to the river (Swamp) were different, following a pattern similar to the river stage fluctuations. During the study period (2008), Colorado River stage never drop below the aquifer elevation. The hydraulic gradients from the river to Swamp and from Swamp to Slitherin and Diablo were negligible during Tamarisk dormancy, but increased in the growing season. Groundwater electrical conductivity, depth, and elevation data all indicated that the direction of the flow is from water resources (old and new river channels) toward the heart of CNWR.

Application of SEBAL model over CNWR with a rough canopy structure and woody matter resulted in overestimation of ET in spring and winter. This was mainly

due to the fixed overpass time of Landsat, which was around 10:00 AM PST. At this time during spring and winter, sun elevation angle is very low, resulting in a significant presence of shadows, which lowers the detected surface temperature. To adjust for this error, a relative SAVI coefficient was defined and applied. Modified remotely-sensed estimates were similar to the groundwater consumption results of the White method. Since the modification presented in this study is based on the same remotely-sensed data, it is not limited to the local conditions of the study area and can be applied over different riparian ecosystems.

Remotely sensed data were averaged over the entire lower CNWR, resulting in an annual Tamarisk water consumption which was only 45% of the annual grass-based reference ET and significantly lower than the values that are currently used by the US Bureau of Reclamation. Projecting this estimate over the entire Tamarisk monocultures and the entire riparian forests along the Lower Colorado River (below Davis dam) resulted in 166.2 Mm<sup>3</sup> and 310.4 Mm<sup>3</sup>, which are again significantly lower than USBR approximations. The findings of this study are consistent with the results of another recent research and provide a more realistic estimate of the gross amount of water that can be salvaged over the Lower Colorado River by removing all Tamarisk monocultures.

Water balance analysis was performed over the stretch of the river containing PVID and CNWR (73,862 ha). The average annual ET for all the irrigated fields, riparian thickets, bare soils, and water bodies of this area was 968 mm. This was about 9% of the river discharge above Palo Verde dam, with an annual average flow rate of 246.5 m<sup>3</sup>/sec. Closure error was only 2%, suggesting that water balance components are accurately identified.



## References

- Allen RG, Tasumi M, Trezza R (2007a) Satellite-based energy balance for mapping evapotranspiration with internalized calibration (METRIC)-model. *Irrig Drain Eng* 133(4):380–394.
- Allen RG, Tasumi M, Morse A, Trezza A, Wright JL, Bastiaanssen W, Kramber W, Lorite-Torres I, Robison CW (2007b) Satellite-based energy balance for Mapping Evapotranspiration with Internalized Calibration (METRIC)-Applications. *Irrig Drain Eng* 133(4):395–406.
- Bastiaanssen WGM, Menenti M, Feddes RA, Holtslang AA (1998a) A remote sensing surface energy balance algorithm for land (SEBAL): 1. Formulation. *J Hydrol* 212–213:198–212.
- Bastiaanssen WGM, Pelgrum H, Wang J, Ma Y, Moreno JF, Roerink GJ, van der Wal T (1998b) A remote sensing surface energy balance algorithm for land (SEBAL): 2. Validation. *J Hydrol* 212–213:213–229.
- Bastiaanssen WGM, Noordman EJM, Pelgrum H, Davids G, Thoreson BP, Allen RG (2005) SEBAL model with remotely sensed data to improve water-resources management under actual field conditions. *Irrig Drain Eng* 131(1):85–93.
- Bawazir AS, Samani Z, Bleiweiss M, Skaggs R, Schmutge T (2009) Using ASTER satellite data to calculate riparian evapotranspiration in the Middle Rio Grande, New Mexico. *Intern J Remote Sens* 30(21):5593–5603.
- Brutsaert W, Sugita M (1992) Application of self-preservation in the diurnal evolution of the surface energy budget to determine daily evaporation. *J Geophys Res* 97:18377–18382.
- Chavez JL, Neale CMU, Prueger JH, Kustas WP (2008) Daily evapotranspiration estimates from extrapolating instantaneous airborne remote sensing ET values. *Irrig Sci* 27:67–81.
- Cleverly JR, Smith SD, Sala A, Devitt DA (1997) Invasive capacity of *Tamarix ramosissima* in a Mojave Desert floodplain: the role of drought. *Oecologia* 111:12–18.
- Colaizzi PD, Evett SR, Howell TA, Tolck JA (2006) Comparison of five models to scale daily evapotranspiration from one-time-of day measurements. *Trans ASABE* 49(5):1409–1417.

- Crago RD (2000) Conservation and variability of the evaporative fraction during the daytime. *J Hydrol* 180(1–4):173–194.
- Dennison PE, Nagler PL, Hultine KR, Glenn EP, Ehleringer JR (2009) Remote monitoring of tamarisk defoliation and evapotranspiration following saltcedar leaf beetle attack. *Remote Sens Environ* 113:1462–1472.
- Devitt DA, Sala A, Mace KA, Smith SD (1997) The effect of applied water on the water use of saltcedar in a desert riparian environment. *J Hydrol* 192:233–246.
- Glenn EP, Tanner R, Mendez S, Kehret T, Moore D, Garcia J, Valdes C (1998) Growth rates, salt tolerance and water use characteristics of native and invasive riparian plants from the delta of the Colorado River, Mexico. *J Arid Environ* 40:281–294.
- Godaire JE, Klinger RE (2007) Tree-ring dating of Tamarisk (*Tamarix ramosissima*), Cibola National Wildlife Refuge, California. US Bureau of Reclamation.
- Goodrich DC, Scott R, Qi J, Goff B, Unkrich CL, Moran MS, Williams D, Schaeffer S, Snyder K, MacNish R, Maddock T, Pool D, Chehbouni A, Cooper DI, Eichinger WE, Shuttleworth WJ, Kerr Y, Marsett R, Ni W (2000) Seasonal estimates of riparian evapotranspiration using remote and in situ measurements. *Agric For Meteorol* 105(1-3):281–309.
- Gowda PH, Chavez JL, Colaizzi PD, Evett SR, Howell TA, Tolck JA (2008) ET mapping for Agric Water Manage: present status and challenges. *Irrig Sci* 26:223–237.
- Gribovszki Z, Szilágyi J, Kalicz P (2010) Diurnal fluctuations in shallow groundwater levels and streamflow rates and their interpretation – A review. *J Hydrol* 385:371–383.
- Groeneveld DP, Baugh WM, Sanderson JS, Cooper DJ (2007) Annual groundwater evapotranspiration mapped from single satellite scenes. *J Hydrol* 344:146–156.
- Horton JL, Kolb TE, Hart SC (2001) Responses of riparian trees to interannual variation in ground water depth in a semi-arid river basin. *Plant, Cell Environ* 24:293–304.
- Huete AR (1988) A soil-adjusted vegetation index (SAVI). *Remote Sens Environ* 25:295–309.
- Huete AR, Didan K, Miura T, Rodriguez E, Gao X, Ferreira L (2002) Overview of the radiometric and biophysical performance of the MODIS vegetation indices. *Remote Sens Environ* 83:195–213.

- Hultine KR, Belnap J, van Riper III C, Ehleringer JR, Dennison PE, Lee ME, Nagler PL, Snyder KA, Uselman SE, West JB (2009) Tamarisk biocontrol in the western United States: ecological and societal implications. *Front Ecol Environ* 8(9):467–474.
- Hultine KR, Nagler PL, Morino K, Bush SE, Burtch KG, Dennison PE, Glenn EP, Ehleringer JR (2010) Sap flux-scaled transpiration by tamarisk (*Tamarix* spp.) before, during and after episodic defoliation by the saltcedar leaf beetle (*Diorhabda carinulata*). *Agric For Meteorol* 150:1467–1475.
- Loheide II SP, Butler Jr JJ, Gorelick SM (2005) Use of diurnal water table fluctuations to estimate groundwater consumption by phreatophytes: a saturated-unsaturated flow assessment. *Water Resource Res* 41.W07030
- Meyboom P (1966) Groundwater studies in the Assiniboine River drainage basin—part I: Evaluation of a flow system in south-central Saskatchewan, *Bull. Geol. Surv. Can.*, 139.
- Murray RS, Nagler PL, Morino K, Glenn EP (2009) An empirical algorithm for estimating agricultural and riparian evapotranspiration using MODIS enhanced vegetation index and ground measurements of ET. II. Application to the Lower Colorado River, U.S. *Remote Sens* 1:1125–1138.
- Nagler PL, Scott RL, Westenberg C, Cleverly JR, Glenn EP, Huete AR (2005) Evapotranspiration on western U.S. rivers estimated using enhanced vegetation index from MODIS and data from eddy covariance and Bowen ratio flux towers. *Remote Sens Environ* 97:337–351.
- Nagler PL, Glenn EP, Didan K, Osterberg J, Jordan F, Cunningham J (2008) Wide-Area Estimates of Stand Structure and Water Use of *Tamarix* spp. on the Lower Colorado River: Implications for Restoration and Water Management Projects. *Restoration Ecology* 16(1):136–145.
- Nagler PL, Morino K, Murray RS, Osterberg J, Glenn EP (2009a) An empirical algorithm for estimating agricultural and riparian evapotranspiration using MODIS enhanced vegetation index and ground measurements of ET. I. Description of method. *Remote Sens* 1:1273–1297.
- Nagler PL, Morino K, Didan K, Erker J, Osterberg J, Hultine KR, Glenn EP (2009b) Wide-area estimates of saltcedar (*Tamarix* spp.) evapotranspiration on the lower Colorado River measured by heat balance and remote sensing methods. *Ecohydrol* 2:18–33.
- Norman JM, Kustas WP, Humes KS (1995) A two-source approach for estimating soil and vegetation energy fluxes from observations of directional radiometric surface temperature. *Agric For Meteorol* 77:263–293.

- Owens MK, Moore GW (2007) Saltcedar water use: realistic and unrealistic expectations. *Rangeland Ecol Manage* 60(5):553–557.
- Prueger JH, Kustas WP (2005) Aerodynamic methods for estimating turbulent fluxes. In: Hatfield JL, Baker JM (eds) *Micrometeorology in Agricultural Systems*, Agronomy Monograph No. 47. American Society of Agronomy, Inc., Crop Science Society of America, Inc., Soil Science Society of America, Inc. Publishers. Madison, WI, USA.
- Ramos JG, Cratchley CR, Kay JA, Casterad MA, Martinez-Cob A, Dominguez R (2009) Evaluation of satellite evapotranspiration estimates using ground-meteorological data available for the Flumen District into the Ebro Valley of N.E. Spain. *Agric Water Manage* 96:638–652.
- Scott RL, Cable WL, Huxman TE, Nagler PL, Hernandez M, Goodrich DC (2008) Multiyear riparian evapotranspiration and groundwater use for a semiarid watershed. *J Arid Environ* 72:1232–1246.
- Tasumi M (2005) A review of evaporation research on Japanese lakes. In: *Proceedings of ASCE/EWRI World Water and Environmental Resources Congress*, ASCE, Reston, VA, USA.
- Trezza R (2002) Evapotranspiration using a satellite-based surface energy balance with standardized ground control. Dissertation, Utah State University, Logan, UT, 339 Pp.
- US Bureau of Reclamation (2009a) Colorado River Accounting and Water Use Report; Arizona, California, and Nevada; Calendar Year 2008. U.S. Department of the Interior, Bureau of Reclamation, Lower Colorado Region, Boulder Canyon Operations Office. Water Conservation & Accounting Group. Accessible at: <http://www.usbr.gov/lc/region/g4000/4200Rpts/DecreeRpt/2008/2008.pdf>
- US Bureau of Reclamation (2009b) Lower Colorado River Accounting System, Evapotranspiration and Evaporation Calculations; Calendar Year 2008. U.S. Department of the Interior, Bureau of Reclamation, Lower Colorado Regional Office, Boulder City, NV. Accessible at: <http://www.usbr.gov/lc/region/g4000/4200Rpts/LCRASRpt/2008/2008LCRAS.pdf>
- Vandersande MW, Glenn EP, Walworth JL (2001) Tolerance of five riparian plants from the lower Colorado River to salinity drought and inundation. *J Arid Environ* 49:147–159.
- Wang J, Sammis TW, Gutschick VP, Gebremichael M, Miller DR (2009) Sensitivity analysis of the surface energy Balance algorithm for land (SEBAL). *Trans ASABE* 52(3):801–811.

Westenburg CL, Harper DP, DeMeo GA (2006) Evapotranspiration by phreatophytes along the lower Colorado River at Havasu National Wildlife Refuge, Arizona: U.S. Geological Survey Scientific Investigations Report 2006-5043, 44 p. Available at <http://pubs.water.usgs.gov/sir20065043>

White WN (1932) A method of estimating ground-water supplies based on discharge by plants and evaporation from soil: results of investigations in Escalante Valley, Utah, U.S. Geol Surv Water Supply Pap, 659-A.

Zavaleta E (2000) The Economic Value of Controlling an Invasive Shrub. *AMBIO* 29(8):462–467.

Zhang L, Lemeur R (1995) Evaluation of daily ET estimates from instantaneous measurements. *Agric For Meteorol* 74:139–154.

## CHAPTER 5

### GENERAL SUMMARY AND CONCLUSIONS

The “Surface Energy Balance Algorithm for Lands (SEBAL)” was implemented to estimate spatially distributed evapotranspiration over Palo Verde Irrigation District (PVID) and Cibola National Wildlife Refuge (CNWR), located on the west bank of the Lower Colorado River in Southern California. As input data to SEBAL model, all available cloud-free Landsat TM5 imagery acquired over the study area between January 2008 and January 2009 (21 images) were acquired and processed. Annual evapotranspiration (ET) estimates were 1,286 mm over PVID, 913 mm over CNWR, and 968 mm over the entire study area on average.

Both PVID and CNWR groundwater level fluctuations manifested a distinct seasonal pattern. Over PVID, water table was at its lowest position in February 2008 and rose gradually as the irrigation applications became more intensive until it reached its peak in September and October. As irrigation decreased during the winter months, groundwater dropped to the same level in February of the next year. This shows that how groundwater in this area is affected by the irrigation and drainage systems. The seasonal variation of groundwater over CNWR was approximately opposite of the variation at PVID, with highest level of water table occurring in spring, and the lowest level in late summer. This was the result of water extraction by the tap roots of the riparian species (mainly Tamarisk).

Several irrigation and drainage performance indicators were estimated over PVID. In general, field water consumption was very uniform. However, 15% of the fields had a

variability higher than 10%. Using the distributed information of ET variability, PVID irrigation managers can easily locate these fields and focus their attention specifically on them to investigate possible reasons behind the observed low uniformity in those fields. PVID full-cover fields had an ET rate 6% greater than their potential rate, estimated by the Priestly-Taylor method. This slightly higher rate of water consumption is detected because the Priestly-Taylor parameter was calibrated using ET estimates over a reference grass surface, while most of PVID fields are under alfalfa, with one of the highest water consumption rates among all agricultural crops. This also indicates that, on average, PVID fields at full cover are provided with adequate water.

Three drainage performance indicators were also estimated over PVID to investigate irrigation sustainability. The drainage ratio was 0.45, a value much higher than the typical leaching requirements of irrigation schemes (0.05 to 0.10). This high amount of drained water would prevent any salt accumulation in the crop root zone. Assuming that the leaching requirement in PVID is not greater than 0.15, water application can be reduced by about 30% without negatively affecting agricultural production. Over-irrigating always raises concerns about water-logging problems. However, the depth to the water table was not only uniformly distributed over PVID, but it was also below the maximum range of crop effective root depth at all times. This means that PVID drains are successfully functioning, and water-logging is not an issue.

In order to demonstrate the potential of remote sensing techniques in studying crop-specific water consumption, remotely-sensed estimates of cotton crop coefficient from two different techniques were compared with tabulated crop coefficients that are currently used by the US Bureau of Reclamation in estimating cotton water consumption

as part of water delivery management on the Lower Colorado River. Remote sensing techniques detected a heavy pre-planting irrigation event, as well as a longer growing season in comparison with tabulated values. These differences resulted in a larger seasonal water consumption that was also verified by interviewing local cotton growers. Remotely-sensed estimates were averaged over the traditional four-stage crop growth period to develop new tabulated values to foster a more efficient water management. Finally, a new and simple linear model was developed to estimate the cotton crop coefficient from satellite-derived vegetation indices. Compared to energy balance models, the developed linear model is significantly less complicated and less time-consuming to implement. A similar approach can be applied to modify crop coefficients that are currently used in approximating water consumption of other major crops in the western US (e.g. alfalfa).

Studying stream-aquifer-phreatophyte interaction over the CNWR revealed that the Colorado River stage never drops below the aquifer elevation during the study period. The hydraulic gradients from the river to Swamp and from Swamp to Slitherin and Diablo were negligible during Tamarisk dormancy, but increased in the growing season. Groundwater electrical conductivity, depth, and elevation data all indicated that the direction of the flow is from water resources (old and new river channels) toward the heart of CNWR.

Application of SEBAL model over CNWR with a rough canopy structure and woody matter resulted in overestimation of ET in spring and winter. This was mainly due to the fixed overpass time of Landsat, which was around 10:00 AM PST. At this time during spring and winter, sun elevation angle is very low, resulting in a significant presence of



shadows, which lowers the detected surface temperature. To adjust for this error, a relative SAVI coefficient was defined and applied. Modified remotely-sensed estimates were similar to the groundwater consumption results of the White method. Since the modification presented in this study is based on the same remotely-sensed data, it is not limited to the local conditions of the study area and can be applied over different riparian ecosystems.

Over the PVID, annual water balance closure error was less than 1%, suggesting that all of the water balance components were accurately estimated. During the study period, precipitation accounted for only 3% of water inputs (71 mm) to this irrigation scheme. The rest (2,479 mm) was diverted from the Colorado River, using the Palo Verde diversion dam on the river. Consumptive use of water by PVID crops in 2008 was about 52% of diverted water and 7% of the Colorado River discharge (7,815 Mm<sup>3</sup>) upstream of the Palo Verde diversion dam. Over the entire stretch of the river under consideration (including both PVID and CNWR), water balance closure error was 2%. The average annual ET for all the irrigated fields, riparian thickets, bare soils, and water bodies of this area was 968 mm. This was about 9% of the river discharge above Palo Verde dam, with an annual average flow rate of 246.5 m<sup>3</sup>/sec.

APPENDIX

Table A.1

Reported coefficients of variation (among and within field,  $CV_s$  and  $CV_w$  respectively) of actual ET estimated over sites with diverse agro-climatological conditions. In all of these studies, SEBAL model was used to estimate evapotranspiration.

<b>Publication</b>	<b>RS Platform</b>	<b>Overpass Dates</b>	<b>Study Area</b>	<b>Study Unit</b>	<b>Main Crops</b>	<b><math>CV_s</math> (%)</b>	<b><math>CV_w</math> (%)</b>
<i>This study</i>	<i>Landsat TM</i>	21	<i>California, USA</i>	<i>1485 Fields</i>	<i>Alfalfa, Cotton</i>	38.2	7.0
Zwart & Leclert (2010)	Landsat ETM	12	Office du Niger, Mali	5 management zones	Rice	2.4	8.9
Ahmad et al. (2009)	MODIS	19	Rechna Doab, Pakistan	9 subdivisions	Rice, Wheat	2.4	4.0
Ahmad et al. (2009)	MODIS	19	Rechna Doab, Pakistan	15 subdivisions	Sugarcane, Wheat	4.9	7.5
Roerink et al. (1997)	Landsat TM	1	Rio Tunuyan, Argentina	10 secondary units	Orchards, Vineyards	8.6	NA
Roerink et al. (1997)	Landsat TM	1	Rio Tunuyan, Argentina	31 tertiary units	Orchards, Vineyards	6.1	NA
Bastiaanssen et al. (1996)	Landsat TM	1	Nile Delta, Egypt	53 irrigation districts	Rice, Cotton, Maize	10	15

Table A.2

Previously developed  $K_c$ -VI relationships for cotton in the literature

Publication	Region	VI source	$K_c$ source	VI- $K_c$ relationship	Considerations
Shuhua et al. (2003)	China	Landsat ETM+	Penman-Monteith	$K_c = 1.12 \text{ NDVI}^2 + 0.809 \text{ NDVI} + 0.251$	NA
Hunsaker et al. (2003)	AZ, USA	Hand-held radiometer	Soil water balance	$K_{cb} = 1.49 \text{ NDVI} - 0.12$	Pre-full-cover
Hunsaker et al. (2003)	AZ, USA	Hand-held radiometer	Soil water balance	$K_{cb} = 2.80 \text{ NDVI} - (5.69e-4) \text{ GDD} - 1.17$	Post-full-cover
Hunsaker et al. (2005)	AZ, USA	Hand-held radiometer	Soil water balance	$K_{cb} = 5.0 \text{ NDVI} - 12.2 \text{ NDVI}^2 + 14.9 \text{ NDVI}^3 - 6.2 \text{ NDVI}^4 - 0.21$	Early-season
Hunsaker et al. (2005)	AZ, USA	Hand-held radiometer	Soil water balance	$K_{cb} = 498 \text{ NDVI} - 662 \text{ NDVI}^2 + 294 \text{ NDVI}^3 - 125$	Late-season

## CURRICULUM VITAE

### SALEH TAGHVAEIAN

32 Aggie Village Apt. C

Logan, UT 84341

(435) 890-0270, [s.t@aggiemail.usu.edu](mailto:s.t@aggiemail.usu.edu)

## EDUCATION

### **PhD, Irrigation Engineering (March 2011)**

Civil and Environmental Engineering Department, Utah State University, Logan, UT  
Dissertation: “Water and Energy Balance of a Riparian and Agricultural Ecosystem along the Lower Colorado River”

### **MS, Irrigation and Drainage Engineering (January 2006)**

Irrigation and Drainage Engineering Department, Ferdowsi University, Mashhad, Iran  
Thesis: “Effects of Sewage Effluent Irrigating and Application of Sludge on Soil Properties”

### **BS, Irrigation and Drainage Engineering (July 2003)**

Irrigation and Drainage Engineering Department, Ferdowsi University, Mashhad, Iran  
Thesis: “Time Domain Reflectometry of Soil Moisture under Different Levels of Salinity”

## RESEARCH EXPERIENCE

### **Research Assistant**

Institute: Remote Sensing Service Lab, Utah State University, Logan, UT, USA

- Flew with USU remote sensing aircraft (Cessna TP206) and operated 3 Kodak Megaplug 4.2i digital cameras (in visible and NIR bands), a FLIR thermal camera, and a LiDAR.
- Processed aerial and satellite imagery using software packages such as ERDAS.
- Modeled spatially distributed energy balance components at different temporal and spatial scales, using SEBAL and METRIC models.
- Developed RS/GIS applications in mapping the performance of large irrigation schemes.
- Integrated remotely sensed, hydro-climatological, and LiDAR data in ArcGIS environment in order to study stream-aquifer interaction.
- Programmed, operated and maintained eddy-covariance systems and several other soil/water/atmosphere sensors, including: TDR's, Neutron Probes, Water Level Loggers, Infrared Thermometers (Apogee), hand-held radiometers (EXOTECH), etc.

Institute: Utah On-Site Wastewater Treatment Training Program, Utah Water Research Laboratory, Utah State University, Logan, UT, USA

- Operated and maintained “The Huntsman On-Site Wastewater Treatment Training and Demonstration Site,” equipped with several soil-based waste treatment systems.
- Designed and installed a small-scale drip irrigation system for disposing municipal effluent. The goal is to give trainees some hands-on experience with maintaining drip systems that run on wastewater (cleaning filters, flushing the system, etc.).

## **TEACHING EXPERIENCE**

### **Teaching Assistant**

Taught undergraduate and graduate courses, developed engaging course materials and lectures, organized and conducted lab sessions, and evaluated exams and lab assignments. Courses: GIS in Water Resources (2010), Remote Sensing of Land Surfaces (2009, 2010, 2011), Irrigation Systems Operation and Maintenance (2011), Irrigation Hydrology (2005), Irrigation Principals (2004).

### **Conferences, Workshops, and Agricultural Extension**

Institute: CEE Department, Utah State University, Logan, UT, USA

- Trained technical staff of Palo Verde Irrigation District to understand and use new GIS tools in managing land and water resources of the district.
- Assisted in holding certification courses, offered by the Utah On-Site Wastewater Treatment Training Program.
- Contributed to organizing, planning, and holding “Remote Sensing & Hydrology 2010 Symposium” and “Spring Runoff Conference” in 2008, 2009, and 2010.
- Hosted “World Water Day” celebration in order to raise the level of awareness about the worldwide issues on water quality and availability.

Institute: IDE Department, Ferdowsi University, Mashhad, Iran

- Guided several week-long field trips to large irrigation schemes.
- Initiated regular meetings between farmers, researchers, and government officials in order to investigate existing challenges.
- Organized irrigation expositions to introduce modern equipments to farmers.

## **SKILLS**

### **Leadership**

- Representative of Utah State University’s irrigation students (2007 – 2008).
- President, Iranian National Committee on Irrigation and Drainage (IRNCID) chapter at Ferdowsi University, Iran (2001 – 2006).

### **Language**

- English (fluent), Persian (native), Arabic (intermediate)

### Computer

- RS/GIS: ERDAS Imagine, ArcGIS, MODTRAN
- Agro-Hydrology: Ref-ET, CropWat, SIRMOD, Catch 3D, RootCanal
- Statistical : Statistical Analysis Software (SAS)
- Microsoft Office Package

### PROFESSIONAL AFFILIATIONS

- American Geophysical Union (AGU)
- American Society of Civil Engineers (ASCE)
- U.S. Committee on Irrigation and Drainage (USCID)
- International Association of Hydrological Sciences (IAHS)
- International Society for Photogrammetry and Remote Sensing (ISPRS)

### PUBLICATIONS

- Taghvaeian, S., Neale, C.M.U., dos Santos, C.A.C., Watts, D., Osterberg, J. & Sritharan, S.I. (2010) Two Different Remote Sensing Techniques for Monitoring Crop Coefficient and Water Requirement of Cotton. In: Red Book of the Remote Sensing and Hydrology 2010 Symposium, September 27-30, 2010, Jackson Hole, WY. (In Press).
- Poormohammadi, S., Rahimian, M.H. & Taghvaeian, S. (2010) Applying Remotely Sensed Energy Balance Models in Iran: Potentials and Limitations. In: Red Book of the Remote Sensing and Hydrology 2010 Symposium, September 27-30, 2010, Jackson Hole, WY. (In Press).
- Taghvaeian, S., Neale, C.M.U., dos Santos, C.A.C., Watts, D., Osterberg, J. & Sritharan, S.I. (2010) Studying Water Balance Components at the Palo Verde Irrigation District, using Remote Sensing, GIS and Hydroclimatological Data. In: Proceeding of the 2<sup>nd</sup> Conference on Evapotranspiration, August 16-18, 2010, Las Vegas, NV., 59–64.
- Taghvaeian, S., Neale, C.M.U., dos Santos, C.A.C., Watts, D., Osterberg, J. & Sritharan, S.I. (2009) Using Remote Sensing and GIS Techniques for Studying Irrigation Performance of Palo Verde Irrigation District. In: Proceeding of USCID 5th International Conference on Irrigation & Drainage, Nov. 3-6, 2009, Salt Lake City, UT., 21–34.
- Ghazanfari, S., Musavi Baygi, M., Sanaei Nejad, H., Naseri, M. & Taghvaeian, S. (2008) Compilation and Implementation of a Thermodynamic Model to Predict the Minimum Temperature Resulted from Cold Air Accumulation in Complex Terrain. In: Proceeding of the IASTED International Symposium on Intelligent Systems and Controls, Nov. 16-18, 2008, Orlando, FL. 638/005.
- Ghahraman, B. & Taghvaeian, S. (2008) Investigation of Annual Rainfall Trends in Iran. *Journal of Agricultural Science and Technology*, 10(1): 93–97.
- Taghvaeian, S., Danesh, S. & Alizadeh, A. (2007) Effects of Sewage Irrigation on Some of the Physical and Chemical Properties of Soil. *Iranian Journal of Irrigation and Drainage*, 1: 49–61.